

ลักษณะสมบัติของแอมิโกลมอลเทศชนิดใหม่จาก
Corynebacterium glutamicum ATCC 13032



นางสาว วิชา ศรีสีมารัตน์

ศูนย์วิทยทรัพยากร
จุฬาลงกรณ์มหาวิทยาลัย

วิทยานิพนธ์นี้เป็นส่วนหนึ่งของการศึกษาตามหลักสูตรปริญญาวิทยาศาสตรดุษฎีบัณฑิต

สาขาวิชาชีวเคมี ภาควิชาชีวเคมี

คณะวิทยาศาสตร์ จุฬาลงกรณ์มหาวิทยาลัย

ปีการศึกษา 2553

ลิขสิทธิ์ของจุฬาลงกรณ์มหาวิทยาลัย

CHARACTERIZATION OF A NOVEL AMYLOMALTASE FROM
Corynebacterium glutamicum ATCC 13032




Miss Wiraya Srisimarat

ศูนย์วิทยทรัพยากร
จุฬาลงกรณ์มหาวิทยาลัย

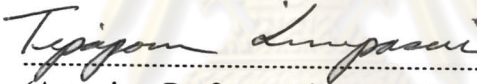
A Dissertation Submitted in Partial Fulfillment of the Requirements
for the Degree of Doctor of Philosophy Program in Biochemistry
Department of Biochemistry
Faculty of Science
Chulalongkorn University
Academic year 2010
Copyright of Chulalongkorn University

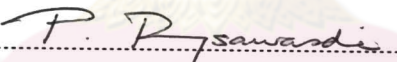
Thesis Title CHARACTORIZATION OF A NOVEL
AMYLOMALTASE FROM *Corynebacterium glutamicum*
ATCC 13032
By Miss Wiraya Srisimarat
Field of Study Biochemistry
Thesis Advisor Professor Piamsook Pongsawasdi, Ph.D.
Thesis Co-Advisor Assistant Professor Jarunee Kaulpiboon, Ph.D.,
Professor Wolfgang Zimmermann, Ph.D.

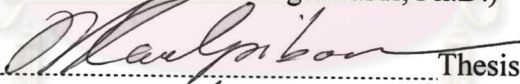
Accepted by the Faculty of Science, Chulalongkorn University in Partial
Fulfillment of the Requirements for the Doctoral Degree


..... Dean of the Faculty of Science
(Professor Supot Hannongbua, Dr.rer.nat.)

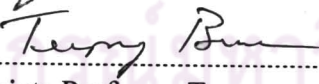
THESIS COMMITTEE

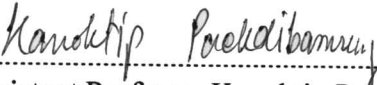

..... Chairman
(Associate Professor Tipaporn Limpaseni, Ph.D.)



..... Thesis Advisor
(Professor Piamsook Pongsawasdi, Ph.D.)


..... Thesis Co-Advisor
(Assistant Professor Jarunee Kaulpiboon, Ph.D.)


..... Thesis Co-Advisor
(Professor Wolfgang Zimmermann, Ph.D.)


..... Examiner
(Associate Professor Teerapong Buaboocha, Ph.D.)


..... Examiner
(Assistant Professor Kanoktip Packdibamrung, Ph.D.)


..... External Examiner
(Associate Professor Jarunya Narangajavana, Ph.D.)

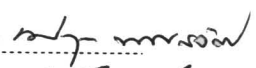
วิทยา ศรีสิมารัตน์ : ลักษณะสมบัติของแอมิโลมอลเตสชนิดใหม่จาก *Corynebacterium glutamicum* ATCC 13032. (CHARACTERIZATION OF A NOVEL

AMYLOMALTASE FROM *Corynebacterium glutamicum* ATCC 13032)

อ. ที่ปรึกษาวิทยานิพนธ์หลัก: ศ.ดร. เปี่ยมสุข พงษ์สวัสดิ์, อ. ที่ปรึกษาวิทยานิพนธ์
ร่วม: ผศ.ดร. จารุณี ควรวินบูลย์, Prof. Wolfgang Zimmermann, Ph.D., 185 หน้า.

งานวิจัยนี้มีวัตถุประสงค์ในการค้นหาแอมิโลมอลเตสชนิดใหม่ และระบุกรดอะมิโนสำคัญในการเร่งปฏิกิริยาการเกิดผลิตภัณฑ์ออลิโกแซ็กคาไรด์วงปิด โดยได้ทำการโคลนยีนแอมิโลมอลเตสจากแบคทีเรีย *Corynebacterium glutamicum* ATCC 13032 และแสดงออกใน *Escherichia coli* BL21 (DE3) โดยใช้เวกเตอร์ pET-19b ได้ยีนขนาด 2,190 นิวคลีโอไทด์ (รวม his-tag) พบว่าลำดับกรดอะมิโนที่แปลมาจากลำดับยีนมีความคล้ายกับที่เคยมีรายงานไว้เพียง 28-45% จากนั้นทำรีคอมบิแนนท์เอนไซม์ให้บริสุทธิ์ด้วยคอลัมน์ HisTrap FF™ ตรวจสอบขนาดได้ 84 kDa และมีภาวะที่เหมาะสมในการเร่งปฏิกิริยาที่ pH 6.0 และอุณหภูมิ 30 °C เอนไซม์สามารถเร่งปฏิกิริยา cyclization ได้ผลิตภัณฑ์ไซโคลเดกซ์ทรินวงใหญ่ (LR-CDs) มีขนาดตั้งแต่ CD19 ขึ้นไป หลังจากทำเอนไซม์ให้บริสุทธิ์แล้วได้ทำการตัด his-tag ออก แต่เอนไซม์ที่ไม่มี his-tag ไม่สามารถทำงานได้ จึงทำการเปลี่ยนเวกเตอร์เป็น pET-17b จากนั้นทำการแสดงออกรีคอมบิแนนท์เอนไซม์และทำให้บริสุทธิ์ด้วยคอลัมน์ DEAE FF™ และ Phenyl FF™ จากการตรวจสอบสมบัติพบว่าไม่มีความแตกต่างกับเอนไซม์ที่มี his-tag จึงทำการกลายพันธุ์เฉพาะตำแหน่งที่ Tyr-172 เมื่อนำเอนไซม์ และเอนไซม์กลาย (Y172A) ไปทำการตรวจสอบลักษณะสมบัติพบว่าเอนไซม์ทั้งสองชนิดมีสมบัติทางกายภาพไม่แตกต่างกัน แต่เมื่อตรวจวัดแอกทิวิตีของ disproportionation, cyclization และ hydrolytic พบว่า Y172A มีทุกแอกทิวิตีต่ำกว่าเอนไซม์ wild-type จากการศึกษาทางจลนพลศาสตร์ด้วยปฏิกิริยา disproportionation โดยใช้มอลโทโทรโอสเป็นซับสเตรต พบว่าเอนไซม์ wild-type และ Y172A มีค่า K_m เท่ากับ 19.6 และ 12.9 มิลลิโมลาร์ และค่า k_{cat} เท่ากับ 9,374 และ 2,165 นาที⁻¹ ตามลำดับ จากการตรวจสอบผลิตภัณฑ์ของปฏิกิริยา cyclization ผลิตภัณฑ์ขนาดเล็กที่สุดของทั้ง 2 เอนไซม์คือ CD19 และรูปแบบผลิตภัณฑ์ LR-CDs ขึ้นกับระยะเวลาในการบ่มและความเข้มข้นของเอนไซม์ที่ใช้ โดยเมื่อระยะเวลาในการบ่มสั้นกว่า จะได้ผลิตภัณฑ์หลักที่มีขนาดใหญ่กว่า และเอนไซม์ wild-type แสดงรูปแบบที่แตกต่างจาก Y172A คาดว่าเกิดจากการที่เอนไซม์ wild-type มีทั้งแอกทิวิตีของ transglucosylation และ hydrolytic สูงกว่า ผลที่ได้แสดงว่าตำแหน่ง Tyr-172 น่าจะมีความสำคัญในการกำหนดรูปแบบผลิตภัณฑ์

ภาควิชา.....ชีวเคมี.....ลายมือชื่อนิสิต.....

สาขาวิชา.....ชีวเคมี.....ลายมือชื่อ อ.ที่ปรึกษาวิทยานิพนธ์หลัก.....

ปีการศึกษา.....2553.....ลายมือชื่อ อ.ที่ปรึกษาวิทยานิพนธ์ร่วม.....

ลายมือชื่อ อ.ที่ปรึกษาวิทยานิพนธ์ร่วม.....

5073910523 : MAJOR BIOCHEMISTRY

KEYWORDS : LARGE-RING CYCLODEXTRIN/ AMYLOMALTASE/ SITE-DIRECTED MUTAGENESIS

WIRAYA SRISIMARAT : CHARACTERIZATION OF A NOVEL AMYLOMALTASE FROM *Corynebacterium glutamicum* ATCC 13032.
 THESIS ADVISOR: PROF. PIAMSOOK PONGSAWASDI, Ph.D.,
 THESIS CO-ADVISOR: ASST. PROF. JARUNEE KAULPIBOON, Ph.D., PROF. WOLFGANG ZIMMERMANN, Ph.D., 185 pp.


The aim of this study is to search for a novel amylomaltase and to identify residue involved in formation of cyclic oligosaccharide product. The amylomaltase gene from *Corynebacterium glutamicum* ATCC 13032 was cloned and expressed in *Escherichia coli* BL21(DE3) using the expression vector pET-19b. The ORF of amylomaltase gene, including His-tag sequence was 2,190 base pairs. The deduced amino acid sequence showed only 28-45% similarity with reported amylomaltases. The enzyme was purified by HisTrap FFTM column. The size was 84 kDa and the conditions for optimal catalysis were at pH 6.0 and 30 °C. The large-ring cyclodextrin (LR-CDs) products were from CD19 up. After purification, removal of his-tag residues resulted in total loss of enzyme activity. The amylomaltase clone was reconstructed using pET-17b. The enzyme was expressed and purified by DEAE FFTM and Phenyl FFTM columns. The basic characters obtained were similar to the enzyme with his-tag. The recombinant plasmid was then used as a template for site-directed mutagenesis at Tyr-172. Both wild-type and mutated enzyme, Y172A, had the same physical characteristics. The Y172A mutant showed lower disproportionation, cyclization and hydrolytic activity than the wild-type enzyme. In disproportionation reaction with maltotriose, kinetic parameters were determined. The K_m were 19.6 and 12.9 mM and k_{cat} were 9,374 and 2,165 min^{-1} in the wild-type and Y172A enzyme, respectively. When the cyclization products were investigated, the smallest LR-CD was CD19 from both enzymes and the product profile was dependent on the incubation time and the enzyme concentration. Shorter incubation time gave larger LR-CDs as principal products. Interestingly, the wild-type enzyme showed different product pattern from that of Y172A mutant. This might be due to higher transglucosylation and hydrolytic activity of the wild-type enzyme. These results suggested that Tyr-172 should be involved in determining LR-CDs product profile.


Department : Biochemistry

Field of Study : Biochemistry

Academic Year : 2010

Student's Signature 

Advisor's Signature 

Co-Advisor's Signature 

Co-Advisor's Signature 

ACKNOWLEDGEMENTS

I would like to express my deepest gratitude to my advisor, Professor Piamsook Pongsawasdi, for her generous advices, technical helps, guidance, attention, stimulating discussion and support throughout this thesis. Without her kindness and understanding, this work could not be accomplished.

My gratitude is also extended to Assistant Professor Jarunee Kaulpiboon and Professor Wolfgang Zimmermann for their valuable comments and insight concerning.

Sincere thanks and appreciation are due to Associate Professor Tipaporn Limpaseni, Associate Professor Teerapong Buaboocha, Assistant Professor Kanoktip Packdibamrung and Associate Professor Jarunya Narangajavana for their valuable suggestion and comments and also dedicating valuable time for thesis examination.

The Department of Biochemistry, Faculty of Science gave a support for most of chemicals and instruments. My appreciate is also expressed to staffs and students especially to Miss Nicole Weizenmann and Mr. Rene Kermer at Department of Microbiology and Bioprocess Technology, Institute of Biochemistry, University of Leipzig, Germany for HPAEC-PAD support and PD Dr. Schiller at Institute of Medical Physics and Biophysics, Faculty of Medicine, University of Leipzig, Germany for MALDI-TOF support and all staff and student in the Starch and Cyclodextrin Research Unit especially to Mr. Surachai Yaiyen.

Finally, the greatest gratitude is expressed to my parents and my family for their infinite love, encouragement, understanding and everything giving to my life.

This work was financially supported by the Royal Golden Jubilee Ph.D. Fellowship from the Thailand Research Fund. Financial supports from the Ratchadapiseksomphot Endowment Fund of Chulalongkorn University to the Starch and Cyclodextrin Research Unit and from Research Institution Partnership Grant of Alexander von Humboldt Foundation are acknowledged.

CONTENTS

	Page
THAI ABSTRACT.....	iv
ENGLISH ABSTRACT.....	v
ACKNOWLEDGEMENTS.....	vi
CONTENTS.....	vii
LIST OF TABLES.....	xiv
LIST OF FIGURES.....	xv
ABBREVIATIONS.....	xix
CHAPTER I INTRODUCTION.....	1
1.1 The 4- α -glucanotransferase (4 α GTase).....	1
1.2 The occurrence and the structure of amyloamylase.....	6
1.3 Physiological roles of amyloamylase.....	16
1.4 Application of amyloamylase.....	18
1.5 Large-ring cyclodextrins.....	19
1.6 <i>Corynebacterium glutamicum</i>	32
1.7 Objectives.....	36
CHAPTER II MATERIALS AND METHODS.....	37
2.1 Equipments.....	37
2.2 Chemicals.....	38
2.3 Enzymes, Restriction enzymes and Bacterial strains.....	41
2.4 Cloning of amyloamylase gene (<i>malQ</i>).....	42
2.4.1 Cultivation and extraction of genomic DNA from <i>Corynebacterium glutamicum</i> ATCC 13032.....	42
2.4.2 Agarose gel electrophoresis.....	43
2.4.3 Amplification of amyloamylase gene (<i>malQ</i>) using PCR technique.....	43
2.4.4 Restriction enzyme digestion.....	44
2.4.5 Ligation of the PCR product with vector pET-19b.....	44
2.4.6 Preparation of competent cells for electroporation.....	45
2.4.7 Plasmid transformation.....	45
2.5 Colony selection and primary screening.....	46
2.5.1 Plasmid size screening.....	46

	Page
2.5.2 Plasmid extraction.....	46
2.5.3 Nucleotide sequencing.....	47
2.6 Site-directed mutagenesis.....	47
2.7 Optimization for amyломaltase gene expression.....	48
2.8 Purification of amyломaltase enzyme.....	49
2.8.1 Starter inoculum.....	49
2.8.2 Cells cultivation and crude extract preparation.....	49
2.8.3 Purification of recombinant wild-type amyломaltase with his-tag residues (p19AM).....	50
2.8.4 Purification of recombinant wild-type amyломaltase (p17AM) and Y172A mutated amyломaltase.....	51
2.8.4.1 DEAE FF™ column chromatography.....	51
2.8.4.2 Phenyl FF™ column chromatography.....	51
2.9 Enzyme assay.....	52
2.9.1 Starch degrading activity.....	52
2.9.2 Starch transglucosylation activity.....	52
2.9.3 Disproportionation activity.....	53
2.9.4 Cyclization activity.....	53
2.9.5 Hydrolytic activity.....	54
2.9.6 Coupling activity.....	54
2.9.6.1 Using DNS reagent.....	54
2.9.6.2 Using bichinonic acid assay.....	55
2.9.6.3 Using glucose oxidase assay.....	55
2.9.6.4 Using HPAEC-PAD analysis.....	56
2.10 Protein determination.....	56
2.11 Polyacrylamide gel electrophoresis (PAGE).....	56
2.11.1 SDS-polyacrylamide gel electrophoresis (SDS-PAGE)...	56
2.11.2 Non-denaturing polyacrylamide gel electrophoresis (Native-PAGE).....	57
2.11.3 Detection of protein bands.....	57
2.11.3.1 Coomassie blue staining.....	57

	Page
2.16 Mass spectrometry (MS).....	65
CHAPTER III RESULTS.....	66
3.1 Identification and expression of amyloamylase gene (<i>malQ</i>) from <i>Corynebacterium glutamicum</i> ATCC 13032.....	66
3.1.1 Extraction of chromosomal DNA.....	66
3.1.2 <i>malQ</i> amplification and preparation.....	66
3.1.3 Transformation.....	66
3.1.4 Nucleotide sequencing.....	69
3.1.5 Expression of amyloamylase gene.....	80
3.1.6 Protein pattern of cells.....	80
3.2 Purification of amyloamylase from the recombinant clone harboring p19AM.....	83
3.2.1 Preparation of crude extract.....	83
3.2.2 HisTrap FF™ column chromatography.....	83
3.2.3 Determination of enzyme purity by SDS and Native- PAGE.....	86
3.3 Characterization of amyloamylase from the recombinant clone harboring p19AM.....	86
3.3.1 Molecular weight determination of amyloamylase.....	86
3.3.2 Effect of temperature on amyloamylase starch transglucosylation activity and stability.....	86
3.3.3 Effect of pH on amyloamylase starch transglucosylation activity and stability.....	90
3.3.4 Transglucosylation reaction of amyloamylase.....	90
3.3.5 The synthesis of large-ring cyclodextrins.....	93
3.4 Construction and expression of recombinant wild-type and Y172A mutated amyloamylase.....	98
3.4.1 Extraction of plasmid DNA.....	98
3.4.2 Transformation.....	98
3.4.3 Nucleotide sequencing.....	100
3.4.4 Site-directed mutagenesis at Y172A of amyloamylase.....	100
3.4.5 Expression of amyloamylase gene.....	101

	Page
3.5 Purification of amyloamylase from the recombinant clone harboring p17AM and Y172A mutant.....	101
3.5.1 Preparation of crude extract.....	101
3.5.2 DEAE FF TM column chromatography.....	101
3.5.3 Phenyl FF TM column chromatography.....	103
3.5.4 Determination of enzyme purity by SDS and Native-PAGE.....	106
3.6 Characterization of amyloamylase from recombinant clone p17AM and Y172A mutant.....	112
3.6.1 Molecular weight determination.....	112
3.6.2 Effect of temperature on starch transglucosylation activity and stability.....	112
3.6.3 Effect of pH on starch transglucosylation activity and stability.....	112
3.6.4 Determination of pI of amyloamylase.....	115
3.6.5 Transglucosylation reaction of amyloamylase.....	115
3.6.6 Activities of the recombinant wild-type and Y172A mutated amyloamylase.....	115
3.6.7 Substrate specificity.....	119
3.6.8 Determination of kinetic parameters.....	119
3.6.9 Time course of hydrolysis reaction.....	121
3.6.10 The synthesis of large-ring cyclodextrins.....	124
3.6.11 Analysis of large-ring cyclodextrins by MALDI-TOF....	129
CHAPTER IV DISCUSSIONS.....	133
4.1 Identification of amyloamylase gene from <i>Corynebacterium glutamicum</i>	133
4.2 Expression of amyloamylase from the recombinant clone harboring p19AM.....	135
4.3 Purification of amyloamylase from the recombinant clone harboring p19AM.....	136
4.4 Characterization of amyloamylase from the recombinant clone with p19AM.....	138

	Page
4.4.1 Molecular weight determination.....	138
4.4.2 Effect of temperature on starch transglucosylation activity and stability.....	138
4.4.3 Effect of pH on starch transglucosylation activity and stability.....	139
4.4.4 Transglucosylation reaction.....	139
4.4.5 The synthesis of large-ring cyclodextrins.....	140
4.5 Construction and expression of recombinant wild-type and Y172A mutated enzyme.....	141
4.6 Purification of amyломaltase from the recombinant clone harboring p17AM and Y172A mutant.....	142
4.7 Characterization of amyломaltase from the recombinant clone with p17AM and Y172A mutant.....	143
4.7.1 Molecular weight determination.....	143
4.7.2 Effect of pH and temperature on starch transglucosylation activity and stability.....	143
4.7.3 Determination of pI	144
4.7.4 Measurement of activities.....	144
4.7.5 Substrate specificity.....	146
4.7.6 Kinetic study.....	147
4.7.7 The synthesis of large-ring cyclodextrins.....	148
4.7.8 Analysis of large-ring cyclodextrins by MALDI-TOF.....	149
CHAPTER V CONCLUSIONS.....	151
REFERENCES.....	153
APPENDICES.....	168
Appendix1 Preparation for SDS-polyacrylamide gel electrophoresis....	169
Appendix 2 Preparation for native-polyacrylamide gel electrophoresis..	172
Appendix 3 Preparation for isoelectric focusing (IEF).....	174
Appendix 4 Preparation for iodine solution.....	176
Appendix 5 Preparation for bicinchoninic acid assay.....	177
Appendix 6 Preparation for DNS reagent.....	178

	Page
Appendix 7 Standard curve for protein determination by Bradford's method.....	179
Appendix 8 Standard curve for starch determination by starch degrading assay.....	180
Appendix 9 Standard curve for glucose determination by glucose oxidase assay.....	181
Appendix 10 Standard curve for glucose determination by bicinchoninic acid assay.....	182
Appendix 11 Restriction map of pET-19b.....	183
Appendix 12 Restriction map of pET-17b.....	184
BIOGRAPHY.....	185



ศูนย์วิทยทรัพยากร
จุฬาลงกรณ์มหาวิทยาลัย

LIST OF TABLES

Table		Page
1.1	Enzyme belonging to the α -amylase family and four highly conserved regions.....	3
1.2	Possible effects of the formation of inclusion complexes on properties of guest molecules.....	26
1.3	Physicochemical properties of small- and large-ring CDs	27
1.4	Studies of inclusion complex formation between LR-CD or mixture of LR-CDs and different guest compounds	29
3.1	Percent similarity of deduced amino acid sequence of recombinant amyloamylase from <i>Corynebacterium glutamicum</i> ATCC 13032 compared with other 4 α GTases.	79
3.2	Purification of amyloamylase from the recombinant clone harboring p19AM.....	85
3.3	Purification of the recombinant wild-type amyloamylase (p17AM)...	108
3.4	Purification of Y172A mutated amyloamylase.....	108
3.5	Activity of the recombinant wild-type and Y172A mutated amyloamylase.....	118
3.6	Kinetic parameters of the recombinant wild-type and Y172A mutated amyloamylase from disproportionation reaction with maltotriose as substrate.....	122
3.7	The effect of amount of enzyme and incubation time on formation of principal large-ring cyclodextrin products of the wild-type and Y172A mutated amyloamylase.....	130

LIST OF FIGURES

Figure		Page
1.1	Different enzymes involved in the degradation of starch.....	2
1.2	Schematic representation of the 4 α GTase catalyzed reactions.....	5
1.3	Structure of the fold of (a) <i>Bacillus circulans</i> CGTase and (b) <i>Thermus aquaticus</i> amyломaltase binding with acarbose.....	8
1.4	Molecular surfaces of (a) α -amylase isozyme II of porcine pancreas in complex with a maltohexaose (part of a larger inhibitor); (b) CGTase from <i>Bacillus circulans</i> strain 8 complexed with β -cyclodextrin derivative and (c), (d) amyломaltase from <i>Thermus aquaticus</i> with a modeled binding mode of a maltohexaose.....	10
1.5	Scheme of the interactions of acarbose bound to the catalytic site of amyломaltase from <i>Thermus aquaticus</i>	13
1.6	Scheme of the interaction of acarbose bound to the secondary binding site of amyломaltase from <i>Thermus aquaticus</i>	15
1.7	Roles of 4 α GTase in glucan utilization by bacteria.....	17
1.8	Comparison of traditional and newly improved processes for IMOs production.....	20
1.9	Structure of small-ring CDs (α , β , and γ).....	21
1.10	Schematic representation in top and side views of the molecular structures of CD9, CD10 and CD14, to show the distortions associated with increasing in ring sized of the large-ring cyclodextrins	22
1.11	Structure of the asymmetric unit of the crystalline complex of CD9 with cycloundecanone.....	25
1.12	Solid state structure of CD26.....	26
1.13	History of amino acid fermentation and strain development technology of <i>Corynebacterium glutamicum</i>	33
1.14	Circular representative of the <i>Corynebacterium glutamicum</i> ATCC 13032 chromosome.....	35

Figure	Page
3.1	Agarose gel electrophoresis of genomic DNA of <i>Corynebacterium glutamicum</i> ATCC 13032..... 67
3.2	Agarose gel electrophoresis of amplified DNA..... 68
3.3	Agarose gel electrophoresis of recombinant <i>malQ</i> inserted in pET-19b vector..... 70
3.4	Nucleotide and deduced amino acid sequences of amyломaltase from <i>Corynebacterium glutamicum</i> ATCC 13032..... 71
3.5	Amino acid sequence alignment of amyломaltase from <i>Corynebacterium glutamicum</i> ATCC 13032 (CG) compared with amyломaltase from <i>Thermus aquaticus</i> (TA) using Stretcher program..... 74
3.6	Amino acid sequence alignment of amyломaltase from <i>Corynebacterium glutamicum</i> ATCC 13032 (CG) compared with amyломaltase from <i>Thermus thermophilus</i> (TT) using Stretcher program..... 75
3.7	Amino acid sequence alignment of amyломaltase from <i>Corynebacterium glutamicum</i> ATCC 13032 (CG) compared with amyломaltase from <i>Aquifex aeolicus</i> (AA) using Stretcher program..... 76
3.8	Amino acid sequence alignment of amyломaltase from <i>Corynebacterium glutamicum</i> ATCC 13032 (CG) compared with amyломaltase from potato <i>Solanum tuberosum</i> (PT) using Stretcher program..... 77
3.9	Amino acid sequence alignment of amyломaltase from <i>Corynebacterium glutamicum</i> ATCC 13032 (CG) compared with amyломaltase from <i>Escherichia coli</i> K12 (EC) using Stretcher program..... 78
3.10	Expression of p19AM in <i>E.coli</i> BL21(DE3) at 0.4 mM IPTG..... 81
3.11	SDS-PAGE of whole cell suspensions of p19AM clone induced by 0.4 mM IPTG at various times..... 82
3.12	Purification profile of amyломaltase from the recombinant clone harboring p19AM by HisTrap FF TM column chromatography..... 84

Figure	Page
3.13	Molecular weight determination of amyloamaltase..... 87
3.14	Native-PAGE of purified amyloamaltase of the recombinant clone (p19AM) incubated with soluble starch substrate and stained with iodine solution..... 88
3.15	Effect of temperature on starch transglucosylation activity and stability..... 89
3.16	Effect of pH on amyloamaltase starch transglucosylation activity and stability..... 91
3.17	TLC chromatogram of the reaction products of amyloamaltase incubated with maltooligosaccharides..... 92
3.18	HPAEC analysis of large-ring cyclodextrins synthesized by amyloamaltase at different incubation time..... 94
3.19	HPAEC analysis of large-ring cyclodextrins synthesized by amyloamaltase at different amount of enzyme..... 97
3.20	Agarose gel electrophoresis of recombinant <i>malQ</i> inserted in pET-17b vector..... 99
3.21	Purification profile of wild-type amyloamaltase from recombinant clone (p17AM) by DEAE FF TM column chromatography..... 102
3.22	Purification profile of Y172A mutated amyloamaltase by DEAE FF TM column chromatography..... 104
3.23	Purification profile of wild-type amyloamaltase from recombinant clone (p17AM) by Phenyl FF TM column chromatography..... 105
3.24	Purification profile of Y172A mutated amyloamaltase by Phenyl FF TM column chromatography..... 107
3.25	SDS-PAGE of the recombinant wild-type (p17AM) from each purification step..... 109
3.26	SDS-PAGE of the Y172A mutated amyloamaltase from each purification step..... 110
3.27	Native-PAGE of the purified amyloamaltase from recombinant wild-type (p17AM) and Y172A mutant incubated with soluble starch substrate and stained with iodine solution..... 111

Figure	Page
3.28	Calibration curve for molecular weight of recombinant wild-type and Y172A mutated amyloamylase by SDS-PAGE..... 113
3.29	Calibration curve for molecular weight of recombinant wild-type and Y172A mutated amyloamylase by gel filtration on Sephacryl S-200 column..... 114
3.30	Isofocusing polyacrylamide gel electrophoresis of recombinant wild-type and Y172A mutated amyloamylase..... 116
3.31	Calibration curve of standard pI markers..... 117
3.32	Substrate specificity of recombinant wild-type amyloamylase (p17AM) in disproportionation reaction..... 120
3.33	Substrate specificity of Y172A mutated amyloamylase in disproportionation reaction..... 120
3.34	Lineweaver-Burk plot of recombinant wild-type and Y172A mutated amyloamylase on disproportionation reaction with maltotriose..... 122
3.35	Glucose released at various time points..... 123
3.36	Profiles of large-ring cyclodextrin products at different incubation time as analyzed by HPAEC-PAD..... 125
3.37	Profiles of large-ring cyclodextrin products at different amount of recombinant amyloamylase as analyzed by HPAEC-PAD..... 127
3.38	HPAEC analysis of the larger-scale production of large-ring cyclodextrins..... 131
3.39	Mass spectra of mixture of large-ring cyclodextrin products..... 132

ABBREVIATIONS

A	absorbance
bp	basepair
BSA	bovine serum albumin
°C	degree Celsius
CDs	cyclodextrins
CAs	cycloamyloses
CGTase	cyclodextrin glycosyltransferase
cm	centrimeter
Da	dalton
D-enzyme	disproportionation enzyme
DP	degree of polymerization
g	gram
GH	glycoside hydrolases family
4 α GTase	4- α -glucanotransferase
h	hour
IMOs	isomaltooligosaccharides
kb	kilobase
kDa	kilodalton
l	litre
μ l	microlitre
LR-CDs	large-ring cyclodextrins
M	molar

mA	milliampere
min	minute
mg	milligram
ml	millilitre
mM	millimolar
MW	molecular weight
n.d.	not detectable
nC	nanocoulomb
nm	nanometer
R _f	relative mobility
R _t	retention time
rpm	revolution per minute
µg	microgram
µM	micromolar
U	unit
V	volt

ศูนย์วิทยทรัพยากร
จุฬาลงกรณ์มหาวิทยาลัย

CHAPTER I

INTRODUCTION

1.1 The 4- α -glucanotransferase (4 α GTase)

Starch is a major product of many economically important crops such as wheat, rice, maize, tapioca and potato. A large-scale starch processing industry has emerged in the last century. In the past decades, the productions of maltodextrin, modified starch and glucose have been changed from the acid hydrolysis of starch to the use of starch-converting enzymes. A large variety of bacteria employ extracellular or intracellular enzymes able to convert starch or glycogen that serves as energy and carbon sources for the cells (Figure 1.1). Besides the use in starch industry, starch-converting enzymes are also used in several other industrial applications, such as laundry and dish detergents or as anti-staling agent in baking. (van der Maarel *et al.*, 2002).

The α -amylase family consists of a number of carbohydrate-metabolizing enzymes which fulfill the following requirements: (i) act on α -glucosidic linkage; (ii) hydrolyze α -glucosidic linkages to produce α -anomeric mono- and oligo-saccharides or form α -glucosidic linkages by transglycosylation reaction; (iii) have four conserved regions in their primary structures which contain all the catalytic and most of the important substrate-binding sites; and (iv) have 2 Asp and Glu residues as catalytic sites (Table 1.1) (Takata *et al.*, 1992; Kuriki *et al.*, 2006). The family includes extensively studied enzymes such as α -amylase (EC 3.2.1.1), isoamylase (EC 3.2.1.68), pullulanase (EC 3.2.1.41), α -glucosidase (EC 3.2.1.20) and cyclomaltodextrin glucano (glycosyl) transferase (CGTase, EC 2.4.1.19).

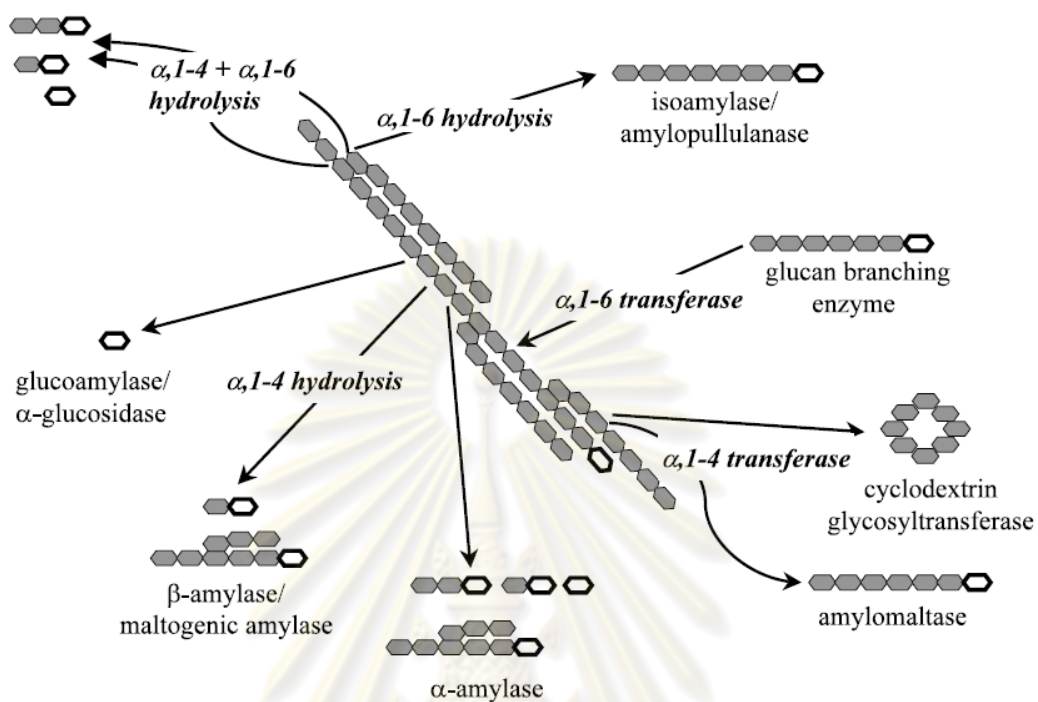


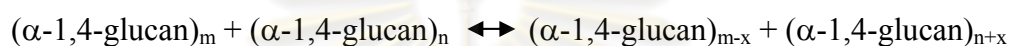
Figure 1.1 Different enzymes involved in the degradation of starch. The open ring structure symbolizes the reducing end of a glucan molecule. (van der Maarel *et al.*, 2002)

ศูนย์วิทยทรัพยากร
จุฬาลงกรณ์มหาวิทยาลัย

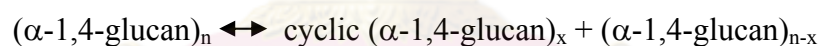
Table 1.1 Enzymes belonging to the α -amylase family and four highly conserved regions. The three invariable catalytic sites are highlighted. Numbering of amino acid starts at the amino-terminal end of each enzyme. (Modified from van der Maarel *et al.*, 2002 and Kuriki *et al.*, 2006)

Enzyme	Origin	Region 1	Region 2	Region 3	Region 4	Accession No.
α -amylase	<i>Aspergillus oryzae</i>	117DVVANH	202GLRIDTVKH	230EVLD	292FVENHD	1506277A
CGTase	<i>Bacillus macerans</i>	135DFAPNH	225GIRFDAVKH	258EWFL	324FIDNHD	P31835
Pullulanase	<i>Klebsiella aerogenes</i>	600DVVYNH	671GFRFDLMGY	704EGWD	827YVSKHD	P07811
Isoamylase	<i>Pseudomonas amyloclavata</i>	292DVVYNH	371GFRFDLASV	435EPWA	505FIDVHD	AAA25855
Branching enzyme	<i>Escherichia coli</i>	335DWVPGH	401ALRVDASV	458EEST	521LPLSHD	ACI76450
Neopullulanase	<i>Bacillus stearothermophilus</i>	242DAVFNH	324GWRLDVANE	357EIIWH	419LLGSHD	AAK15003
Amylopullulanase	<i>Thermoanaerobacter ethanolicus</i>	487DGVFNH	593GWRLDVANE	626ELWG	698LLGSHD	P38939
α -glucosidase	<i>Saccharomyces cerevisiae</i>	106DLVINH	210GFRIDTAGL	276EVAH	344YIENHD	P07265
Oligo-1,6-glucosidase	<i>Bacillus cereus</i>	98DLVVNH	195GFRMDVINP	255EMPG	324YWNNHD	P21332
Dextran glucosidase	<i>Streptococcus mutans</i>	98DLVVNH	190GFRMDVIDM	236ETWG	308FWNNHD	AAA26939
Amylomaltase	<i>Thermus aquaticus</i>	213DMPIFV	289LVRIIDHFRG	340EDLG	390YTGTHTD	O87172
Glycogen debranching enzyme	<i>Homo sapiens</i>	298DVVYNH	504GVRLDNCHS	534ELFT	603MDITHD	NP_000019
Amylosucrase	<i>Neisseria polysaccharea</i>	190DFIFNH	290ILRMDAVAF	336EAIIV	396YVRSHD	CAA09772

Amylomaltase (EC 2.4.1.25), an intracellular 4- α -glucanotransferase (4 α GTase), is also a member of α -amylase family. The 4 α GTase group composes of 4 types of enzyme: CGTase (Type I), amylomaltase or D-enzyme (in plant) (Type II), glycogen debranching enzyme (Type III) and other 4 α GTases (Type IV). This group of enzymes catalyzes the transfer of a part of α -1,4-D-glucan from a donor to an acceptor molecule, such as glucose or another α -1,4-glucan with a free 4-hydroxyl group as shown in the following equation,



This is an inter-molecular transglycosylation reaction, and is often referred to as a disproportionation reaction. CGTase and amylomaltase can also catalyze an intramolecular glucan transfer reaction within a single linear glucan molecule (cyclization reaction) to produce a cyclic α -1,4-glucan (cycloamylose, CA, or so called cyclodextrin, CD), as follows:



This reaction is reversible, by a reaction called coupling. In addition to these three reactions as described, both CGTase and amylomaltase also show a weak hydrolytic activity (Takaha and Smith, 1999). All these reactions can be summarized as shown in Figure 1.2.

จุฬาลงกรณ์มหาวิทยาลัย

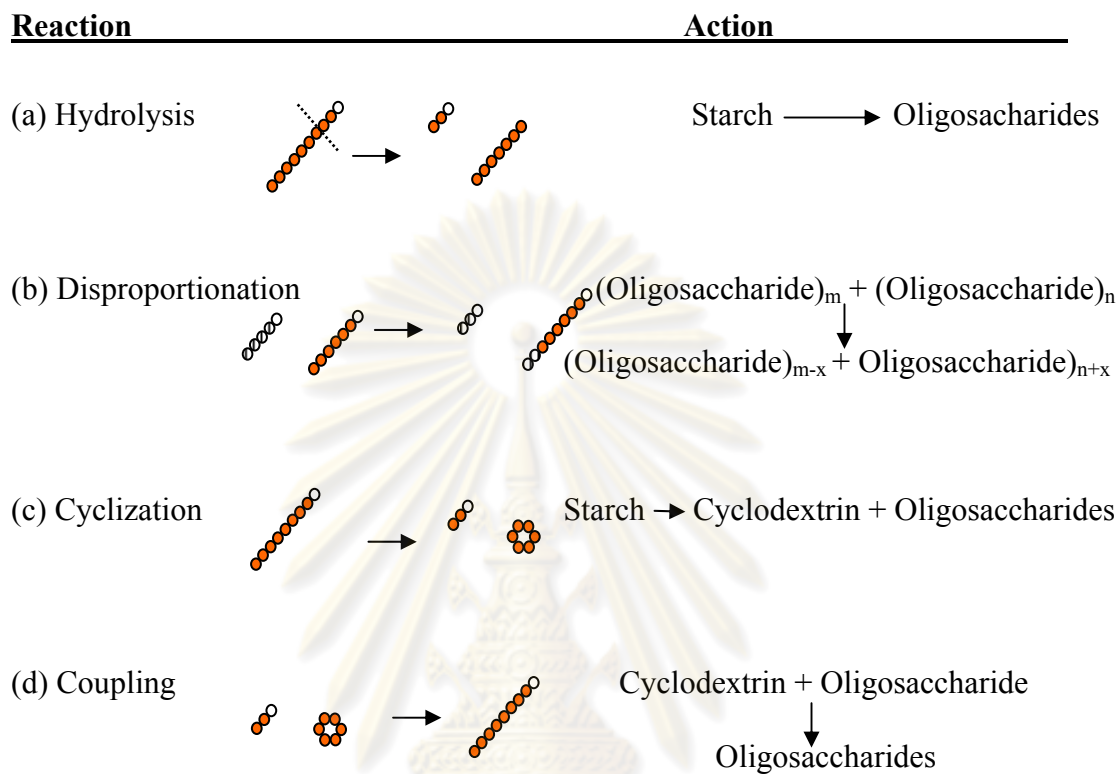


Figure 1.2 Schematic representation of the $4\alpha\text{GTase}$ catalyzed reactions. The circles represent glucose residues; the white circles indicate the reducing end sugars. (a) hydrolysis; (b) disproportionation; (c) cyclization; (d) coupling reaction (van der Veen *et al.*, 2000)

ศูนย์วิทยทรัพยากร
จุฬาลงกรณ์มหาวิทยาลัย

1.2 The occurrence and the structure of amyloamylase

Amyloamylases have been studied in various sources. In microorganisms, amyloamylase was first found in *Escherichia coli* as a maltose-inducible enzyme which is essential for the metabolism of maltose (Monod and Torriani, 1984). The amyloamylase gene has been cloned from *Streptococcus pneumoniae* (Stassi *et al.*, 1981), *E. coli* (Pugsley and Dubreuil, 1988), *Clostridium butyricum* NCIMB 7423 (Goda *et al.*, 1997), hyperthermophilic archaeon *Thermococcus litoralis* (Jeon *et al.*, 1997), *Thermus aquaticus* ATCC 33923 (Terada *et al.*, 1999), *Aquifex aeolicus* (Bhuiyan *et al.*, 2003), *Pyrobaculum aerophilum* IM2 (Kaper *et al.*, 2005) and *Thermus brockianus* (Bo-young *et al.*, 2006). In plant, this enzyme is comparable to disproportionation enzyme or D-enzyme which has been reported to be involved in starch metabolism (Lütken *et al.*, 2010). D-enzyme was first found in potato tuber (Peat *et al.*, 1956), carrot roots (Manner and Rowe, 1969), tomato fruits (Manner and Rowe, 1969), germinated barley seed (Yoshio *et al.*, 1986), pea leaves (Kakefuda and Duke, 1989) and *Arabidopsis* leaves (Lin and Preiss, 1988).

Although amyloamylase and CGTase catalyze similar reactions as mentioned, the two enzymes are different in both structure and function. Amyloamylase and CGTase differ in cycloamylose production properties. Main products of CGTase are small-ring CDs which are composed of glucose with a degree of polymerization (DP) of 6-8 units (α , β , γ -CD, respectively), but main products of amyloamylase are large-ring CDs (LR-CDs) consisted of glucose with DP of 16 up (Takaha and Smith, 1999, Bhuiyan *et al.*, 2003). For the structural difference, amyloamylases have been classified as part of glycoside hydrolase family 77 (GH77) (based on amino acid sequence similarities), while the enzyme α -amylases and CGTases are parts of GH13. GH77 enzyme is efficient 4- α -glucanotransferase and exhibits remarkably low

hydrolytic activities that are at least one order of magnitude lower than that of CGTases of GH13 (van der Maarel *et al.*, 2002; Kaper *et al.*, 2007).

From a number of reported amyloamylase genes that have been cloned, only a few have been studied at the level of enzyme and production of LR-CDs e.g. *E. coli* K12 (Takaha and Smith, 1999), *Thermus aquaticus* ATCC 33923 (Terada *et al.*, 1999), *Aquifex aeolicus* (Bhuiyan *et al.*, 1999) and *Synechocystis* sp. PCC 6803 (Lee *et al.*, 2009). In addition, only five amyloamylases have been determined for their X-ray structures: *T. aquaticus* (1esw) (Przylas *et al.*, 2000), *T. thermophilus* (2owx, 2owc, 2oww) (Barends *et al.*, 2007), *T. thermophilus* HB8 (1fp8) (Uitdehaag *et al.*, 2000), *A. aeolicus* (1tz7) (Barends *et al.*, 2004) and *T. brockianus* (Jung *et al.*, 2010). Structurally, amyloamylase contains several insertions between the strands of the central ($\beta\alpha$)₈-barrel localized in domain A. All insertions are presented at the C-terminal side of the barrel, where the substrate binding site also is located. These insertions are divided into three subdomains (subdomain B1, B2, and B3), in order to facilitate comparison to related enzymes (Figure 1.3b). The insertions between the third and fourth barrel strand of the central barrel (domain A) and between the fourth and fifth strand build subdomain B1. Subdomain B2 consists of a large insertion between the second and third barrel strand. The remaining insertions, between the first and second strand, between the seventh and eighth strand and after the eighth barrel strand build subdomain B3. Thus, subdomains B1-B3 form an almost continuous ring around the C-terminal edge of the barrel and might participate in binding the large amylose substrates (Przylas *et al.*, 2000; Sträter *et al.*, 2002).

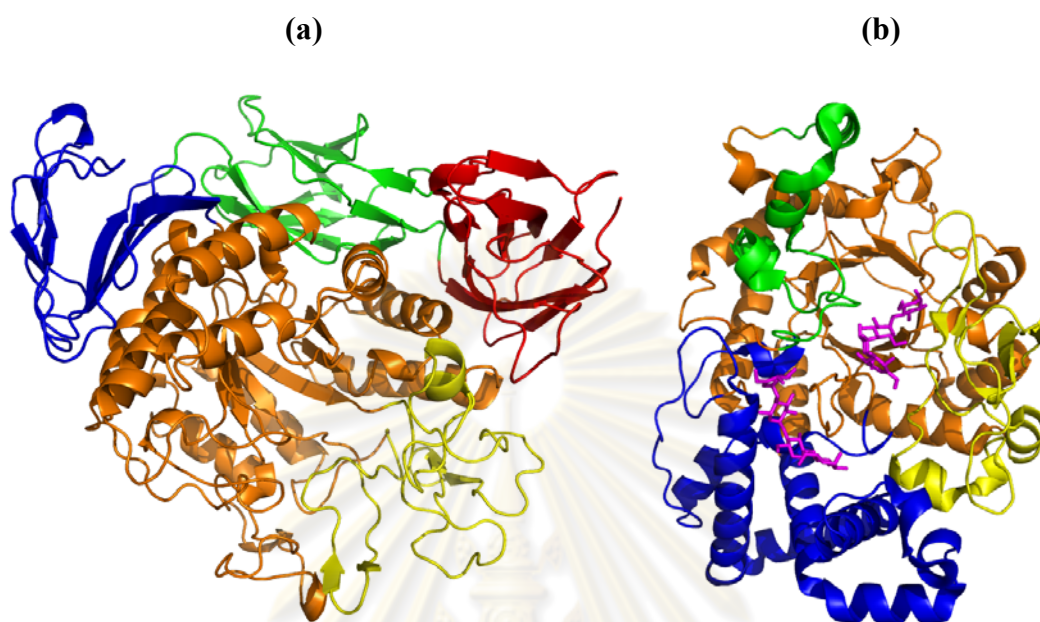


Figure 1.3 Structure of the fold of (a) *Bacillus circulans* CGTase and (b) *Thermus aquaticus* amyloamylase binding with acarbose. Domain A, B, C, D and E of CGTase are shown in the orange, yellow, blue, green and red, respectively. Domain A, subdomain B1, B2 and B3 of amyloamylase are shown in the orange, yellow, blue and green, respectively. The acarbose molecules are displayed as stick model in (b).

ศูนย์วิทยทรัพยากร
จุฬาลงกรณ์มหาวิทยาลัย

Subdomain B1 corresponds to domain B in CGTase and the related α -amylase family enzymes (Figure 1.3). In amyloamylase, the insertion between the fourth and the fifth strand are part of subdomain B1, whereas in CGTase and the related α -amylase, the insertion between the second and third strand complete domain B. In fact, amyloamylase also contains the insertion between the second and third strand (subdomain B2). This insertion, however, is considerably larger in amyloamylase and mainly α -helical. Subdomain B2 is unique to amyloamylase. The most difference between amyloamylase and CGTase is the absence of domain C. When the amyloamylase structure is superimposed onto CGTase, subdomain B3 of amyloamylase is located at approximately the same position as domain C in CGTase (Sträter *et al.*, 2002).

To characterize topographical difference which might be responsible for the reaction specificity and for the product ring size, the amyloamylase structure was compared with those of an α -amylase and CGTase for which enzyme-substrate complexes have been structurally characterized: pig pancreatic α -amylase isozyme II bound to a linear maltooligosaccharide derivative (Machius *et al.*, 1996) and a *Bacillus circulans* CGTase bound to a β -cyclodextrin derivative (Schmidt *et al.*, 1998) (Figure 1.4). The α -amylase has a relatively open active site cleft, which is formed by residues of domain A and B (Figure 1.4a). In CGTase, domain A and B also forms part of the active site pocket (Figure 1.4b). In a co-crystal structure with β -cyclodextrin derivative, a tyrosine or phenylalanine side chain (e.g. Tyr-195 in CGTase from *Bacillus circulans* strain 8) from domain B is oriented nearly perpendicular to the plane defined by the cyclodextrin ring (Figure 1.4b). This hydrophobic side chain has been shown to affect the cyclization reaction and it has been proposed to favor the synthesis of cyclodextrins by forming a non-polar core

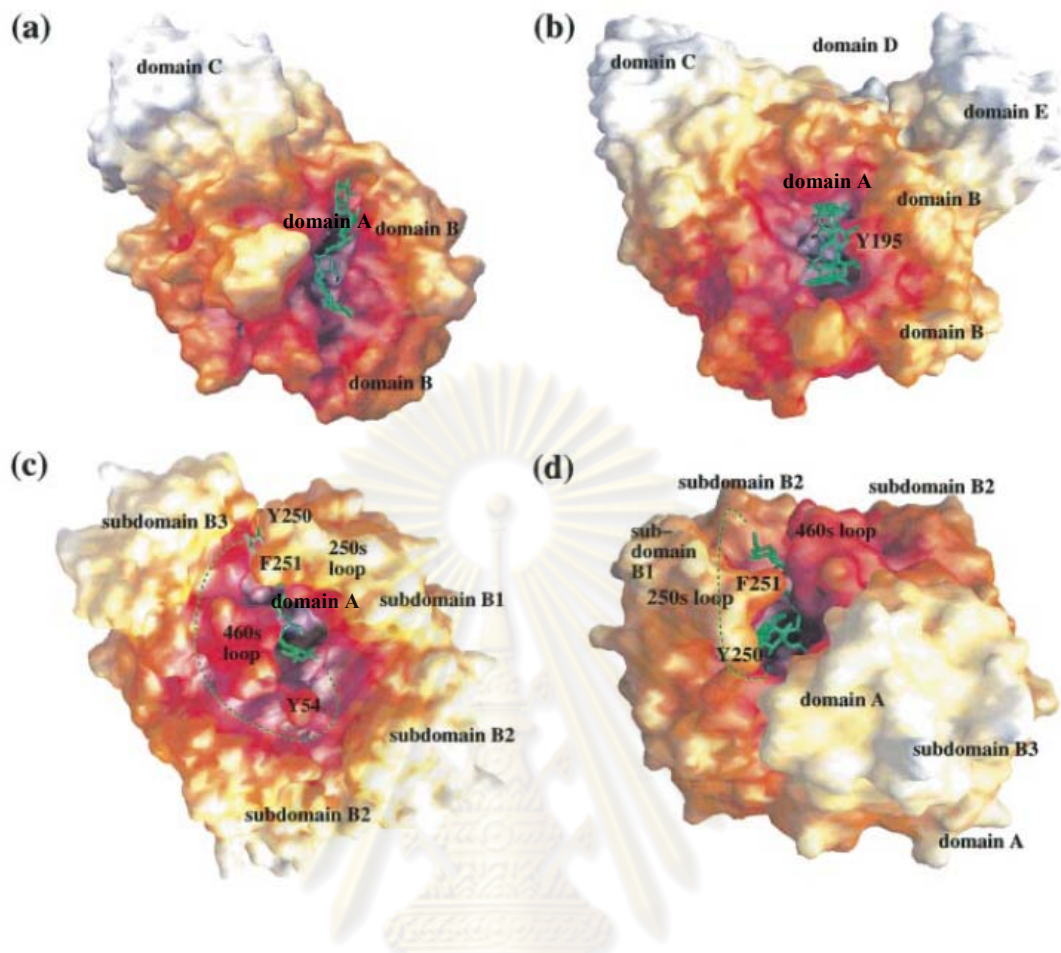


Figure 1.4 Molecular surfaces of (a) α -amylase isozyyme II of porcine pancreas in complex with a maltohexaose (part of a larger inhibitor) (Machius *et al.*, 1996); (b) CGTase from *Bacillus circulans* strain 8 complexed with β -cyclodextrin derivative (Schmidt *et al.*, 1998) and (c), (d) amylomaltase from *Thermus aquaticus* with a modeled binding mode of a maltohexaose. The surfaces are colored according to the distance to the center of mass. The domains, subdomains and two loops, the 250s loop and the 460s loops, are labeled. The bound or modeled inhibitors are shown in green. Possible binding paths for a cycloamylose product to amylomaltase are indicated as broken green line in (c) and (d). The active center of amylomaltase is located at the center of the modeled oligosaccharide in (c) and (d). (Przylas *et al.*, 2000)

around which the α -glucan could wrap (Nakamura *et al.*, 1994; Penninga *et al.*, 1995). The tyrosine or phenylalanine residue is part of domain B and is replaced by glycine, serine or valine residue in α -amylases. A tryptophan residue (Trp-258) is near this residue in amylomaltase, which might have a similar function. In amylomaltase the active-site cleft is partially covered by a long extended loop (250s loop) formed by residues 247-255 between subdomain B1 (Figure 1.4c and 1.4d). Two hydrophobic side chains, Tyr-250 and Phe-251, are located at the tip of the loop and point toward subdomain B3. This loop might be important for binding of substrates and dissociation of products (Figure 1.4d). On the other side of the active site groove, the loop between 460s loop and Tyr-54 derived from the loop might restrict the formation of smaller cyclic products (Figure 1.4c) (Przylas *et al.*, 2000; Sträter *et al.*, 2002)

The co-crystal structure of *T. aquaticus* amylomaltase with acarbose (Przylas *et al.*, 2000) demonstrated that acarbose molecule bound at two binding sites, the catalytic site and the second binding site. All amylomaltase have seven conserved residues in their structures: the three catalytic residues Asp-293, Glu-340 and Asp-395 and residues Tyr-59, Asp-213, Arg-291 and His-394 (numbering in amylomaltase of *T. aquaticus*). These seven residues build up the core of the catalytic cleft. Except for Tyr-59, they are part of the four conserved motifs of family 13. The presence of these core residues except for Tyr-59 is also found in CGTase and α -amylase, this supports a similar reaction mechanism for amylomaltase and other enzymes of this family, as previously indicated by homologous signature of the amino acid sequences. A mechanism involving a covalent intermediate, Glu-340 protonates the glycosidic oxygen atom of the scissile bond and a planar oxocarbenium-like transition state is formed. The Asp-293 is the nucleophile which attacks the C1 atom of the substrate under formation of the covalent intermediate. The Asp-395 presumably exerts strain

on the substrate in the Michaelis complex and specifically stabilizes the planar oxocarbenium-like transition state (Uitdehaag *et al.*, 1999). Obviously, the environment of the three acidic residues plays an important role in governing reaction specificity.

For the other four additional conserved amino acid residues of amylomaltase (Tyr-59, Asp-213, Arg-291 and His-394), they are also part of catalytic cleft. From 3D structure of amylomaltase, catalytic site is divided into subsites. The tyrosine residue in the catalytic subsite -1 (Figure 1.5) helps to orientate the sugar by forming a stacking interaction with the hexose ring, while His-394 and Arg-291 interact with the O2 atom of the substrate hexose in the -1 subsite. Asp-213 is part of a hydrogen bonding network that shows some flexibility in the substrate-bound and intermediate structure (Uitdehagg *et al.*, 1999).

As has been previously noticed on the basis of sequence comparisons, the histidine residue of the first conserved region (His-122 of α -amylase, Table 1.1), which is conserved in most other α -amylase family members, is not presented in amylomaltase. In addition, the co-crystal structure with acarbose was that the acarviosine moiety was not bound to substrate -1 and +1, as in the related family 13 enzymes (the glycosidic linkage is broken between subsites -1 and +1). Instead, the inhibitor occupies subsites -3 to +1 of the active center (Figure 1.5) (Sträter *et al.*, 2002).

In the co-crystal structure of amylomaltase with acarbose, a second glucan binding site which is located in a groove close to the active center was suggested. The distance between the reducing end of the maltotetraose part and the non-reducing end of the substrate analog bound to the active site is ~ 14 Å. Hydrophobic contacts of Tyr-

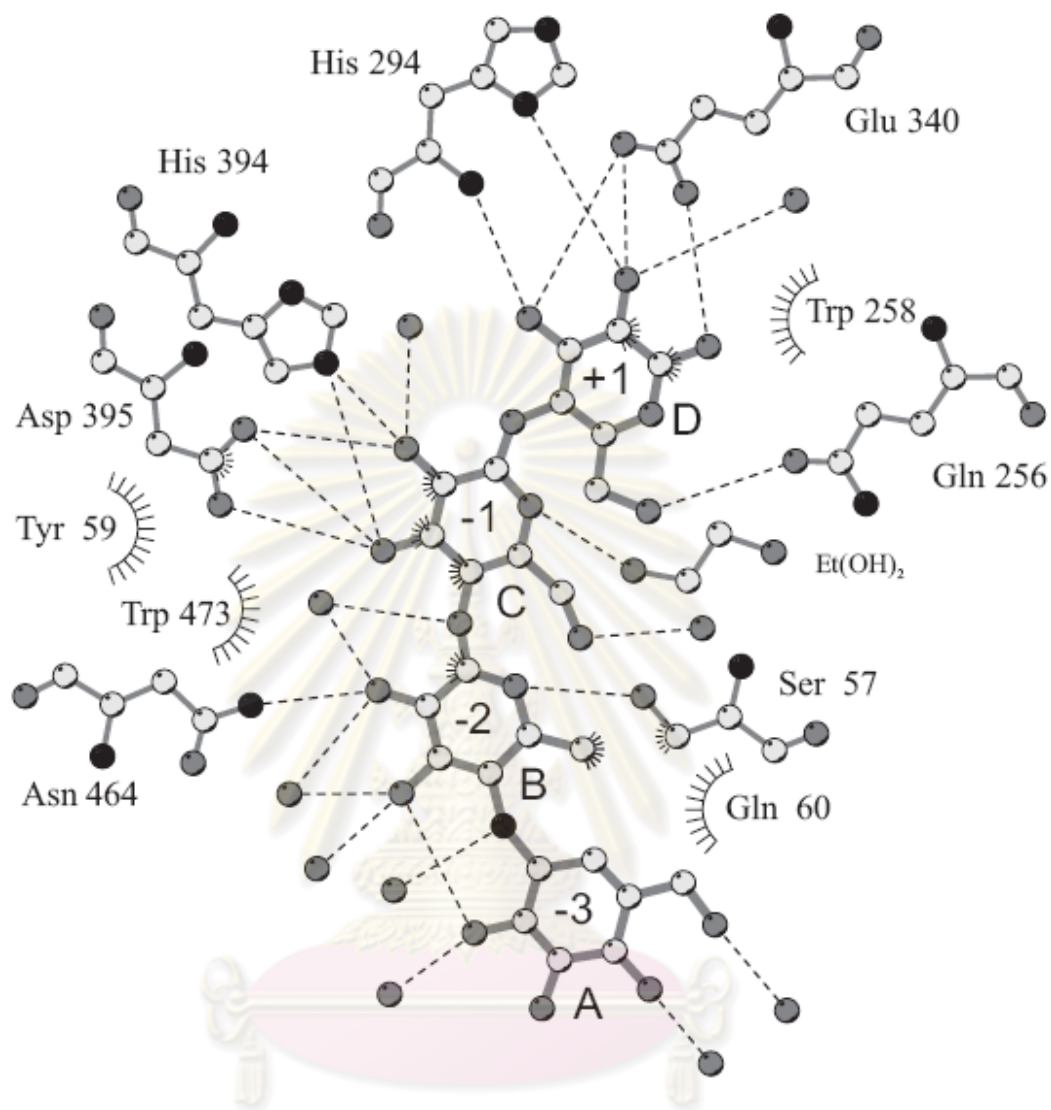


Figure 1.5 Scheme of the interactions of acarbose bound to the catalytic site of amyloamylase from *T. aquaticus*. Hydrogen bonds of less than 3.5 Å are shown as dashed lines. (Sträter *et al.*, 2002)

54 with glucose unit B and of Tyr-101 with unit C of the inhibitor are probable the most interactions that determine the conformation and binding of the inhibitor to this site (Figure 1.6). The acarbose winds around Tyr-54, which is highly solvent-exposed in the unliganded structure. Tyr-101 is involved in a hydrophobic stacking interaction with glucose unit C. Overall, the second acarbose has significantly fewer interactions with the protein compared to the acarbose bound to the active site (Figure 1.5).

In addition to Tyr-250, Phe-251 and Tyr-54 (Figure 1.4c), the hydrophobic side chains of Tyr-101 and Tyr-465 are solvent exposed and located near the catalytic cleft along an alternative glucan binding groove. These side chains may be involved in stacking interactions with the hydrophobic face of the glucan rings of the substrate. For the formation of cyclic products, the non-reducing end of glucan chain has to fold back to the active center. In *T. aquaticus* amyloamylase, the secondary binding site around Tyr-54 might help to form a curved conformation of the amylose chain in this region, which would favor the formation of cyclic products. Thus, one putative binding pathway for the smallest large-ring cyclodextrin products is obtained by connecting the two acarbose molecules bound to amyloamylase as indicated in Figure 1.4c by a broken green line. The path indicated in Figure 1.4c has a length of about 110 Å. Large ring cyclodextrins consisting of n glucose units which form a planar ring have a length of $\sim 4.6n$ (Å) and a radius of $\sim 0.73n$ (Å), assuming that the distance of two neighboring glucose units is about 4.6 Å. Therefore, an extended CD22 ring has a radius of about 16 Å and a length of ~ 100 Å, the dimensions that fit within 110 Å in length from the obtained 3D structure (Przylas *et al.*, 2000).

An alternative pathway appears possible, which goes around the 250s loop (broken green line in Figure 1.4d). The flexibility of the 250s loop conformation

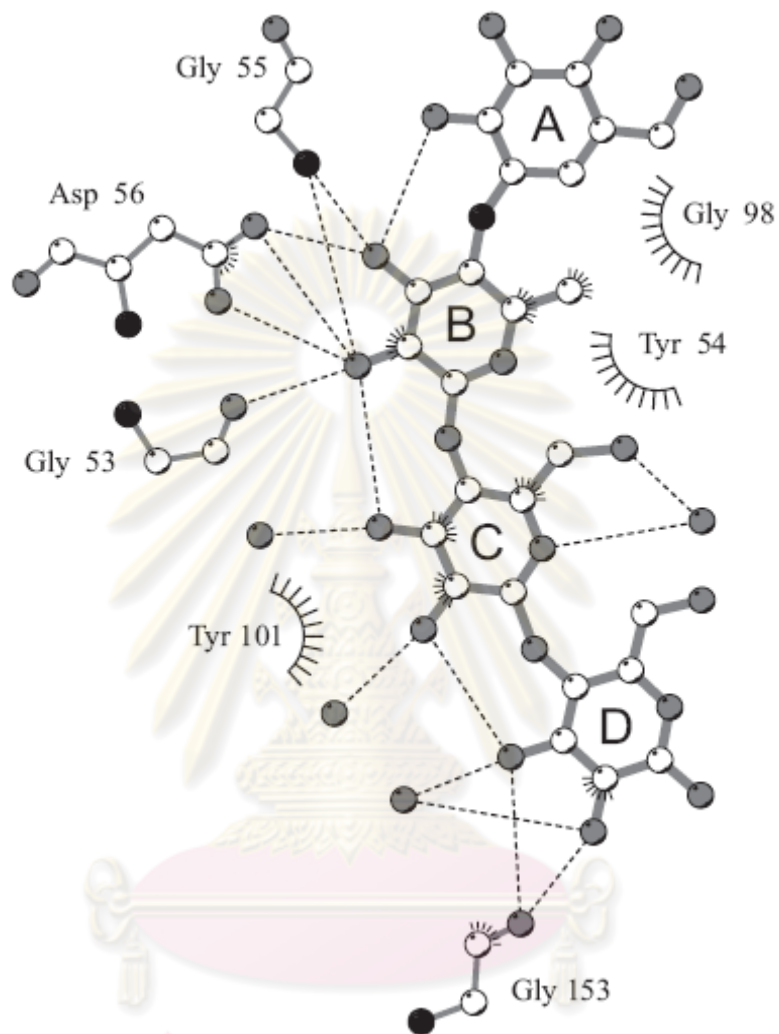


Figure 1.6 Scheme of the interaction of acarbose bound to the secondary binding site of amylomaltase from *T. aquaticus*. (Sträter *et al.*, 2002)

might be important for binding of substrates and dissociation of products. It is also clear that the formation of small cyclic products like cyclodextrins is sterically hindered by the presence of this loop near the active site. If the large-ring cyclodextrin product wraps around the 250s loop during the cyclization reaction, the minimum ring size might be restricted to about 18 residues by the size of this loop (Figure 1.4d) (Przylas *et al.*, 2000).

1.3 Physiological roles of amyloamylase

In *Escherichia coli*, amyloamylase (4 α GTase) is a part of maltooligosaccharide transport and utilization system which includes maltodextrin phosphorylase and maltose transport proteins (Schwartz, 1987). The role of amyloamylase apparently to convert short maltooligosaccharides into longer chain of which glucan phosphorylase can act on (Figure 1.7). This phosphorylase, like that in plant, degrades maltooligosaccharides to maltotetraose. The genes for amyloamylase and glucan phosphorylase constitute the *malPQ* operon. A similar operon structure was also found in *S. pneumoniae* (Lacks *et al.*, 1982), *Klebsiella pneumoniae* (Bloch *et al.*, 1986) and *C. butyricum* (Goda *et al.*, 1997), so the function of these amyloamylases is expected to be the same as the *E. coli* enzyme. On the other hand, the genes for amyloamylase found in the genome of *Haemophilus influenzae* (Fleischmann *et al.*, 1995) and *Aquifex aeolicus* (Deckert *et al.*, 1998) are part of the glycogen operon, which include genes for glycogen synthesis and degradation. Furthermore, these organisms do not have the genes homologous to *E. coli malE*, *malF*, *malG* which are involved in the transport of maltooligosaccharides into the cytoplasm. All these observations suggest that in *H. influenzae* and *A. aeolicus*, amyloamylase may not be involved in exogenous maltooligosaccharide utilization, but is involved in glycogen

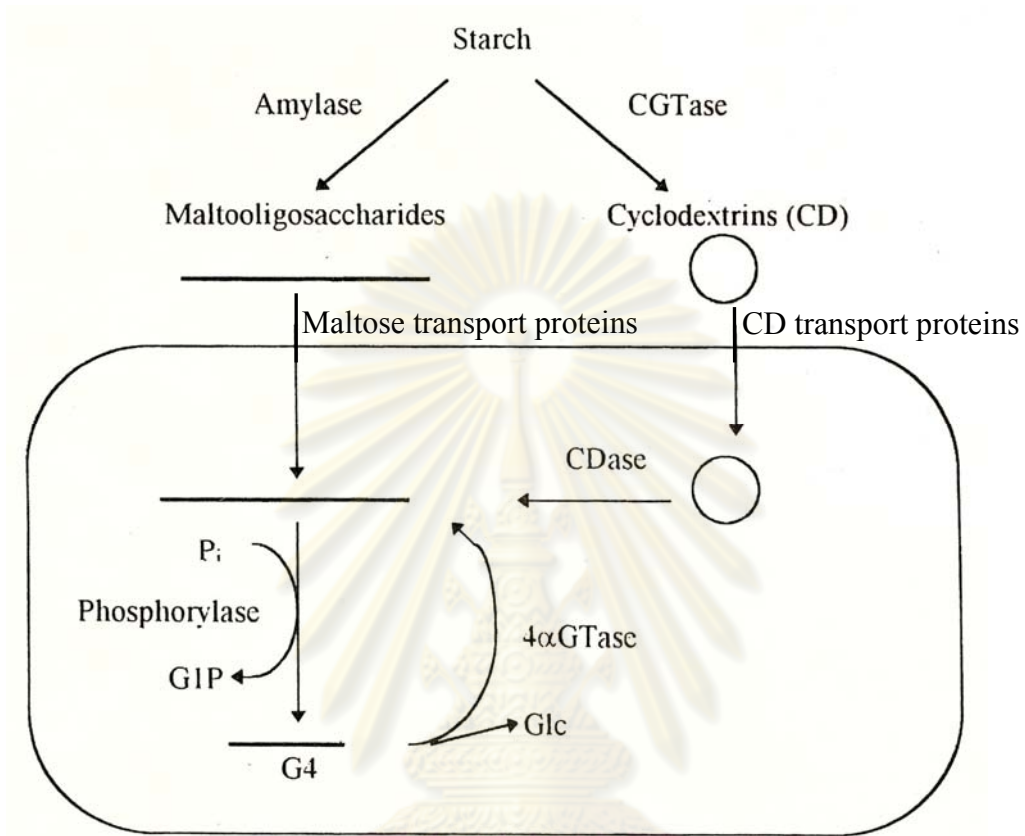


Figure 1.7 Roles of 4 α GTase in glucan utilization by bacteria (Takaha and Smith, 1999)

ศูนย์วิทยทรัพยากร
จุฬาลงกรณ์มหาวิทยาลัย

metabolism. Thus, the physiological role of amyloamylase may be different in each organism (Takaha and Smith, 1999).

1.4 Application of amyloamylase

Amyloamylases have been recently explored for their potential applications. A first application of amyloamylase is for the production of large-ring cyclodextrins (LR-CDs) with a degree of polymerization (DP) ranging from 16 to a few hundreds (Terada *et al.*, 1999, Bhuiyan *et al.*, 2003, Kaper *et al.*, 2004). LR-CDs are highly soluble in water, assumed to form a single helical V-amylose conformation and a toroidal shape, with an anhydrophilic channel-like cavity (Gessler *et al.*, 1999). They can form inclusion complexes with inorganic (Kitamura *et al.*, 1999) and organic molecules (Takaha and Smith, 1999) and have several potential applications in pharmaceuticals, food science and biotechnology (see section 1.5) (Endo *et al.*, 2002, Tomono *et al.*, 2002).

A second application of amyloamylase is in the production of isomalto-oligosaccharides (IMOs). The enzyme from *Thermotoga maritima* was used in combination with a maltogenic amylase from *Bacillus stearothermophilus* to produce IMOs from starch (Lee *et al.*, 2002). Syrups of IMOs are resistant to crystallization and have a reduced sweetness and low viscosity. IMOs are non-digestible oligosaccharides which can be applied as a substitute sugar for diabetics, to improve the intestinal microflora, or to prevent dental caries. The role of the 4 α GTase in this process is to produce longer (iso) malto-oligosaccharides that act as a substrate for amylase and to elongate the IMOs produced by the amylase. At present, industrial production of IMOs was by the use of α -glucosidase (transglucosidase) acting on maltose substrate. The advantage of using amylase and 4 α GTase was a reduction of

the number of enzymes involved and of the reaction time in combination with a higher yield of IMO (Figure 1.8) (Lee *et al.*, 2002).

A third application is in the production of thermoreversible starch gel that is of commercial interest since it can be used as a substitute for gelatin which will be of beneficial for vegetarian foods. This product could be dissolved in water and formed a firm gel after heating and cooling. The gel could be dissolved again by a new heating step (Kaper *et al.*, 2005, Lee *et al.*, 2006, Hansen *et al.*, 2008, Hansen *et al.*, 2009). In addition, the amyloamylase-treated starch was used to improve food product, such as improvement of creaminess of low-fat yoghurt (Alting *et al.*, 2009) and combination with xanthan gum for fat substitution in reduced-fat mayonnaise (Mun *et al.*, 2009).

1.5 Large-ring cyclodextrins

Cyclodextrins (Schardinger dextrans or Cycloamylose) are the oligomers of anhydroglucose units join to form a ring structure with α -1,4 glycosidic bonds. The main CDs synthesized naturally by CGTase are composed of 6, 7 and 8 glucose units called α - or CD6, β - or CD7 and γ -cyclodextrin or CD8 (Figure 1.9) (Szejtli, 1998). CDs are hydrophilic outside, thus dissolves in water, with an apolar cavity which provides a hydrophobic matrix, enabling them to form “inclusion complexes” with appropriate hydrophobic “guest” molecules (Figure 1.10). Result of the complexation between cyclodextrins and guests includes alteration of the solubility of the guest compound, stabilization against the effects of light, heat, and oxidation, masking of unwanted physiological effects, reduction of volatility, and others as shown in Table 1.2. As a result, they have applications in many fields such as pharmaceutical, food and cosmetic industries (Hashimoto, 2002).

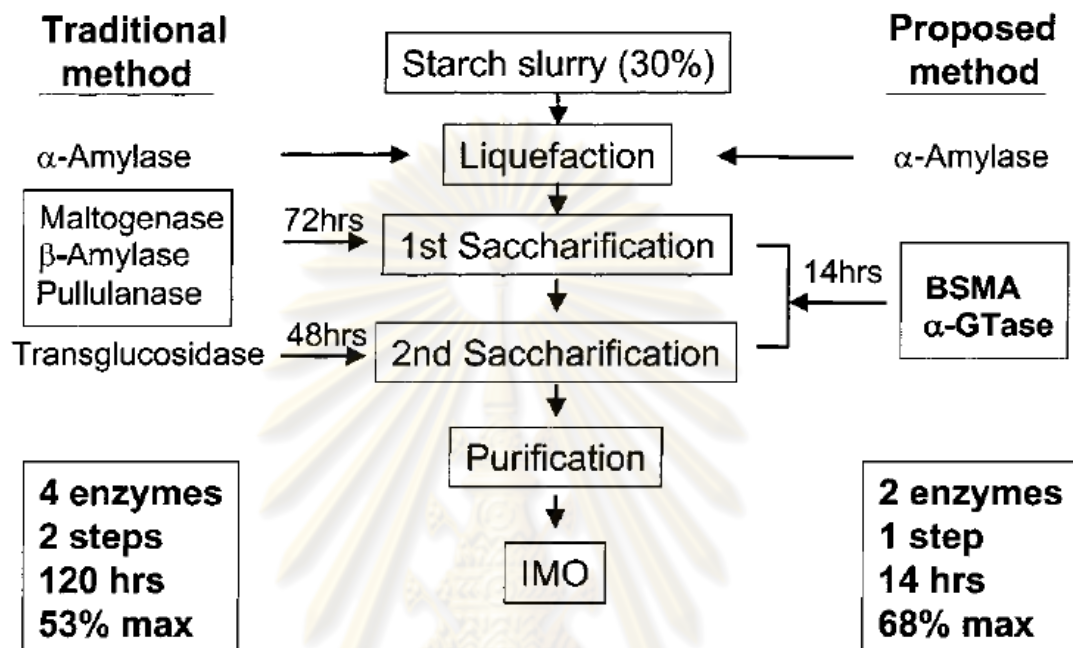


Figure 1.8 Comparison of traditional and newly improved processes for IMOs production. The new developed method improves the process of IMOs production by employing fewer enzymes, taking shorter process time, and yielding more IMOs. (Lee *et al.*, 2002)

ศูนย์วิทยทรัพยากร
จุฬาลงกรณ์มหาวิทยาลัย

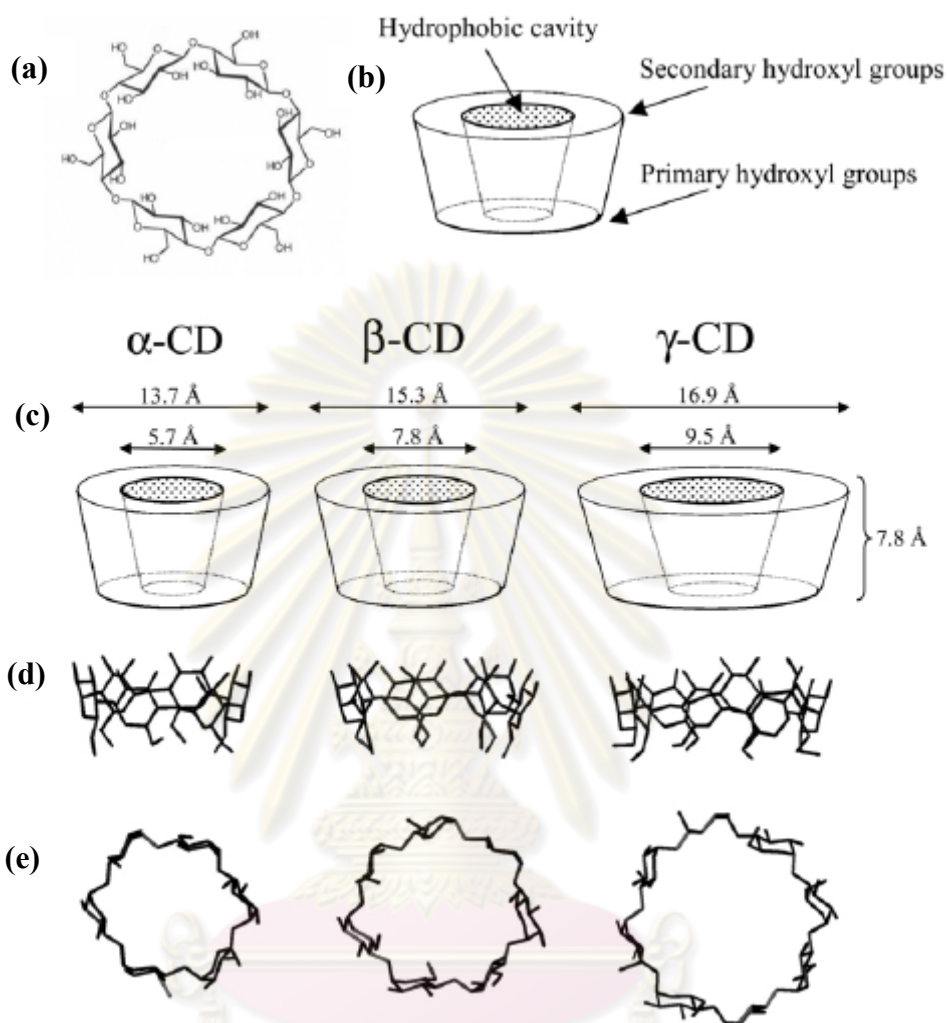


Figure 1.9 Structure of small-ring CDs (α , β , and γ). (a) Schematic presentation of α -CD. (b) Basic graphical illustration of a CD molecule. A hollow truncated cone is often used to illustrate CDs, where the C6 primary hydroxyl groups crown the narrow rim and the C2 and C3 secondary hydroxyl groups crown the wide rim. (c) Approximate molecule dimensions of α -, β -, and γ -CD. (d) Side view of α -, β -, and γ -CD stick models. (e) Stick models of α -, β -, and γ -CD viewed from the wide rim (Larsen, 2002)

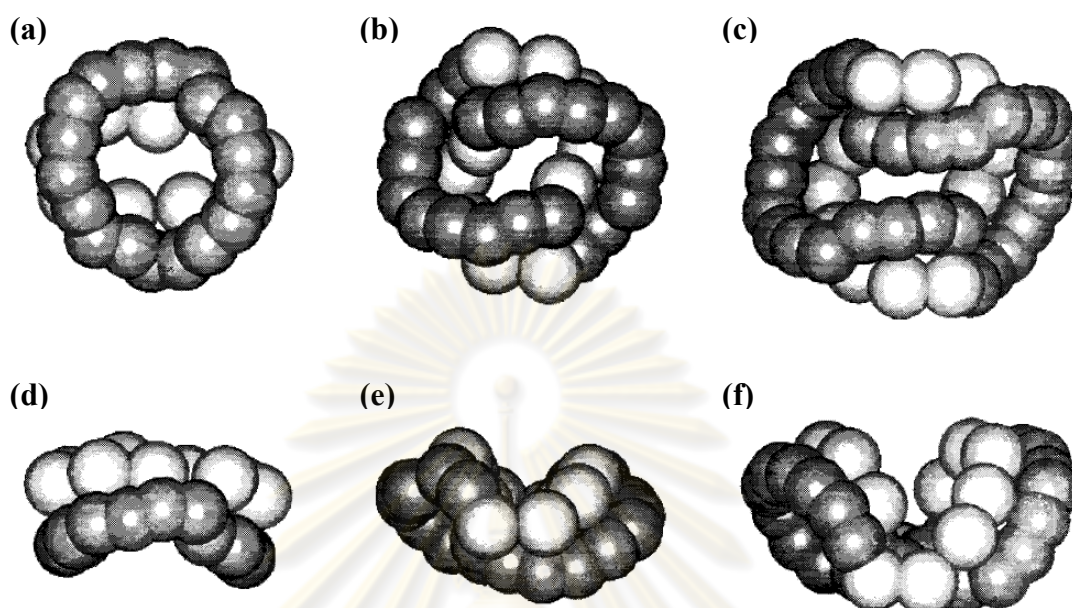


Figure 1.10 Schematic representation in top and side views of the molecular structures of CD9 (a,d), CD10 (b,e) and CD14 (c,f), to show the distortions associated with increase in ring size of the large-ring cyclodextrins (Saenger *et al.*, 1998)

ศูนย์วิทยทรัพยากร
จุฬาลงกรณ์มหาวิทยาลัย

Table 1.2 Possible effects of the formation of inclusion complexes on properties of guest molecules (Szejtli, 1998)

Stabilization of light- or oxygen-sensitive compounds

Stabilization of volatile compounds

Alteration of chemical reactivity

Improvement of solubility

Improvement of smell and taste

Modification of liquid compounds to powders

ศูนย์วิทยทรัพยากร
จุฬาลงกรณ์มหาวิทยาลัย

Large-ring cyclodextrins (LR-CDs) which are composed of more than nine D-glucopyranose units, were not studied until the end of the 20th century, with the exception of two papers on LR-CDs with a degree of polymerization (DP) of 9 to 13 (Pulley and French, 1961; French *et al.*, 1965; Endo and Ueda, 2007). The structure of conventional CDs, a truncated cone with a round cavity, is well known (Figure 1.9c). Due to flexibility, LR-CDs form variety of structures. In CD10 and CD14, the macrocyclic rings are deformed elliptical shapes, and the cavity shape is a narrow groove (Figure 1.10). CD9 has an intermediate structure between that of small-ring CDs, and CD10 and CD14, it displays a distorted elliptical macrocyclic ring without a band flips (Figure 1.10 and 1.11) (Saenger *et al.*, 1998; Larsen, 2002; Endo and Ueda, 2007). CD26 has a structure where two antiparallel V-amylose helices are bound through band flips (Figure 1.12). Table 1.3 lists some physicochemical properties of small- and large-ring CDs with DPs ranging from 9 to 21. The aqueous solubilities of CD9, CD10 and CD14 are lower than those of α - and γ -CD, however, the other LR-CDs have high aqueous solubilities over 100 g/ 100 ml (Ueda, 2002; Endo and Ueda, 2007).

Because LR-CDs can form inclusion complexes with inorganic (Kitamura *et al.*, 1999) and organic molecules (Takaha and Smith, 1999), they have been proposed to be used in many kinds of application. The first report about inclusion complex of LR-CD is the effect of complex formation with CD9 on the solubility of drugs that are poorly soluble or insoluble in water. This study reported the inclusion complexes between CD9 with spironolactone and digitoxin (Miyazawa *et al.*, 1995). In addition, the inclusion complex of CD9 and C₇₀ (Buckminster fullerene) could also be prepared, and an effective solubilization of this molecule in water has been observed (Furuishi *et al.*, 1998). Nevertheless, since the LR-CDs are able to present a variety of

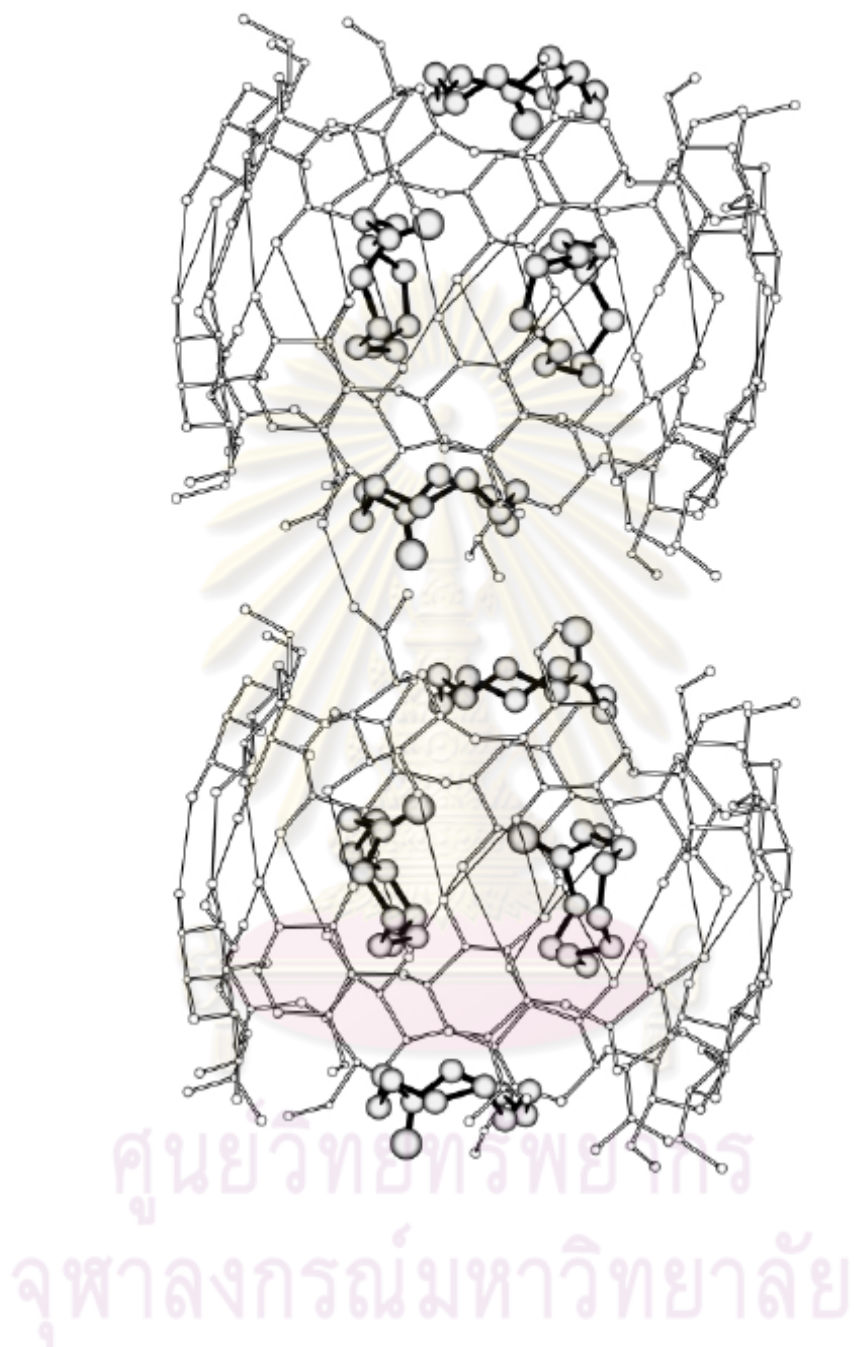


Figure 1.11 Structure of the asymmetric unit of the crystalline complex of CD9 with cycloundecanone. The cycloundecanone molecules are shaded. Thin lines denote the intermolecular hydrogen bonds between CD9 molecules. (Harata *et al.*, 2002)

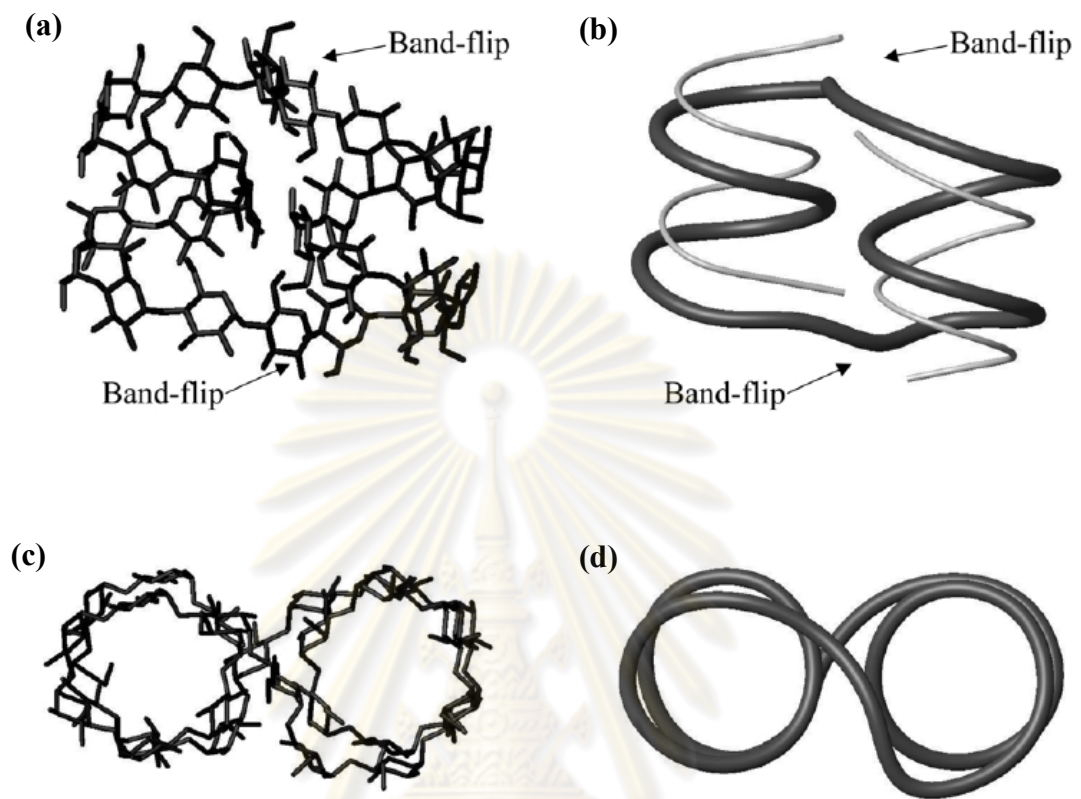


Figure 1.12 Solid state structure of CD26. (a) Structure of CD26 indicating the position of the band-flips and the V-amylose like segments. (b) Same structure as A, the thick dark tube traces the position of C1, whereas the thin light grey tube traces the position of C6. The band-flipped positions are clearly seen. (c) CD26 viewed from the top. (d) Same structure as C, the thick dark tube traces the position of C1. (Larsen, 2002)

Table 1.3 Physicochemical properties of small- and large-ring CDs (Ueda, 2002)

	Number of glucopyranose units	Aqueous ^a solubility (g/100 ml)	Surface ^a tension (mN/m)	Specific rotation [α] _D ²⁵	Half-life of ^b ring opening (h)
α -CD	6	14.5	72	+147.8	33
β -CD	7	1.85	73	+161.1	29
γ -CD	8	23.2	73	+175.9	15
δ -CD	9	8.19	73	+187.5	4.2
CD10	10	2.82	72	+204.9	3.2
CD11	11	>150	72	+200.8	3.4
CD12	12	>150	72	+197.3	3.7
CD13	13	>150	72	+198.2	3.7
CD14	14	2.30	73	+199.7	3.6
CD15	15	>120	73	+203.9	2.9
CD16	16	>120	73	+204.2	2.5
CD17	17	>120	72	+201.0	2.5
CD18	18	>100	73	+204.0	3.0
CD19	19	>100	73	+201.0	3.4
CD20	20	>100	73	+199.7	3.4
CD21	21	>100	73	+205.3	3.2

^a Observed at 25 °C

^b In 1 mol/l HCl at 50 °C

ศูนย์วิทยทรัพยากร
จุฬาลงกรณ์มหาวิทยาลัย

cavity sizes, compared to the conventional cyclodextrins, they may be useful for special applications. Moreover, it is very likely that LR-CDs will be able to display more than one cavity and in the case of very large cyclodextrins even a nanotube / V-amylose-like cavity (Larsen *et al.*, 2002).

A mixture of LR-CDs has also become of interest, since the effect of an LR-CDs mixture as an artificial chaperone for protein refolding was reported (Machida *et al.*, 2000). At present, a protein refolding kit containing a mixture of LR-CDs as one of the active components is on the market (Machida and Hayashi, 2001). Furthermore, it was also reported in 2003 that the LR-CDs mixture provided an efficient method for refolding denatured antibody to correct active structure (Machida *et al.*, 2003). The interaction between LR-CDs mixture with DPs of 20 to 50 (average molecular weight, 7720) and drugs such as prednisolone, cholesterol, digoxin, digitoxin and nitroglycerin were evaluated (Tomono *et al.*, 2002) Although nitroglycerin did not interact with the LR-CDs mixture, the solubilities of prednisolone, cholesterol, digoxin, and digitoxin were enhanced by the presence of the LR-CDs mixture, and the phase solubility diagrams showed the occurrence of complex formations. In particular, the LR-CDs mixture showed the highest solubilization effect for cholesterol in comparison with β - and γ -CD (Tomono *et al.*, 2002). Table 1.4 summarizes studies on the inclusion complex formation between LR-CD or mixture of LR-CDs and guest compounds.

Table 1.4 Studies of inclusion complex formation between LR-CD or mixture of LR-CDs and different guest compounds (Endo *et al.*, 2007)

LR-CD	Indicator or Method	Guest
Pure LR-CD	Enhancement of solubility (UV/VIS absorption)	Anthracene Amphotericin B Ajmalicine Ajmaline Carbamazepine Digitoxin Sprironolactone 9,10-Dibromoanthracene Perylene-3,4,9,10 tetracarboxylic dianhydride
CD9	Solubility method Enhancement of solubility (Spectrophotometry)	Spironolactone Fullerene C ₇₀
CD9	Enhancement of solubility (Spectrophotometry)	Reserpine [2,2]-Paracyclophane Perylene Triphenylene 1,8-Naphthalic anhydride Naphthalene-1,4,5,8-tetracarboxylic dianhydride Digitoxin Gitoxin Digoxin Methyldigoxin Lanatoside C G-Strophanthin Proscillaridin A

Table 1.4 (continued) Studies of inclusion complex formation between LR-CD or mixture of LR-CDs and different guest compounds (Endo *et al.*, 2007)

LR-CD	Indicator or Method	Guest
CD9	Solubility method and NMR Simple precipitation	Digitoxin
		1,5-Cyclooctadiene
		Cyclononane
		Cyclodecanone
		Cycloundecanone
		Cyclododecanone
		Cyclotridecanone
		Cyclopentadecanone
		Cycloundecanone
		Cyclododecanone
CD9-CD13	Powder X-ray diffraction DSC Capillary electrophoresis	Benzoate
		2-Methyl benzoate
		3-Methyl benzoate
		4-Methyl benzoate
		2,4-Dimethyl benzoate
		2,5-Dimethyl benzoate
		3,5-Dimethyl benzoate
		3,5-Dimethoxy benzoate
		Salicylate
		3-Phenyl propionate
4-tert-Butyl benzoate		
Ibuprofen anion		
1-Adamantane carboxylate		

Table 1.4 (continued) Studies of inclusion complex formation between LR-CD or mixture of LR-CDs and different guest compounds (Endo *et al.*, 2007)

LR-CD	Indicator or Method	Guest
CD14-CD17	Capillary electrophoresis	Salicylate 4-tert-Butyl benzoate Ibuprofen anion
CD21-CD32	Isothermal titration calorimetry	Iodine
Mixture of LR-CDs		
CA(S)* and CA(L)**	Spectrofluorometry	8-Anilino-1-naphthalene sulfonic acid
CA(S)* and CA(L)**	Simple precipitation	1-Octanol 1-Butanol Oleic acid

* CA(S): Mixture of LR-CDs with DP around 20 to 55, mainly DP of 25 to 50.

** CA(L): Mixture of LR-CDs with average DP of ca. 150.

ศูนย์วิทยทรัพยากร
จุฬาลงกรณ์มหาวิทยาลัย

1.6 *Corynebacterium glutamicum*

In the mid-1950s, a bacterium which was shown to excrete large quantities of L-glutamic acid into the culture medium was isolated (Kinoshita *et al.*, 1957; Ukada, 1960). It was reported as a novel bacterium, *Corynebacterium glutamicum* (initially identified as *Micrococcus glutamicus*), with a unique ability to produce significant amounts of L-glutamate directly from cheap sugar and ammonia (Ikeda *et al.*, 2003). *Corynebacterium glutamicum* is a fast-growing, rod-shaped, aerobic, non-sporulating, non-pathogenic, non-motile, saprophytic, Gram-positive microorganism that can be isolated from soil samples (Kumagai, 2000; Vertès *et al.*, 2005). *Corynebacteria* belong to the order *Actinomycetales* of the eubacteria that is characterized by a high G+C content and that constitutes a different evolutionary line from that formed by a low G+C content microorganism such as bacilli or clostridia (Stackebrandt *et al.*, 1997). The genus *Corynebacterium* is closely related to *Mycobacterium* and *Norcardia*, among other genera, which form the *Corynebacteria* suborder. The genus includes both aerobes and facultative anaerobes (Liebl, 2005). Nonmedical corynebacteria are widely disseminated in nature and have been isolated from a number of different environments other than soil, including dairy products, plant materials, faeces and animal skin (Liebl, 2001).

Figure 1.13 shows the main issues in the history and strain development technology of *C. glutamicum*. In the early stages, the breeding of production strains depended mostly on repeated random mutation and selection. This classical method has generated a variety of mutants, such as auxotrophs, analog-resistant mutants and transport mutants. By stepwise assembly of beneficial phenotypic characters with the use of the mutagenic approach, many commercially potent producers have been developed and these are used predominantly in industrial fermentation processes

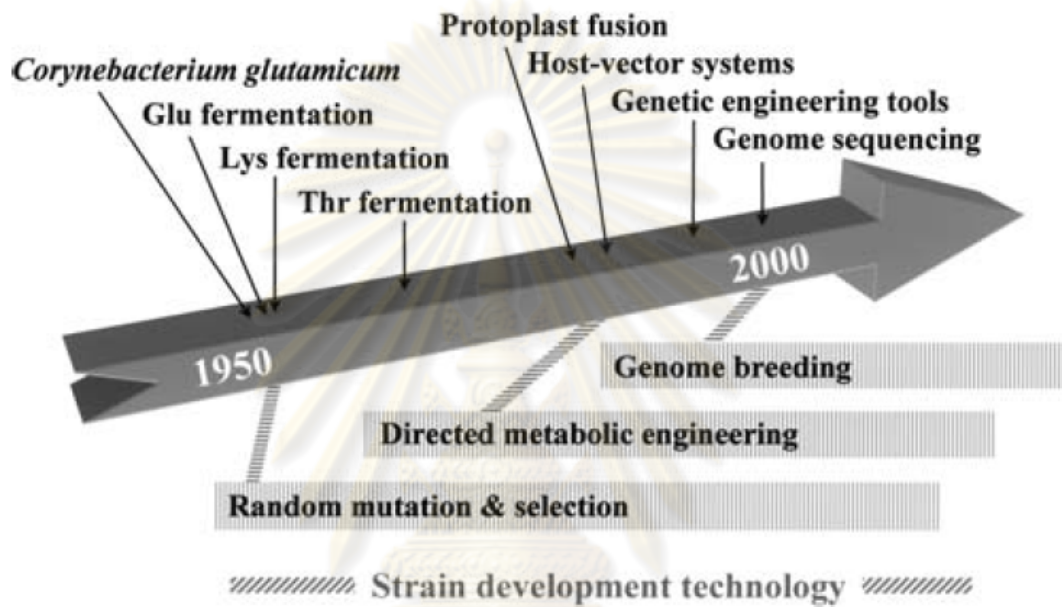


Figure 1.13 History of amino acid fermentation and strain development technology of *Corynebacterium glutamicum* (Ikeda and Nakagawa, 2003)

ศูนย์วิทยทรัพยากร
จุฬาลงกรณ์มหาวิทยาลัย

(Kinoshita and Nakayama, 1978; Leuchtenberger, 1996; Kumagai 2000). Since the mid-1980s, several genes in the biosynthetic pathways of the aspartate derived amino acids (L-lysine, L-threonine, and L-isoleucine) and the vitamin D-pantothenate have been cloned and analyzed (Sahm *et al.*, 2000). These genes were mainly identified by heterologous complementation of *Escherichia coli* mutants, and occasionally, in the homologous system by conferring an amino acid-analog resistance. These studies already led to a general understanding of metabolic pathways, but a complete picture of the complex interactions could not be achieved due to the lack of detailed genetic information. Genomic sequencing followed by automatic and manual annotation turned out to represent the ideal method to obtain the missing genetic information for the development of industrial *C. glutamicum* strains. For this reason, the genome of *C. glutamicum* was sequenced and completed in 2003 (Figure 1.14) (Ikeda and Nakagawa, 2003; Kalinowski *et al.*, 2003). The total genome sequence of *C. glutamicum* ATCC 13032 contains 3,309,401 bp and comprises of 3,099 genes on the genome (accession number: BA00036) (Figure 1.14a) (Ikeda and Nakagawa, 2003). Another research group reported the total genome sequence of 3,282,708 bp with 3,002 genes on the genome (accession number: NC_006958) (Figure 1.14b) (Kalinowski *et al.*, 2003).

In the reported coding sequences (CDS), one sequence was identified as 4- α -glucanotransferase (EC 2.4.1.25) with 2,121 bp in length (accession number: NC_006958 and NC_003450). This sequence encodes 706 amino acids protein (accession number: YP_226540 and NP_601497). Interestingly, this enzyme has not been further investigated and we found that the sequence of 4- α -glucanotransferase from *C. glutamicum* has low similarity to 4- α -glucanotransferase from *T. aquaticus*

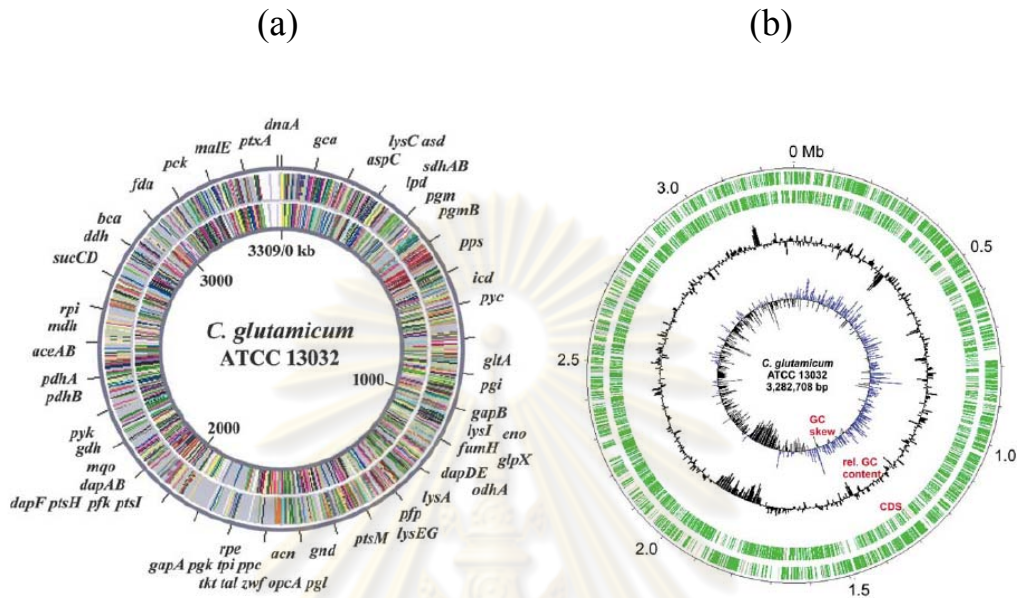


Figure 1.14 Circular representative of the *Corynebacterium glutamicum* ATCC 13032 chromosome. ((a) from Ikeda and Nagakawa, 2003; (b) from Kalinowski *et al.*, 2003)

ศูนย์วิทยทรัพยากร
จุฬาลงกรณ์มหาวิทยาลัย

(Terada *et al.*, 1999) and *A. aeolicus* (Bhuiyan *et al.*, 2003) of which LR-CDs production has been reported.

1.7 Objectives

Although LR-CDs are commercially available, their market has been very limited due to a few number of useful amyloamylases and the lack of efficient and practical production process for LR-CDs. At present, LR-CDs are added in a commercial product as artificial chaperone for protein refolding kit. In addition, the potential use of LR-CDs in various applications has been realized. It is, therefore, beneficial to search for a novel amyloamylase and to characterize the enzyme for understanding of its structure-function relationship. The basic knowledge of the enzyme will be of useful for the improvement of LR-CDs production. From the list of microorganisms with the genome deposited in Genbank, we explored those with the coding sequence for amyloamylase and chose *Corynebacterium glutamicum* for our study since preliminary work showed that the enzyme has low homology with those previously studied.

The objectives:

1. To clone and express *amyloamylase* gene of *Corynebacterium glutamicum* ATCC 13032
2. To purify and characterize amyloamylase
3. To identify residue involved in catalysis by site-directed mutagenesis
4. To analyze and identify parameters influencing large-ring cyclodextrin product profile

CHAPTER II

MATERIALS AND METHODS

2.1 Equipments

Autoclave: Model H-88LL, Kokusan Ensinki Co., Ltd., Japan

Autopipette: Pipetman, Gilson, France

Centrifuge, refrigerated centrifuge: Model J2-21, Beckman Instrument Inc., USA

Electrophoresis unit:

- Mini protein, Bio-Rad, USA
- Submarine agarose gel electrophoresis unit, Bio-Rad, USA
- Mini IEF-CELL Model 111, Bio-Rad, USA

FPLC AKTA Amersham Pharmacia Biotech unit:

Column: Amersham Biosciences HisTrap FFTM, HiTrap FFTM DEAE FFTM and HiPrep Phenyl FFTM (High Sub) 16/10

Detector: UPC-900

Pump: P-920

Fraction collector: Frac-900

Gene Pulser[®]/*E. coli* PulserTM Cuvettes: Bio-Rad, USA

Gel Document: SYNGEND, England

Gel support film for polyacrylamide, Bio-Rad, USA

HPAEC DX-600: Dionex Corp., Sunnydale, USA

Column: Carbopac PA-100TM 4 x 250 mm

Pulsed amperometry detector: DIONEX ED40

Autosampler: DIONEX AS40

Column oven: DIONEX ICS-3000 SP

Incubator, waterbath: Model M20S, Lauda, Germany and BioChiller

2000, FOTODYNE Inc., USA and ISOTEMP 210, Fisher Scientific, USA

Incubator shaker: Innova™ 4080, New Brunswick Scientific, USA

Light box: 2859 SHANDON, Shandon Scientific Co., Ltd., England

Laminar flow: HT123, ISSCO, USA

Magnetic stirrer: Model Fisherbrand, Fisher Scientific, USA

Matrix-assisted laser desorption/ionization-time of flight mass spectrometry (MALDI-TOF MS) : Model “Autoflex” II system, Bruker Daltonic, Germany

Membrane filter: polyethersulfone (PES), pore size 0.45 µm, Whatman, England

Microcentrifuge: Eppendorf, Germany

Orbital incubator: Model 1H-100, Gallenkamp, England

Orbital shaker: Orbital shaker 03, Stuart Scientific, England

pH meter: Model PHM95, Radiometer Copenhagen, Denmark

Power supply: Model POWER PAC 300, Bio-Rad, USA

Sephacryl S-200: Amersham Pharmacia Biotech Inc., USA

Shaking waterbath: Model G-76, New Brunswick Scientific Co., Inc., USA

Sonicator: Bendelin, Germany

Spectrophotometer: DU Series 650, Beckman, USA

Thermal cycler: Mastercycler, Eppendorf, Germany

Vortex: Model K-550-GE, Scientific Industries, Inc, USA

2.2 Chemicals

Acrylamide: Merck, Germany

Agar: Merck, Germany

Agarose: SEKEM LE Agarose, FMC Bioproducts, USA

Ammonium persulphate: Sigma, USA

Ammonium sulphate: Carlo Erba Reagenti, Italy

Ampicillin: Sigma, USA

L-aspartic acid: Fluka, Switzerland

Beef extract: Biomark laboratories, India

Bovine serum albumin: Sigma, USA

Boric acid: Merck, Germany

Bromphenol blue: Merck, Germany

Casein hydrolysate: Merck, Germany

Chloroform: LAB-SCAN Analytical Science, Ireland

Coomassie brilliant blue R-250: Sigma, USA

Copper sulfate: Carlo Erba Reagenti, Italy

4,4'-Dicarboxy-2,2'-biquinoline: Sigma, USA

Dimethyl sulfoxide (DMSO): Merck, Germany

di-Potassium hydrogen phosphate anhydrous: Carlo Erba Reagenti, Italy

di-Sodium ethylene diamine tetra acetic acid: M&B, England

1 kb DNA ladderTM: New England BioLabs Inc., USA and Fermentas, Canada

dNTP: Stratagene, USA

Ethidium bromide: Sigma, USA

Ethyl alcohol absolute: Carlo Erba Reagenti, Italy

Ethylene diamine tetraacetic acid (EDTA): Merck, Germany

Glacial acetic acid: Carlo Erba Reagenti, Italy

Glucose: BDH, England

Glucose liquicolor (Glucose oxidase kit): HUMAN, Germany

Glycerol: Merck, Germany

Glycine: Sigma, USA

Hydrochloric acid: Carlo Erba Reagenti, Italy

Iodine: Baker chemical, USA

Isoamyl alcohol: Merck, Germany

Isopropanol: Merck, Germany

Isopropylthio- β -D-galactoside (IPTG): Sigma, USA

Maltoheptaose: Hayashibara biochemical laboratories Inc., Japan

Maltohexaose: Hayashibara biochemical laboratories Inc., Japan

Maltopentaose: Hayashibara biochemical laboratories Inc., Japan

Maltose: Conda, Spain

Maltotetraose: Hayashibara biochemical laboratories Inc., Japan

Maltotriose: Fluka, Switzerland

β -Mercaptoethanol: Fluka, Switzerland

Methylalcohol: Merck, Germany

N,N-Dimethyl-formamide: Fluka, Switzerland

N,N'-Methylene-bis-acrylamide: Sigma, USA

N,N,N',N'-Tetramethyl-1, 2-diaminoethane (TEMED): Carlo Erba Reagenti, Italy

Pea starch: Emsland-Stärke GmbH, Germany

Peptone: Scharlau microbiology, Spain

Phenol: Fisher Scientific, England

Phenylmethylsulfonyl fluoride (PMSF): Sigma, USA

Plasmid Mini Kit: Bio-Rad, USA

Potassium iodide: Mallinckrodt, USA

Potassium phosphate monobasic: Carlo Erba Reagenti, Italy

QIA quick Gel Extraction Kit: QIAGEN, Germany

Riboflavin (Lactoflavine); BDH, England

5-Sulfosalicylic acid: Mallinckrodt, USA

Sodium acetate: Merck, Germany

Sodium carbonate anhydrous: Carlo Erba Reagenti, Italy

Sodium chloride: Carlo Erba Reagenti, Italy

Sodium citrate: Carlo Erba Reagenti, Italy

Sodium dodecyl sulfate: Sigma, USA

Sodium hydroxide: Merck, Germany

Soluble starch (potato): Scharlau microbiology, Spain

Standard protein marker: Amersham Pharmacia Biotech Inc., USA

Tris (hydroxymethyl)-aminomethane: Carlo Erba Reagenti, Italy

Tryptone: Scharlau microbiology, Spain

Yeast extract: Scharlau microbiology, Spain

2.3 Enzymes, Restriction enzymes and Bacterial strains

Glucoamylase from *Aspergillus niger*: Fluka, Switzerland

E. coli BL21 (DE3): Novagen, Germany

Corynebacterium glutamicum ATCC 13032, Thailand Institute of Scientific and

Technological Research, Thailand

PfuTurbo[®] DNA polymerase: Promega, USA

Plasmid pET-19b: Novagen, Germany

Plasmid pET-17b: Novagen, Germany

Restriction enzymes: New England BioLabs Inc., USA and Fermentas, Canada.

RNaseA: Sigma, USA

T₄ DNA ligase: New England BioLabs, Inc, USA

2.4 Cloning of amyloamylase gene (*malQ*)

2.4.1 Cultivation and extraction of genomic DNA from *Corynebacterium glutamicum* ATCC 13032

The *C. glutamicum* ATCC 13032 was cultivated in Nutrient broth (0.3% beef extract and 0.5% peptone) at 30 °C, with rotary shaking at 250 rpm overnight. The cells were collected by centrifugation at 4 °C, 6,000 xg for 15 minutes. Then genomic DNA extraction was performed. The cells were washed with TE buffer then centrifuged and resuspended with 10 ml of TE buffer. After that, the cells suspension was frozen at -20 °C for 10 minutes then thawed at 65 °C. TE buffer (30 ml) was added (total volume should be 40 ml), followed by 7 ml of 10% SDS and 200 µl of proteinase K. The sample was gently mixed and then incubated at 37 °C for 1 hour. To the reaction mixture, 7.2 ml of 5 M NaCl was added and mixed, followed by the addition of 5.7 ml of CTAB solution. The mixture was then incubated at 65 °C for 20 minutes. Phenol-chloroform extraction was performed by addition of an equal volume of phenol-chloroform to the mixture, mixed thoroughly and centrifuged at 15,000 xg for 10 minutes. The upper solution was extracted again with equal volume of chloroform solution, then collected. After that, 2 volume of ethanol or 0.6 volume of isopropanol was added. Genomic DNA was collected, washed with 70% ethanol and resuspended in TE buffer. Amount of genomic DNA was quantitated by measuring absorbance at 260 nm (Sambrook and Russel, 2001).

$$\text{Concentration of original DNA solution in } \mu\text{g/ml} = A_{260} \times 50$$

The purity of this DNA was monitored by the ratio of $A_{260/280}$ values and by 1% agarose gel electrophoresis.

2.4.2 Agarose gel electrophoresis

Electrophoresis through agarose is the standard method used to separate, identify, and purify DNA fragments. The agarose powder (1%) was added to 100 ml electrophoresis buffer (89 mM Tris-HCl, 8.9 mM boric acid and 2.5 mM EDTA, pH 8.0) in an Erlenmeyer flask and heated until complete solubilization in a microwave oven. The agarose solution was cooled down to 60 °C until all air bubbles were completely eliminated, then poured into an electrophoresis mold. When ready, the DNA samples were mixed with one-fifth volume of the desired gel-loading buffer (0.025% bromphenol blue, 40% ficoll 400 and 0.5% SDS) and slowly loaded the mixture into agarose gel. Electrophoresis was performed at constant voltage of 10 volt/cm until the faster migration dye (bromphenol blue) migrated to approximately 1 cm from the bottom of the gel. The gel was stained with 2.5 µg/ml ethidium bromide solution for 5 minutes and destained to remove unbound ethidium bromide in distilled water for 10 minutes. DNA fragments on agarose gel were visualized under a long wavelength UV light and photographed using Gel Document apparatus. The molecular weight of DNA sample was compared with the relative mobility of the standard 1 kb DNA ladderTM fragment.

2.4.3 Amplification of amyloamylase gene (*malQ*) using PCR technique

The extracted genomic DNA from *C. glutamicum* ATCC 13032 was used as template to amplify the *malQ*. The forward and reverse primers were designed from the start to stop codons and contained a restriction site of *Nde*I and *Xho*I, respectively as shown below.

NdeI

fwdCGAM: GGG AAT TCC ATA TGA CTG CTC GCA GAT TTT TGA ATG

XhoI

revCGAM: CCG CTC GAG CTA ATC TCG CTT GCT TGC CTT TGC C

* Note: The bold letters are start and stop codon, respectively. The underlined letters were designed for the restriction site of *NdeI* and *XhoI*.

PCR was performed in a 50 µl reaction mixture containing 50 ng of chromosomal DNA from *C. glutamicum* ATCC 13032, 1x *Pfu* buffer with MgSO₄, 0.2 mM each dNTPs, 1 µl of 10 µM of each primer and 1U of *Pfu* DNA polymerase. PCR condition consisted of predenaturation at 95 °C for 2 minutes, denaturation at 95 °C for 1 minute, annealing at 60 °C for 30 seconds, extension at 72 °C for 3 minutes and final extension at 72 °C for 5 minutes. The cycle was repeated for 30 times. PCR products were detected by 1% agarose gel electrophoresis. The desired DNA band of *malQ* was extracted from agarose gel by the gel extraction kit (QIAGEN).

2.4.4 Restriction enzyme digestion

The PCR product and plasmid vector pET-19b were separately double digested with *NdeI* and *XhoI* in the reaction mixture of 20 µl containing 1x NEB buffer 4 (New England BioLabs Inc., USA), 1 µg BSA, 10 U of *NdeI*, 20 U of *XhoI* and 50 µg of DNA template. The reaction was performed at 37 °C for 16 hours.

2.4.5 Ligation of the PCR product with vector pET-19b

The purified digested PCR product and vector pET-19b were then ligated at 16 °C overnight in the 10 µl reaction mixture that composed of 1x ligation buffer

(New England BioLabs Inc., USA), 5 U of T4 DNA ligase, 30 µg of PCR product and 50 µg of pET-19b.

2.4.6 Preparation of competent cells for electroporation (Sambrook and Russel, 2001)

A fresh overnight culture of *E. coli* BL21(DE3) was inoculated into 300 ml of LB medium with 1% inoculum size. The cell culture was cultivated with shaking at 250 rpm until A_{600} reached 0.5 to 0.6. The culture was chilled on ice for 15 minutes and then centrifuged at 8,000 xg for 15 minutes at 4 °C. The cells were washed with 300 ml of cold water, spun down and washed again with 150 ml of cold water. After centrifugation, the cells were resuspended in approximately 15 ml of 10% glycerol in distilled water and centrifuged at 8,000 xg for 15 minutes at 4 °C. Finally the cell pellets were resuspended to final volume of 600 µl in 10% glycerol. This cell suspension was divided into 40 µl aliquots and store at -80 °C until used.

2.4.7 Plasmid transformation

The recombinant plasmids from section 2.4.5 were introduced into a competent of *E. coli* strain BL21(DE3) by electroporation. In the electroporation step, 0.2 cm cuvettes and sliding cuvette holder were chilled on ice. The Gene Pulser® apparatus was set to the 25 µF capacitor, 2.5 kV, and the pulse controller unit was set to 200Ω. Competent cells, which were prepared as described in section 2.4.6, were gently thawed on ice. One to five microliter of recombinant plasmid from section 2.4.5 was mixed with 40 µl of the competent cells and then placed on ice for 1 minute. This mixture was transferred to a chilled cuvette. The cuvette was applied one

pulse at the above settings. Subsequently, one milliliter of LB medium (1% tryptone, 0.5% yeast extract and 0.5% NaCl, pH 7.2) was added immediately to the cuvette. The cells were quickly resuspended with a Pasteur pipette. Then the cell suspension was transferred to new tube and incubated at 37 °C for 1 hour with shaking. Finally, this suspension was spread onto the LB agar plates containing 100 µg/ml ampicillin. After incubation at 37 °C for 16 hours, the colonies were picked.

2.5 Colony selection and primary screening

2.5.1 Plasmid size screening

The colonies were picked and resuspended in 20 µl of the size screening buffer containing lysis buffer (1% (w/v) lysozyme, 0.1% (w/v) heat treated RNase A, 50% (v/v) glycerol, 0.05 mM Tris-HCl, pH 8.0) which was pre-warmed at 37 °C for 10 minutes. Then, the solution was incubated at 40 °C for 5 minutes. The viscous sample was centrifuged at 12,000 xg for 10 minutes. To estimate the size of plasmid, 20 µl of the supernatant was loaded onto 1% agarose gel and compared with relative mobility of DNA markers.

2.5.2 Plasmid extraction

The recombinant *E. coli* BL21(DE3) was grown in LB-medium containing 100 µg/ml ampicillin overnight at 37 °C with rotary shaking. The cell culture was collected by centrifugation at 10,000 xg for 5 minutes. The recombinant plasmid pET-19b vector harboring *malQ* was extracted by QIAquick Plasmid Extraction kit (QIAGEN, Germany). The concentration of plasmid was determined by spectrophotometric method ($A_{260/280}$) and agarose gel electrophoresis.

2.5.3 Nucleotide sequencing

About 50-100 ng of the extracted recombinant plasmid pET-19b harboring *malQ* from section 2.5.2 was subjected to automated DNA sequencing (Macrogen, Korea). The sequencing was performed using primers of T7 promoter for DNA sequence at 5'-terminus and T7 terminator for DNA sequence at 3'-terminus of the inserted *malQ*, respectively. The obtained DNA sequence was used to design primers f2CGAM and r2CGAM for determining the residual sequence which was localized in the middle of the gene. The primers used were as shown below. The sequences were analyzed by GENETYX-WIN software.

f2CGAM: TCT ACT CTG TGC GTT CCA CGT TG

r2CGAM: CCT GCG AGT TCT GCT TAT AGG

2.6 Site-directed mutagenesis

Mutagenesis was carried out by PCR amplification using a pair of oligonucleotide with a desired point mutation as primers and the recombinant plasmid as a template. The PCR product was digested with *Dpn* I endonuclease (target sequence: 5'-GA_{CH}³TC-3') which is specific for methylated as well as hemimethylated DNA. This enzyme is used to digest the parental DNA template to select for mutation-containing synthesized DNA. DNA isolated from almost all *E. coli* strains is *dam* methylated and therefore susceptible to *Dpn* I digestion. The nicked plasmid of the *Dpn* I-treated was then transformed into the host *E. coli* competent cells.

The recombinant plasmid pET-17b containing *malQ* was extracted as described in section 2.5.2 to be used as a template. The mutagenic primers were

designed for substitution of Tyr residue by Ala residue at the desired point. The sequences of mutagenic primers were shown below.

Y172A_FWD: CTG CTG ATA AGG_CGC TTG ATT CCC

Y172A_REV: GGG AAT CAA GCG_CCT TAT CAG CAG

* Note: The underlined letters were desired residues

PCR was performed in a 50 μ l reaction mixture containing 50-100 ng of the recombinant plasmid, 1x *Pfu* buffer with MgSO₄, 0.1 μ mole of each dNTP, 10 pmoles of each primer and 1 U of *Pfu* DNA polymerase. PCR condition was predenaturation at 95 °C for 2 minutes, denaturation at 95 °C for 1 minute, annealing at 60 °C for 1 minute, extension at 72 °C for 12 minutes. The cycle was repeated for 16 times. Then, 30 μ l of PCR product was transferred to a new tube and settled on ice for 2 minutes. Then incubated with 1 μ l (10 U) of *Dpn* I for 1 hour at 37 °C.

The *Dpn* I digested PCR product was prepared for transformation by gently mixed with competent *E. coli* BL21(DE3) cells. The transformation was performed as described in section 2.4.7. Cells containing the recombinant mutated plasmids were picked and the mutated plasmids were further extracted. To confirm the mutation, the plasmids were extracted and checked their size by agarose gel electrophoresis as described in section 2.5.2 and 2.4.2, respectively. The point of mutation was further confirmed by nucleotide sequencing as in section 2.5.3 and compared with the parent *malQ*.

2.7 Optimization for amyloamylase gene expression

The transformants of *E. coli* BL21(DE3) were grown overnight at 37 °C in 5 ml of LB medium containing 100 μ g/ml ampicillin. After that, 1% of the cell culture was transferred into 100 ml of the same medium and was cultured at 37 °C with

shaking at 250 rpm. When A_{600} reached 0.5, the transformant was induced by IPTG at a final concentration of 0.4 mM. After various times of induction of 0, 1, 2, 3, 4, 5 and 6 hours, the cells were harvested by centrifugation at 6,000 xg for 15 minutes and then washed by 0.85% NaCl and extraction buffer (50 mM phosphate buffer, pH 7.4 containing 0.1 mM PMSF, 0.01% β -mercaptoethanol, 1.0 mM EDTA), respectively. Bacterial cells were resuspended in extraction buffer then disrupted cells by sonication. Cell debris was removed by centrifugation at 12,000 xg for 30 minutes. The supernatant was dialyzed against 50 mM phosphate buffer, pH 7.4 before determination of enzyme activity and protein concentration as described in section 2.9.2 and 2.10, respectively.

The protein pattern of cells during IPTG induction was followed. The 1.0 ml of cell culture was harvested at various times after IPTG induction (0, 1, 2, 3, 4, 5 and 6 hours) by centrifugation. The cell pellets were resuspended in 100 μ l of 5x sample buffer (Appendix 1). The protein patterns of cell samples (10 μ l) were determined by SDS-PAGE as described in 2.11.1.

2.8 Purification of amyloamylase enzyme

2.8.1 Starter inoculum

The *E. coli* BL21(DE3) transformant colony was transferred into LB medium containing 100 μ g/ml ampicillin at 37 °C with 250 rpm rotary shaking overnight.

2.8.2 Cells cultivation and crude extract preparation

Starter inoculum (1%) was transferred into LB medium in Erlenmeyer flask and cultured at 37 °C with shaking. When A_{600} of the culture reached 0.5, IPTG was added to a final concentration of 0.4 mM to induce amyloamylase and cultivation was

continued at 37 °C for 2 hours. After cultivation, cells were harvested by centrifugation at 6,000 xg for 15 minutes, then washed by 0.85% NaCl and extraction buffer, respectively. Bacterial cells were resuspended in extraction buffer then disrupted by sonication of 40% pulse for 1 minute and stopped for 2 minutes, then repeated sonication process for 10 cycles. Cell debris was removed by centrifugation at 12,000 xg for 30 minutes. The supernatant was dialyzed against 50 mM phosphate buffer, pH 7.4 before determination of enzyme activity and protein concentration as described in section 2.9.2 and 2.10, respectively.

2.8.3 Purification of recombinant wild-type amyloamylase with his-tag residues (p19AM)

The crude extract from 2.8.2 was initially purified by HisTrap FFTM at 4 °C. The HisTrap FFTM was equilibrated with at least 5 times column volume of 20 mM phosphate buffer, pH 7.4 containing 0.5 M NaCl and 20 mM imidazole at the flow rate of 1 ml/minute. The dialyzed protein solution from section 2.8.2 was applied to HisTrap FFTM column (1 ml, two columns consecutively) and washed with the same buffer until A_{280} of eluent decreased to baseline. The bound protein was eluted by 500 mM imidazole in the same buffer at the flow rate of 1 ml/minute. Fractions of 3 ml were collected and the enzyme activity was determined. The active fractions were pooled and dialyzed against 20 mM phosphate buffer, pH 7.4 before determination of the enzyme activity and protein concentration as described in section 2.9.2 and 2.10, respectively.

2.8.4 Purification of recombinant wild-type amyloamylase (p17AM) and Y172A mutated amyloamylase

The crude extract from 2.8.2 was purified by the following steps. All operations were performed at 4 °C.

2.8.4.1 DEAE FFTM column chromatography

The DEAE FFTM was equilibrated with at least 5 times column volume of 50 mM phosphate buffer, pH 7.4 containing 0.01% β -mercaptoethanol at the flow rate of 1 ml/minute. The dialyzed protein solution from section 2.8.2 was applied to a DEAE FFTM column and washed with the same buffer until A_{280} of eluent decreased to baseline. The bound proteins were stepwise eluted by 0.2 M NaCl, 0.3 M NaCl and 1 M NaCl in the same buffer at the flow rate of 1 ml/minute. Fractions of 3 ml were collected and the enzyme activity was determined. The active fractions were pooled and dialyzed against 50 mM phosphate buffer, pH 7.4 before determination of the enzyme activity and protein concentration as described in section 2.9.2 and 2.10, respectively.

2.8.4.2 Phenyl FFTM column chromatography

The Phenyl FFTM was equilibrated with at least 5 times column volume of 50 mM phosphate buffer, pH 7.4 containing 1 M ammonium sulfate and 0.01% β -mercaptoethanol at the flow rate of 1 ml/minute. The dialyzed protein solution from section 2.8.4.1 which was added ammonium sulfate to a final concentration of 1 M was applied to a Phenyl FFTM column. The column was washed with the same buffer until A_{280} of eluent decreased to baseline. The bound proteins were stepwise eluted by 0.2 M ammonium sulfate and 0 M ammonium sulfate in the same buffer at the flow

rate of 1 ml/minute. Fractions of 3 ml were collected and the enzyme activity was determined. The active fractions were pooled and dialyzed against 50 mM phosphate buffer, pH 7.4 before determination of the enzyme activity and protein concentration as described in section 2.9.2 and 2.10, respectively.

2.9 Enzyme assay

Amylomaltase activity was determined by five types of assay as described below.

2.9.1 Starch degrading activity

Starch degrading activity was measured by iodine method. The reaction mixtures contained 100 μ l of 0.75% (w/v) soluble starch (potato), 50 μ l of enzyme, and 100 μ l of 50 mM phosphate buffer pH 6.0. Incubation was at 30 °C for 10 minutes, reaction was stopped by adding 500 μ l of 1 N HCl. Then 100 μ l aliquot was withdrawn and mixed with 900 μ l iodine solution (0.005% I₂ in 0.05% KI, (w/v)). The absorbance at 660 nm was measured.

One unit is defined as the amount of enzyme required to degrade 1 mg starch/ml in 10 minutes reaction time under described condition.

2.9.2 Starch transglucosylation activity

Starch transglucosylation activity was measured by iodine method. The reaction mixture contained 250 μ l of 0.2% (w/v) soluble starch, 50 μ l of 1% maltose, 100 μ l of enzyme and 600 μ l of 50 mM phosphate buffer pH 6.0. Incubation was at 30 °C for 10 minutes, reaction was stopped by boiling. Then 100 μ l aliquot was withdrawn and mixed with 1 ml of iodine solution (0.02% (w/v) I₂ in 0.2% KI). The decrease in the absorbance at 600 nm was monitored.

One unit of enzyme is defined as the amount of enzyme which produces 1% reduction in the intensity of the color of the starch-iodine complex per minute under described condition (modified from Park *et al.*, 2007).

2.9.3 Disproportionation activity

Disproportionation activity was measured by glucose oxidase method. The reaction mixture contained 30 μ l of 5% maltotriose and 20 μ l of enzyme. Incubation was at 30 °C for 10 minutes, reaction was stopped by adding 30 μ l of 1 N HCl. Then 920 μ l of glucose oxidase reagent was added, then incubated at room temperature for 10 minutes. The absorbance at 505 nm was measured.

One unit is defined as the amount of enzyme required for the production of 1 μ mol of glucose per minute under described condition.

2.9.4 Cyclization activity

Cyclization activity was measured by HPAEC-PAD analysis. The reaction mixture contained 150 μ l of 2% pea starch, 50 μ l of enzyme and 1.3 ml of phosphate buffer pH 6.0. Incubation was at 30 °C for 90 minutes, reaction was stopped by boiling. Then added 8 U of glucoamylase (Fluka, Switzerland), then incubated at 40 °C for 30 minutes and inactivated by boiling. The reaction was analyzed by HPAEC-PAD.

One unit is defined as the amount of enzyme required for the production of 1 nC*minute of CD34 per minute under described condition.

2.9.5 Hydrolytic activity

Hydrolytic activity was measured by bicinchoninic acid assay (Appendix 5) (Sinner and Puls, 1978). The reaction mixture contained 30 μ l of LR-CDs (0.5 mg/ml), 10 μ l of enzyme and 10 μ l of phosphate buffer pH 6.0. Incubation was at 30 $^{\circ}$ C for 10 minutes, reaction was stopped by adding 30 μ l of 1 N HCl. Then 950 μ l of bicinchoninic acid reagent was added, then incubated at 80 $^{\circ}$ C for 25 minutes and inactivated on ice for 5 minutes. The absorbance at 562 nm was measured.

One unit is defined as the amount of enzyme required for the production of 1 μ mol of reduced glucose per minute under described condition.

2.9.6 Coupling activity

2.9.6.1 Using DNS reagent

Coupling activity was measured by DNS reagent (Appendix 6) (Chaplin and Kennedy, 1994). The reaction mixture contained 100 μ l of LR-CDs (3 mg/ml), 100 μ l of cellobiose (1 mg/ml), 100 μ l of enzyme and 200 μ l of phosphate buffer pH 6.0. Incubation was at 30 $^{\circ}$ C for 10 minutes, reaction was stopped by boiling. Then added 8 U of glucoamylase (Fluka, Switzerland), incubated at 40 $^{\circ}$ C for 30 minutes and inactivated by boiling. Then 500 μ l of DNS reagent was added, boiled for 5 minutes, inactivated the reaction on ice for 5 minutes and added 4 ml of distilled water. The absorbance at 540 nm was measured.

One unit is defined as the amount of enzyme required for the production of 1 μ mol of reduced glucose per minute under described condition.

2.9.6.2 Using bicinchoninic acid assay

Coupling activity was measured by bicinchoninic acid assay (Appendix 5) (Sinner and Puls, 1978). The reaction mixture contained 10 μl of LR-CDs (3 mg/ml), 10 μl of cellobiose (1 mg/ml), 10 μl of enzyme and 20 μl of phosphate buffer pH 6.0. Incubation was at 30 °C for 10 minutes, reaction was stopped by boiling. Then added 2 U of glucoamylase (Fluka, Switzerland), incubated at 40 °C for 30 minutes and inactivated by boiling. Then 950 μl of bicinchoninic acid reagent was added, incubated at 80 °C for 25 minutes, inactivated on ice for 5 minutes. The absorbance at 562 nm was measured.

One unit is defined as the amount of enzyme required for the production of 1 μmol of reduced glucose per minute under described condition.

2.9.6.3 Using glucose oxidase assay

Coupling activity was measured by glucose oxidase method. The reaction mixture contained 20 μl of LR-CDs (3 mg/ml), 20 μl of cellobiose (1 mg/ml), 20 μl of enzyme and 40 μl of phosphate buffer pH 6.0. Incubation was at 30 °C for 10 minutes, reaction was stopped by boiling. Then added 2 U of glucoamylase (Fluka, Switzerland), incubated at 40 °C for 30 minutes and inactivated by boiling. Then 900 μl of glucose oxidase reagent was added, and incubated at room temperature for 10 minutes. The absorbance at 505 nm was measured.

One unit is defined as the amount of enzyme required for the production of 1 μmol of glucose per minute under described condition.

2.9.6.4 Using HPAEC-PAD analysis

Coupling activity was measured by HPAEC-PAD analysis. The reaction mixture contained 100 μ l of LR-CDs (0.25 mg/ml), 100 μ l of cellobiose (0.1 mg/ml), 50 μ l of enzyme and 250 μ l of phosphate buffer pH 6.0. Incubation was at 30 °C for 60 minutes, reaction was stopped by boiling. Then added 8 U of glucoamylase (Fluka, Switzerland), incubated at 40 °C for 30 minutes and inactivated by boiling. The reaction was analyzed by HPAEC-PAD.

One unit is defined as the amount of enzyme required for the decrease of 1 nC*minute of CD34 per minute under described condition.

2.10 Protein determination

Protein concentration was determined by the method of Bradford (1976) with bovine serum albumin as the standard protein (Appendix 7).

2.11 Polyacrylamide gel electrophoresis (PAGE)

Two types of PAGE were performed for analysis of enzyme purification, the denaturing and non-denaturing gels. The gels were visualized by coomassie blue staining. For non-denaturing gel, starch degrading activity stain was also undertaken.

2.11.1 SDS-polyacrylamide gel electrophoresis (SDS-PAGE)

The denaturing gel was performed according to the method of Bollag *et al.*, 1996. The slab gel system consisted of 0.1% SDS (w/v) in 7.5% separating and 5.0% stacking gel with Tris-glycine buffer, pH 8.0 containing 0.1% SDS as electrode buffer. The gel preparation was described in Appendix 1. Samples to be analyzed were treated with sample buffer and boiled for 5 minutes prior to loading to the gel.

The electrophoresis was run from cathode towards anode at constant current of 20 mA per slab, at room temperature on a Mini-Gel electrophoresis unit (Bio-rad). The standard molecular weight markers were phosphorylase b (MW 97,000 Da), albumin (MW 66,000 Da), ovalbumin (MW 45,000 Da), carbonic anhydrase (MW 30,000 Da), trypsin inhibitor (MW 20,100) and α -lactalbumin (MW 14,400). After electrophoresis, proteins in the gel were visualized by coomassie blue staining.

2.11.2 Non-denaturing polyacrylamide gel electrophoresis (Native-PAGE)

Discontinuous PAGE was performed on the slab gel of 7.5% separating gel and 5% stacking gel. Tris-glycine buffer, pH 8.3 was used as electrode buffer. Preparation of solution and polyacrylamide gel was described in Appendix 2. Samples to be analyzed were treated with sample buffer prior loading to the gel. The electrophoresis was run from cathode towards anode at constant current of 16 mA per slab, at 4 °C on a Mini-Gel electrophoresis unit (Bio-rad). For activity staining, the experiment was done at 30 °C.

2.11.3 Detection of protein bands

2.11.3.1 Coomassie blue staining

The gel was stained by agitating with coomassie staining solution (1% Coomassie blue R-250, 45% methanol and 10% glacial acetic acid) for 2 hours. It was then destained by destaining solution (10% methanol and 10% glacial acetic acid) for several times until gel background was clear.

2.11.3.2 Starch degrading activity staining

After electrophoresis at 4 °C, the gel was stained for activity in a 10 ml of substrate solution containing 2% (w/v) soluble starch in 50 mM phosphate buffer, pH 6.0 and incubated at 30 °C for 10 minutes. The gel was rinsed several times with distilled water and 10 ml of iodine solution (0.2% I₂ in 2% KI) was added for color development at room temperature. The clear zone on the dark blue background indicated starch degrading activity of enzyme.

2.12 Determination of the isoelectric point by isoelectric focusing polyacrylamide gel electrophoresis (IEF)

2.12.1 Preparation of gel support film

A few drops of water were pipetted onto the plate. The hydrophobic side of the gel support film was then replaced against the plate and flatly rolled with a test tube to remove excess water and bubbles. Subsequently, it was placed on the casting tray with the gel support film face down resting in the space bars.

2.12.2 Preparation of the gel

A monomer-ampholyte solution was prepared (Appendix 3) and degassed for 5 minutes under vacuum. A catalyst solution (Appendix 3) was added to the degassed monomer solution and swirled gently. The mixed solution was carefully pipetted into the space between the glass plate and casting tray with a smooth flow rate to prevent air bubbles. The gel was left to polymerize for about 45 minutes, and then lifted from the casting tray using a spatula. The gel was fixed on the gel support film. A template for sample application was placed in the middle of the polymerized gel and ready for use.

2.12.3 Sample application and electrophoresis gel

The sample (1-4 μl) was loaded on the template. Standard protein markers with known pI's in the range of 3-10 were included in each run. Samples were allowed to diffuse into the gel for 5 minutes and the template was carefully removed from the gel. The gel with the absorbed samples was turned upside-down and directly placed on top of the graphite electrodes. Focusing was carried out stepwise under constant voltage conditions: 100 V for 30 minutes, 200 V for 15 minutes and finally 400 V for an additional 120 minutes. After completing electrofocusing, the gel was stained with coomassie brilliant blue R-250. The pI's of sample proteins were determined using a standard curve constructed from the pI's of the standard proteins and their migrating distance from cathode. The standard proteins consisted of amyloglucosidase (3.50), soybean trypsin inhibitor (4.55), β -lactoglobulin A (5.20), bovine carbonic anhydrase B (5.85), human carbonic anhydrase B (6.55), horse myoglobin-acidic band (6.85), horse myoglobin-basic band (7.35), lentil lectin-acidic band (8.15), lentil lectin-middle band (8.45), lentil lectin-basic band (8.65) and trypsinogen (9.30).

2.13 Characterization of amyloamylase

2.13.1 Molecular weight determination

2.13.1.1 Determination from SDS-polyacrylamide gel electrophoresis (SDS-PAGE)

The subunit molecular weight of purified amyloamylase was determined by SDS-PAGE as described in section 2.11.1. The standard curve of protein markers was constructed from the molecular weight of the standard proteins and their relative mobility (R_f).

2.13.1.2 Determination from gel filtration column chromatography

The molecular weight of purified amyloamylase was determined by gel filtration on Sephacryl S-200 column (2 x 80 cm) with 50 mM phosphate buffer, pH 7.4 containing 150 mM NaCl at the flow rate of 0.5 ml/minute. The marker proteins were: catalase (MW 232,000 Da), bovine serum albumin (MW 66,000 Da) and ovalbumin (MW 44,000 Da).

2.13.2 Effect of temperature on amyloamylase activity

The effect of temperature on the amyloamylase activity was examined in 50 mM phosphate buffer, pH 6.0 at various temperatures in the range of 20-60 °C. The activity was determined as described in section 2.9.2. The results were shown as a percentage of the relative activity. The temperature at which maximum activity was observed for each reaction was set as 100%.

2.13.3 Effect of temperature on amyloamylase stability

The effect of temperature on the stability of the enzyme was determined at 20-60 °C. The purified enzyme was incubated at various temperatures for 0-120 minutes before determination of enzyme activity under the standard assay condition as described in section 2.9.2. The results were shown as a percentage of the relative activity. The highest activity was defined as 100%.

2.13.4 Effect of pH on amyloamylase activity

The effect of pH on the amyloamylase activity was determined at 30 °C at various pHs. The buffers at concentration of 50 mM were used: acetate buffer, pH 4.0-6.0; phosphate buffer, pH 6.0-8.0 and Tris-HCl, pH 7.0-9.0. The activity was

determined as described in section 2.9.2. The results were shown as a percentage of the relative activity. The pH at which maximum activity was observed for each reaction was set as 100%.

2.13.5 Effect of pH on amyloamylase stability

The effect of pH on the stability of the enzyme was determined at pH 4.0-9.0. The purified enzyme was incubated with buffers of various pHs at 30 °C for 1 hour before determination of enzyme activity under the standard assay condition as described in section 2.9.2. The buffers used were as in 2.13.4. The results were shown as a percentage of the relative activity. The highest activity was defined as 100%.

2.13.6 Transglucosylation reaction on linear maltooligosaccharides

The transglucosylation reaction on linear maltooligosaccharide of amyloamylase was determined using glucose (G1), maltose (G2), maltotriose (G3), maltotetraose (G4), maltopentaose (G5), maltohexaose (G6) and maltoheptaose (G7) as substrate. The reaction mixtures contained 0.2% (w/v) substrate and 0.25 U of enzyme in 50 mM phosphate buffer, pH 6.0. Incubation was at 30 °C for 2 hours, reaction was stopped by boiling. Then 10 µl aliquot was withdrawn and analyzed by TLC as described in section 2.15.1.

2.13.7 Synthesis of large-ring cyclodextrins

The synthesis of large-ring cyclodextrins was determined using pea starch as substrate. Two important parameters, incubation time and enzyme amount, were varied.

2.13.7.1 Effect of incubation time

The reaction mixtures contained 0.2% pea starch and 0.05 U or 0.15 U (starch degrading activity) of enzyme in 50 mM phosphate buffer, pH 6.0. The reactions were incubated at 30 °C at various time points for 1-24 hours, reaction was stopped by boiling. Then added 4 U of glucoamylase (Fluka, Switzerland) and incubated at 40 °C for 2 hours and inactivated by boiling. The reaction products were analyzed by HPAEC-PAD as described in section 2.15.2.

2.13.7.2 Effect of the amount of enzyme

The reaction mixtures contained 0.2% pea starch and various amounts of enzyme (0.05 U, 0.1 U and 0.15 U of starch degrading activity) in 50 mM phosphate buffer, pH 6.0. The reactions were incubated at 30 °C at time point 1 and 24 hours, reactions were stopped by boiling. Then added 4 U of glucoamylase (Fluka, Switzerland), incubated at 40 °C for 2 hours and inactivated by boiling. The reaction products were analyzed by HPAEC-PAD as described in section 2.15.2.

2.13.8 Time course of hydrolysis reaction

The glucose released from hydrolytic reaction was determined by bicinchoninic acid assay (Sinner and Puls, 1978). The reaction mixture contained 30 µl of 0.5 mg/ml LR-CDs, 10 µl of enzyme and 10 µl of phosphate buffer pH 6.0. Incubation was at 30 °C at various time points for 1-24 hours, reaction was stopped by adding 30 µl of 1 N HCl. Then the amount of glucose was determined by bicinchoninic acid assay as described in section 2.9.4.

2.13.9 Substrate specificity of amyloamylase

The ability of enzyme to catalyze maltooligosaccharides was determined using maltose (G2), maltotriose (G3), maltotetraose (G4), maltopentaose (G5), maltohexaose (G6) and maltoheptaose (G7) as substrate. The reaction mixtures contained 50 mM of substrate and 0.2 U of enzyme in 50 mM phosphate buffer, pH 6.0. Incubation was at 30 °C for 10 minutes, reaction was stopped by boiling. Then the amount of glucose was determined by glucose oxidase method as described in section 2.9.3.

2.13.10 Determination of kinetic parameters

Kinetic parameters of the disproportionation activity were determined by incubating various concentrations of maltotriose (G3), ranging from 0-200 mM at 30 °C for 5 minutes in 50 mM phosphate buffer, pH 6.0. The suitable amount of amyloamylase used was 1 µg of each purified amyloamylase. The reaction was stopped by boiling for 10 minutes. Then the amount of glucose was determined by glucose oxidase method as described in section 2.9.3. Kinetic parameters were determined from the Michaelis-Menten equation, using Lineweaver-Burk plot.

2.14 Precipitation of large-ring cyclodextrins

2.14.1 The large-scale production of large-ring cyclodextrins

The reaction mixture 500 ml contains 0.2% pea starch and 12 U (starch degrading activity) of enzyme in 50 mM phosphate buffer, pH 6.0. The reaction was incubated at 30 °C for 24 hours, reaction was stopped by boiling. Then added 175 U of glucoamylase (Fluka, Switzerland) and incubated at 40 °C for 24 hours and inactivated by boiling.

2.14.2 Precipitation of large-ring cyclodextrins

Five hundred milliliter of large-scale production (section 2.14.1) was filtrated and concentrated at 50 °C under vacuum pressure at 30 mbar until volume reduced to 100 ml. Then 3 times volume of acetone was added to the concentrated reaction and left at room temperature overnight. The supernatant was removed and the precipitate was washed by 50 ml of acetone. The precipitate was further stirred manually using a spatula. The supernatant was removed and washing was repeated twice with acetone. The supernatant was removed, then washed again by 20 ml of ethanol and stirred manually with spatula. The precipitate was dispersed and finely grounded by magnetic stirred for 1 hour. The supernatant was removed and the precipitate was dried in the desiccator. The large-ring cyclodextrins pellet was dissolved with water and analyzed by HPAEC-PAD as described in section 2.15.2.

2.15 Analysis of oligosaccharides and large-ring cyclodextrins

2.15.1 Thin layer chromatography (TLC)

The analysis of oligosaccharides by TLC was performed as described by Dawson *et al.*, 1986. The TLC system was n-propanol : ethyl acetate : water (7:1:2) by volume. Detection of components on a thin layer chromatogram can readily be achieved using a non-selective charring technique by heating the chromatogram at 110 °C for 15 minutes after spraying it with a reagent prepared from concentrated sulphuric acid : ethanol (1:9) (Kennedy and Pagliuca, 1994).

2.15.2 High performance anion exchange chromatography with pulses amperometric detection (HPAEC-PAD)

HPAEC-PAD was used to analyze large-ring cyclodextrins (Koizumi *et al.*, 1999). The model ICS 3000 system (Dionex, USA) was used with Carbopac PA-100 column (4 x 250 mm, Dionex, USA). A sample of 25 μ l was loaded onto the column and eluted with a linear gradient of sodium nitrate (0-2 minutes, increasing from 4% to 8%; 2-10 minutes, increasing from 8% to 18%; 10-20 minutes, increasing from 18% to 28%; 20-40 minutes, increasing from 28% to 35%; 40-55 minutes, increasing from 35% to 45%; 55-60 minutes, increasing from 45% to 63%) in 150 mM NaOH with a flow rate of 1 ml/minute. The size of LR-CD products were compared with standard LR-CDs (CD20 and CD21).

2.16 Mass spectrometry (MS)

The mixture of large-ring cyclodextrins was analyzed by Matrix-assisted laser desorption/ionization-time of flight mass spectrometry (MALDI-TOF MS) (Endo *et al.*, 2007). The MALDI-TOF MS profile was recorded on a “Autoflex” II system (Bruker Daltonic, Germany) at the Institute of Medical Physics and Biophysics, Faculty of Medicine, University of Leipzig, Germany, using 2,5-dihydroxybenzoic acid as a matrix.

CHAPTER III

RESULTS

3.1 Identification and expression of amyloamylase gene (*malQ*) from *Corynebacterium glutamicum* ATCC 13032

3.1.1 Extraction of chromosomal DNA

The genomic DNA was extracted and checked by agarose gel electrophoresis (Figure 3.1 Lane 1). The result showed that the size of DNA template was larger than 10 kb. The ratio of $A_{260/280}$ values was 1.8 indicated that the purity of this extracted DNA was sufficient to be used as template for PCR amplification.

3.1.2 *malQ* amplification and preparation

The product from the PCR amplification was found as a single band on agarose gel electrophoresis shown in Figure 3.2 Lane 2. The size of PCR product was 2.1 kb as expected for *malQ*. This product was then subjected to digestion with the restriction enzymes *NdeI* and *XhoI*.

3.1.3 Transformation

The 2.1 kb amplified gene fragment was digested with *NdeI* and *XhoI*, ligated with *NdeI-XhoI* digested pET-19b vector (Appendix 11) by T4 DNA ligase. The recombinant plasmid was constructed and transformed into the competent cells of *E. coli* BL21(DE3) by electroporation as described in section 2.4.7. One hundred μ l of the transformant was spread on LB agar plate containing 100 μ g/ml ampicillin and incubated at 37 °C for overnight. The *E. coli* BL21(DE3) containing pET-19b vector harboring *malQ* was grown on the plate. To verify the insertion of PCR product into

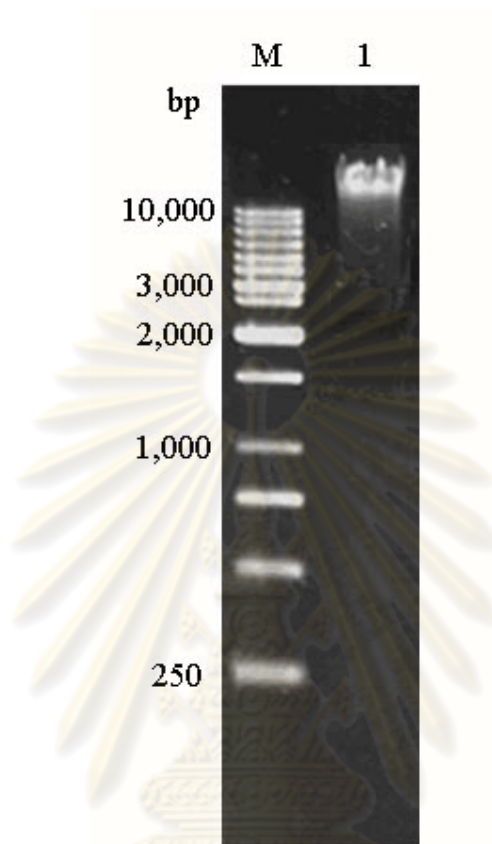


Figure 3.1 Agarose gel electrophoresis of genomic DNA of *Corynebacterium glutamicum* ATCC 13032. The DNA samples were separated on 1% agarose gel and visualized by ethidium bromide staining.

Lane M = GeneRuler™ 1 kb DNA ladder (Fermentas, Canada)

Lane 1 = Genomic DNA of *Corynebacterium glutamicum* ATCC 13032

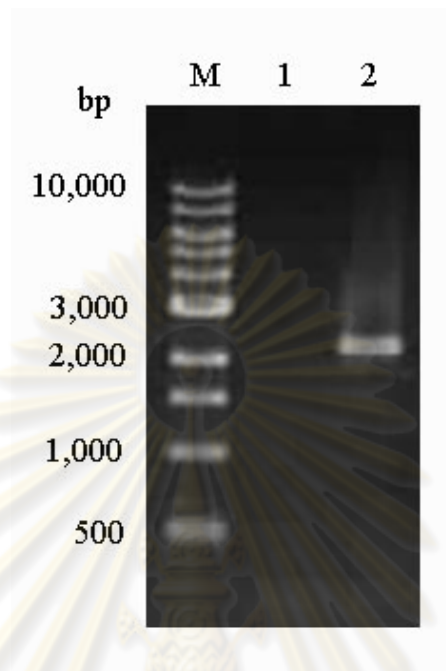


Figure 3.2 Agarose gel electrophoresis of amplified DNA. The DNA samples were separated on 1% agarose gel and visualized by ethidium bromide staining.

Lane M = 1 kb DNA ladder (New England BioLabs Inc., USA)

Lane 1 = Negative control

Lane 2 = Amplified PCR product of *malQ* fragment (2.1 kb)

ศูนย์วิทยทรัพยากร
จุฬาลงกรณ์มหาวิทยาลัย

pET-19b, the transformant was picked for plasmid extraction and digested with *Nde*I-*Xho*I as described in section 2.4.4. The agarose gel electrophoresis pattern of the recombinant plasmid containing *malQ* is shown in Figure 3.3. The size of linear form of the recombinant plasmid and 2.1 kb corresponded to the expected size for the PCR product of *malQ*.

3.1.4 Nucleotide sequencing

To confirm whether the inserted fragment was indeed *malQ*, the recombinant plasmid (p19AM) was subjected to DNA sequencing by using the primers of T7 promoter and T7 terminator which can sequence through the 5'-terminus and 3'-terminus of the inserted *malQ* in plasmid, respectively. The sequence was extended by using primer fCGAM2 and rCGAM2 as described in section 2.5.3 and searched for overlapping regions. The nucleotide sequence of *malQ* and deduced amino acid sequence are shown in Figure 3.4. The nucleotide sequence consisted of *malQ* (2,121 bp) and his-tag residues from pET-19b (69 bp), and was deduced to 729 amino acid residues.

The alignment of the obtained deduced amino acid sequence with other published 4α GTases which were reported about large-rings cyclodextrins synthesis in NCBI and Swiss-Prot amino acid database was performed (Figure 3.5 to 3.9). The result of the alignment is shown in Table 3.1. The amyloamylase from *C. glutamicum* was the largest, the size was similar to amyloamylase from *E. coli*, however, the similarity between these two amyloamylases was only 45%. And when compared amyloamylase from *C. glutamicum* with other published 4α GTases, amino acid sequence similarity was very low, in the range of 28-33%.

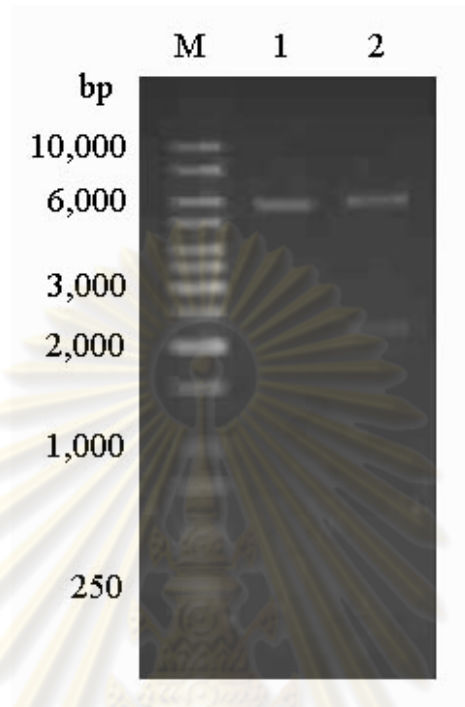


Figure 3.3 Agarose gel electrophoresis of recombinant *malQ* inserted in pET-19b vector. The DNA samples were separated on 1% agarose gel and visualized by ethidium bromide staining.

Lane M = GeneRuler™ 1 kb DNA ladder (Fermentas, Canada)

Lane 1 = pET-19b vector digested with *NdeI* and *XhoI*

Lane 2 = pET-19b vector harboring *malQ*, digested with *NdeI* and *XhoI*

จุฬาลงกรณ์มหาวิทยาลัย

```

      10      20      30      40      50      60
ATGGGCCATCATCATCATCATCATCATCACAGCAGCGGCCATATCGACGACGAC
M G H H H H H H H H H S S G H I D D D
      70      80      90     100     110     120
GACAAGCATATGACTGCTCGCAGATTTTTGAATGAACTCGCCGATCTCTACGGCGTAGCA
D K H M T A R R F L N E L A D L Y G V A
      130     140     150     160     170     180
ACTTCCTACACTGATTACAAAGGTGCCCATATTGAGGTCAGCGATGACACATTAGTGAAA
T S Y T D Y K G A H I E V S D D T L V K
      190     200     210     220     230     240
ATCCTGCGTGCTCTGGGTGTGAATTTAGATACAAGCAACCTCCCCAACGATGACGCTATC
I L R A L G V N L D T S N L P N D D A I
      250     260     270     280     290     300
CAACGCCAAATTGCCCTCTTCCATGATCGAGAGTTCACTCGCCACTGCCTCCATCGGTG
Q R Q I A L F H D R E F T R P L P P S V
      310     320     330     340     350     360
GTTGCAGTTGAAGGTGATGAACTAGTTTTCCCGGTGCATGTGCACGACGGTTCCCCTGCA
V A V E G D E L V F P V H V H D G S P A
      370     380     390     400     410     420
GATGTCCACATCGAATTGGAAGACGGCACGCAGCGGGATGTTTCTCAGGTGGAAAAGTGG
D V H I E L E D G T Q R D V S Q V E N W
      430     440     450     460     470     480
ACAGCGCCACGGGAAATTGATGGGATTAGGTGGGGCGAGGCATCGTTTAAGATTCCCTGGT
T A P R E I D G I R W G E A S F K I P G
      490     500     510     520     530     540
GATCTCCCCTTGGGTTGGCACAAGCTTCACCTTAAATCCAATGAACGCTCAGCTGAGTGC
D L P L G W H K L H L K S N E R S A E C
      550     560     570     580     590     600
GGTTTGATCATCACCCCGGCTCGTCTGTCTACTGCTGATAAGTATCTTGATTCCCCTCGC
G L I I T P A R L S T A D K Y L D S P R
      610     620     630     640     650     660
AGTGGTGTGATGGCGCAGATCTACTCTGTGCGTTCCACGTTGTCGTGGGGCATGGGTGAT
S G V M A Q I Y S V R S T L S W G M G D
      670     680     690     700     710     720
TTCAATGATTTAGGAAAAGTTGGCAAGTGTGGTTGCCAGGATGGAGCAGACTTCCTGCTC
F N D L G N L A S V V A Q D G A D F L L
      730     740     750     760     770     780
ATCAACCCCATGCACGCTGCAGAGCCGCTGCCTCCTACTGAGGACTCTCCTTATCTGCC
I N P M H A A E P L P P T E D S P Y L P
      790     800     810     820     830     840
ACAACCAGGCGCTTTATCAACCCGATCTACATTCGGGTAGAAGATATTCGGAGTTTAAT
T T R R F I N P I Y I R V E D I P E F N
      850     860     870     880     890     900
CAGCTTGAGATTGATCTACGCGATGATATCGCAGAGATGGCTGCCGAATTCCGCGAACGC
Q L E I D L R D D I A E M A A E F R E R
      910     920     930     940     950     960
AATCTGACCTCAGACATCATTGAGCGCAATGACGTCTACGCTGCAAAGCTTCAAGTGCTG
N L T S D I I E R N D V Y A A K L Q V L

```

Figure 3.4 Nucleotide and deduced amino acid sequences of amyломaltase from *Corynebacterium glutamicum* ATCC 13032. The underlined letters indicate residues containing his-tag.

```

          970          980          990          1000          1010          1020
CGCGCCATTTTTGAAATGCCTCGTTCCAGCGAACGTGAAGCCAACCTTTGTCTCCTTCGTG
R A I F E M P R S S E R E A N F V S F V
    1030          1040          1050          1060          1070          1080
CAACGGGAAGGCCAAGGTCTTATTGATTTTCGCCACCTGGTGC GCGGACCGCGAAACTGCA
Q R E G Q G L I D F A T W C A D R E T A
    1090          1100          1110          1120          1130          1140
CAGTCTGAATCTGTCCACGGAACCTGAGCCAGACCGCGATGAGCTGACCATGTTCTACATG
Q S E S V H G T E P D R D E L T M F Y M
    1150          1160          1170          1180          1190          1200
TGGTTGCAGTGGCTATGTGATGAGCAGCTGGCGGCAGCTCAAAAAGCGCGCTGTCGATGCC
W L Q W L C D E Q L A A A Q K R A V D A
    1210          1220          1230          1240          1250          1260
GGAATGTCGATCGGCATCATGGCAGACCTGGCAGTTGGTGTGCATCCAGGTGGTGTGAT
G M S I G I M A D L A V G V H P G G A D
    1270          1280          1290          1300          1310          1320
GCCCAGAACCTCAGCCACGTACTTGTCTCCGGATGCGTCAGTGGGCGCCCCACCAGATGGA
A Q N L S H V L A P D A S V G A P P D G
    1330          1340          1350          1360          1370          1380
TACAACCAGCAGGGCCAAGACTGGTCCCAGCCACCATGGCATCCAGTGCCTCTTGCAGAG
Y N Q Q G Q D W S Q P P W H P V R L A E
    1390          1400          1410          1420          1430          1440
GAAGGCTACATTCCGTGGCGTAATCTGCTGCGCACTGTGCTGCGTCACTCCGGCGGAATC
E G Y I P W R N L L R T V L R H S G G I
    1450          1460          1470          1480          1490          1500
CGCGTGGACCACGTTCTTGGTTTGTTCAGGCTCTTTGTTCATGCCACGCATGCAATCCCCT
R V D H V L G L F R L F V M P R M Q S P
    1510          1520          1530          1540          1550          1560
GCTACGGGCACCTATATCCGCTTTCGACCATAATGCGTTGGTAGGCATTCTAGCCCTAGAA
A T G T Y I R F D H N A L V G I L A L E
    1570          1580          1590          1600          1610          1620
GCAGAACTCGCAGGCGCCGTTGTCATTGGTGAAGATCTGGGAACGTTTGGCCTTGGGTA
A E L A G A V V I G E D L G T F E P W V
    1630          1640          1650          1660          1670          1680
CAAGATGCATTGGCTCAGCGTGGCATCATGGGCACCTCGATCCTATGGTTTCGAGCATTCC
Q D A L A Q R G I M G T S I L W F E H S
    1690          1700          1710          1720          1730          1740
CCAAGCCAGCCGGGTCTCGCCGCCAGGAAGAGTATCGTCCGCTGGCCTTGACCACTGTG
P S Q P G P R R Q E E Y R P L A L T T V
    1750          1760          1770          1780          1790          1800
ACCACTCATGATCTCCCTCCGACTGCTGGTTATTGGAGGGCGAGCACATTGCTCTTCGT
T T H D L P P T A G Y L E G E H I A L R
    1810          1820          1830          1840          1850          1860
GAGCGATTGGGGGTGCTCAACACTGATCCTGCTGCAGAACTCGCTGAGGATCTGCAGTGG
E R L G V L N T D P A A E L A E D L Q W
    1870          1880          1890          1900          1910          1920
CAAGCGGAGATCCTTGATGTGCGAGCATCTGCCAACGCATTGCCAGCCCGGGAATACGTG
Q A E I L D V A A S A N A L P A R E Y V

```

Figure 3.4 (continued) Nucleotide and deduced amino acid sequences of amylo maltase from *Corynebacterium glutamicum* ATCC 13032.

```

1930      1940      1950      1960      1970      1980
G G A C T C G A A C G C G A T C A G C G C G G T G A G T T G G C T G A G C T G T T G G A A G G C C T G C A C A C T T T C
G L E R D Q R G E L A E L L E G L H T F
1990      2000      2010      2020      2030      2040
G T T G C G A A A C C C C T T C A G C A C T G A C C T G T G T C T G C T T G G T A G A C A T G G T C G G T G A A A A G
V A K T P S A L T C V C L V D M V G E K
2050      2060      2070      2080      2090      2100
C G G G C A C A G A A T C A G C C G G G C A C A A C G A G G G A T A T G T A T C C C A A C T G G T G T A T C C C A C T G
R A Q N Q P G T T R D M Y P N W C I P L
2110      2120      2130      2140      2150      2160
T G T G A C A G C G A A G G C A A C T C C G T G C T C A T T G A A T C G C T G C G T G A A A A T G A G C T G T A T C A C
C D S E G N S V L I E S L R E N E L Y H
2170      2180      2190
C G T G T G G C A A A G G C A A G C A A G C G A G A T T A G
R V A K A S K R D *

```

Figure 3.4 (continued) Nucleotide and deduced amino acid sequences of amyломaltase from *Corynebacterium glutamicum* ATCC 13032.

* indicates termination codon

ศูนย์วิทยทรัพยากร
จุฬาลงกรณ์มหาวิทยาลัย

CG	1	MTARRFLNELADLYGVATSYTDYKGAHIEVSDDTLVKILRALGVNLDTSNLPNDDAIQRQ	60
		:.: .: .: .: .: .	
TA	1	M-----ELPRAFGLLLHPTSLPG-----	18
CG	61	IALFHDREFTRPLPPSVVAVEGDELVFPVHVHDGSPADVHIELEDGTQRDVSVQVENWTAP	120
		.: .: .: .: .: .	
TA	19	-----PYGVGVLGREA-----RDFLRFL-----	36
CG	121	REIDGIRWGEASFKIPGDLPLGWHKHLHLSNERSAECGLIITPARLSTADKYLDSPRSGV	180
		: .: .: .: .: .: .	
TA	37	KEAGGRYWQV-----LPLG-----PTGYGDSP----	58
CG	181	MAQIYSVRSTLSWGMGDFNDLGNLASVVAQDGADFLINPMHAAEPLPPTEDSPYLPTR	240
		.: .: .: .: .: .	
TA	59	----YQSFSFAFA-----GN-----PYLIDLR	75
CG	241	RFINPIYIRVEDIPEFNQLEIDLRDDIAEMAAEFRENRNLTSDIIERNVDVYAAKLQVLRAI	300
	: .: .: .: .: .	
TA	76	PLAERGYVRLLED-PGFPQGRVDYG-----LLYAWKWPALKEAFRGFKEKASPEEREAFAA	129
CG	301	FEMPRSSEREANFVSFVQREGQGLIDFATWCADRETAQSESVHGTEPDRDELTMFYMWLQ	360
		.: .: .: .: .: .	
TA	130	FREREAWLEDYALFMALKGAHGGLPWNRWPLPLRKREEKALREAKSALAEVAFHAFTQ	189
CG	361	WLCDEQLAAAQKRAVDAGMSIGIMADLAVGVHPGGADAQ-----NLSHVLAPDASVGAP	414
		.: .: .: .: .: .	
TA	190	WLFFRQWGALKAEAEALG--IRIIGDMPIFVAEDSAEVWAHPPEWFLDDEGRPTVVAGVP	247
CG	415	PDGYNQGGQDWSQPPWHPVRLAEEGYIPWRNLLRRTLVRHSGGIRVDHVLGLFRLFVMPRM	474
		.: .: .: .: .: .	
TA	248	PDYFSETGQRWGNPLYRWDVLEREGFSFWIRRLKALELPHLVRIDHFRGFEEAYWEIPAS	307
CG	475	QSPAT-GTYIRFDHNALVGILALELAGAVVIGEDLGTFFEPWVDALAQRGIMGTSILW	533
	: .: .: .: .	
TA	308	CPTAVEGRVWKAPGEKL--FQKIQEVFGEVPLAEDLGVITPEVEALRDRFGLPGMKVLQ	365
CG	534	FEHSPSQPGRRQEEYRPLALTTVTT--HDLPPTAGYLEGEHIALRERLGLVNTDPAEEL	591
		.: .: .: .: .: .	
TA	367	FAFDDGMENPFLPHNYPAGRNVVYTGTHDNDTTLGWYR-----TATPHEK	411
CG	592	AEDLQWQAEILDVAASANALP-AREYVGLERDQRGELAELEGLHTFVAKTPSALTCVCL	650
		.: .: .: .: .: .	
TA	412	AFMARYLADWGITFREEEVVPWALMHLGMKSVAR-----LAVYPQDVLAL-----	457
CG	641	VDMVGEKRAQNQPGTTRDMPNWCIPLCDSEGNVLIESLRENELYHRVAKASKRD	706
		.: .: .: .: .: .	
TA	453	----GSEARMNYPGRPSG--NWAWRLLPGELSPEHGARLRA-----MAEATERL	500

Figure 3.5 Amino acid sequence alignment of amyloamylase from *Corynebacterium glutamicum* ATCC 13032 (CG) compared with amyloamylase from *Thermus aquaticus* (TA) using Stretcher program. Amino acid conservation across the aligned sequences is shown as (markup line) identical, (colon) conserved substitutions and (dot) semi-conserved substitutions. Catalytic residues are shown as highlight. The letters in squared box indicate Tyr-172 and Tyr-54 residues of *C. glutamicum* and *T. aquaticus*, respectively.

CG	1	MTARFLNELADLYGVATSYTDYKGAHIEVSDDTLVKILRALGVNLDTSNLPNDDAIQRQ	60
		:. . : . . . : .	
TT	1	M-----ELPRAFGLLLHPTSLPG-----	18
CG	61	IALFHDREFTRPLPPSVVAVEGDELVFPVHVHDGSPADVHELEDGTQRDVSQVENWTAPR	120
	 : . .	
TT	19	-----PYGVGVLGQEA-----RDFLRFL-----	36
CG	121	IEIDGIRWGEASFKIPGDPLGWHKHLHLSNERSAECGLIITPARLSTADKYLDSPRSGV	180
		: 	
TT	37	KEAGGRYWQV-----LPLG-----PTGYGDSP----	58
CG	181	MAQIYSVRSTLSWGMGDFNDLGNLASVVAQDGADFLINPMHAAEPLPPTEDSPYLPTR	240
	 : 	
TT	59	----YQSFSAFA-----GN-----PYLIDLR	75
CG	241	RFINPIYIRVEDIPEFNQLEIDLRDDIAEMAAEFRENLTSDIIERNDVYAAKLQVLRAI	300
	 : : : :	
TT	76	PLAERGYVRLLED-PGFPQGRVDYG-----LLYAWKWPALKEAFRGFKKASPEEREAFAA	129
CG	301	FEMPRSSEREANFVSFVQREGQGLIDFATWCADRETAQSESVHGTEPDRDELTMFYMWLQ	360
	 : : : : . .	
TT	130	FREREAWLEDYALFMALKGAHGGLPWNRWPLPLRKREEKALREAKSALAEVAFHAFTQ	189
CG	351	WLCDEQLAAAQKRAVDAGMSIGIMADLAVGVHPGGADAQ-----NLSHVLAPDASVGAP	414
	 : : : . . . : 	
TT	180	WLFFRQWGALKAEAEALG--IRIIGDMPIFVAEDSAEVWAHPEWFHLDDEGRPTVVAGVP	247
CG	415	PDGYNQQGQDWSQPPWHPVRLAEEGYIPWRNLLRRTLVRHSGGIRVDHVLGLFRLFVMPRM	474
		. . : : : : : : . .	
TT	248	PDYFSETGQRWGNPLYRWDVLEREGFSFWIRRLKALELPHLVRIDHFRGFEEAYWEIPAS	307
CG	445	QSPAT-GTYIRFDHNALVGILALELAGAVVIGEDLGTFFEPWQDALAQRGIMGTSILW	533
	 : : : : . . . : .	
TT	278	CPTAVEGRWVKAPGEKL--FQKIQEVFGEVPLAEDLGVITPEVEALRDRFGLPGMKVLQ	365
CG	504	FEHSPSQPGRRQEEYRPLALTTVTT--HDLPPTAGYLEGEHIALRERLGLVNTDPAEEL	591
	 :	
TT	326	FAFDDGMENPFLPHNYPAHGRVVVYTGTHDNDTTLGWYR-----TATPHEK	411
CG	592	AEDLQWQAEILDVAASANALP-AREYVGLERDQRGELAELEGLHTFVAKTPSALTCVCL	650
	 : : : . . . : :	
TT	412	AFMARYLADWGITFREEEVVPWALMHLGMSVAR-----LAVYPQDVLAL-----	457
CG	641	VDMVGEKRAQNQPGTTRDMPNWCIPLCDSEGNVLIESLRENELYHRVAKASKRD	690
	 : : : .	
TT	453	----GSEARMNYPGRPSG--NWAWRLLPGELSPEHGARLRA-----MAEATERL	490

Figure 3.6 Amino acid sequence alignment of amyloamylase from *Corynebacterium glutamicum* ATCC 13032 (CG) compared with amyloamylase from *Thermus thermophilus* (TT) using Stretcher program. Amino acid conservation across the aligned sequences is shown as (markup line) identical, (colon) conserved substitutions and (dot) semi-conserved substitutions. Catalytic residues are shown as highlight.

CG	1	MTARRFLNELADLYGVATSYTDYKGAHIEVSDDTLVKILRALGVNLDTSNLPNDDAIQRQ	60
AA	1	M-----RLAGILLHVTSLPS-----	15
CG	61	IALFHDREFTRPLPPSVVAVEGDELVFPVHVHDGSPADVHIELEDGTQRDVQSQVENWTAP	120
AA	16	-----PYGIGDLGKE-----AY	27
CG	121	REIDGIRWGEASFKIPGDLPLGWHKHLHLSNERSAECGLIITPARLSTADKYLDSPRSGV	180
AA	28	RFLDFLK--ECGFSLWQVLP-----NPTSLEAG-----NSP----	57
CG	181	MAQIYSVRSTLSWGMGDFNDLGNLASVVAQDGADFLINPMHAAEP-LPPTEDSPYLPTT	239
AA	58	---YSSNSLFA-----GN-----YVLIDPEELLEEDLIKERDLKRFPLG	93
CG	240	RRFINPIYIRVEDIPEFNQLEIDLRRDIAEMAAE-FRERNLTSDIERNVDVYAAKLQVLR	298
AA	94	EALYEVVY-----EYKELLEKAFKNFRFELLEDFLKEHSYWLDRDYALYM	139
CG	299	AIFEMPRSSEREANFVSFVQREGQGLIDFATWCADRETAQSESVHGTEPDRDELTMFYMW	358
AA	140	AIKE-----EEGK---EWYEWDEELKRREKEALKRVLNKLKGRFYFHFV	180
CG	359	LQWLCDQLAAAQKRAVDAGMSIGIMADLAVGVHPGGADAQN-----LSHVLAPDASVG	412
AA	181	VQVFVFKQWEKLRRYARERGISI--VGDLPYPSYSSADVWTNPELFLKLDGDLKPLFVAG	238
CG	413	APPDGYNQGGDWSQPPWHVRLAEEGYIPWRNLLRVLRLHSGGIRVDHVLGLFRLFVMP	472
AA	239	VPPDFFSKTGQLWGNPVYNWEEHEKEGFRWWIRRVHHLKLFDFLRLDHFGRGFEAYWEVP	298
CG	473	RMQSPAT-GTYIRFDHNALVGILALEAELAGAVVIGEDLGTFFEPWVQDALAQRGIMGTSI	531
AA	299	YGEETAVNGRWVKAPGKTL--FKKLLSYFPKNPFIADLGFITDEVRYLRETFKIPGSRV	356
CG	532	LWFEH--SPSQGPRRQEEYRPLALTVTTHDLPPTAGYLEGEHIALRERLGVLNTDPAA	589
AA	357	IEFAYDKSEHLPHNVEENN--VYTTSTHDLPPIRGWFENLGEESRKRLF-----	405
CG	590	ELAEDLQWQAEILDVAASANALPAREYVGLERDQRGELAEELLEGLHTFVAKTPSALTVCVC	649
AA	406	-----EYLGREIKEEKVNEELIRLV--LISRAKFAIQMQ	438
CG	650	LVDMPVEKRAQNQPGTTRDMYPNWCIPLCDSEGNVLIESLRENELYHRVAKASKRD-	706
AA	439	DLLNLGNearmNYPGRP---FGNWRWRIKE-----DYTQKKEFIKKLLGIYGREV	485

Figure 3.7 Amino acid sequence alignment of amylomaltase from *Corynebacterium glutamicum* ATCC 13032 (CG) compared with amylomaltase from *Aquifex aeolicus* (AA) using Stretcher program. Amino acid conservation across the aligned sequences is shown as (markup line) identical, (colon) conserved substitutions and (dot) semi-conserved substitutions. Catalytic residues are shown as highlight.

CG	1	MTARFLNELADLYGVATSYTDYKGAHIEVSDDTLVKILRALGVNLDTSNLPNDDAIQRQ	60
	:..:.....: ..: .:.: .	
PT	1	MAIHTCFSLIP-----SSFSSPKLPYPKNTTFQ-----SPTPK---LSRP	37
CG	61	IALFHDREFTRPLPPSVVAVEGDELVPVHVHDGSPA-DVHIELEDGTQRDVSQVENWTA	119
		..: :.....: ... : :..... .. . :..... . :.....:..	
PT	38	TFMF-DRKGSFQNGTAAVPAVGED--FPIDYADWLPKRDPNDRRRAGI---LLHPTSFPG	91
CG	120	PREIDGIRWGEASFKIPGDLPLGWHLHLKSNERSAECGLIITPARLSTADKYLDSPRSG	179
		..:..: ..: : . :	
PT	92	PYGIGDL--GPQAFKF-----LDW--LHLAGCSLWQVPLPV-PPGKRGNED---GSPYSG	138
CG	180	VMAQIYSVRSTLSWGMGDFNDLGNLASVVAQDGADFLINPMHAAEPLPPTEDSPYLPTT	239
		.. : : : . :	
PT	139	QDA-----NCGNTLLISLEELVDDGLLKMEELPEPLPT--DRVNYSTI	179
CG	240	RRFINPIYIRVEDIPEFNQLEIDLRDDIAEMAAEFRERNLTSDIIEERNVYAAKQLVRA	299
	: :..... :..... : : :..... : : : : :... : :	
PT	180	SEIKDPLITKAA--KRLLSSEGELKQLENFR---RDPNISSWL--EDAAYFAAI-----	227
CG	300	IFEMPRSSEREANFVSFVQREGQGLIDFATWCADRETAQSESVHGTEPDRDELTMFYMWL	359
		... : : : :.....: : : ..:: :...:	
PT	228	-----DNSVNTISWY-----DWPEPLKNRHLAALAEVYQSEKDFIDI---FIAQ	268
CG	360	QWLCDEQLAAAQKRAVDAGMSIGIMADLAVGVHPGGADAQNLSHVLA----PDASVGAPP	415
		:: ... : : 	
PT	269	QFLFQRQWKVRYARSKGISIMGDMPIYVGYHSADVWANKQFLNLRKGFPLIVSGVPP	328
CG	416	DGYNQGGQDWSQPPWHPVRLAEEGYIPWRNLLRRTVLRHSGGIRVDHVLGLFRLFVMPRMQ	475
		:~:~: . . : : : : : : : : : :	
PT	329	DAFSETGQLWGSPLYDWKAMEKDGFSWWVRRIQRATDLDFEFRIDHFRGFAGFVAVPSEE	388
CG	476	SPATGTYIRFDHNALVIGILALEAELAGAVVIGEDLGTFFEPWQDALAQRGIMGTSILWFE	535
	:.....:..... : :.....: : : . .	
PT	389	KIAILGRWKVGPGLFDAILQA-VGKINI IAEDLGVITEDVVQLRKSIEAPGMAVLQFA	447
CG	536	HSPSQPGPRRQEYRPLALTVTTHDLPPTAGYLEGEHIALRERLGLVNTDPAAELEAEDL	595
	:.....:..... :~:~: . . : :	
PT	448	FGSDAENPHLPHNHEQNQVVYTGTHNDTIRGWWD-----TLPQEEKSNVL	493
CG	596	QWQAEILDVAASANALPAREYVGLERDQRGELAELEGLHTFVAKTPSALTCVCLVDMVG	655
		:~:~: :~: : : : : :	
PT	494	KYLSNIEE-----EETSRG----LIEGAVSSVARI--AIIIPMQDVLGLG	531
CG	656	EKRAQNQPGTTRDMPNWCIPLCDSEGN-SVLIESLRENELYHRVAKASKRD 706	
	 :: : : : :	
PT	541	SDSRMNI PATQFGNW-SWRIPSSTSFDNLDAAEAKKLRD-----ILATYGRL 576	

Figure 3.8 Amino acid sequence alignment of amylomaltase from *Corynebacterium glutamicum* ATCC 13032 (CG) compared with amylomaltase from potato *Solanum tuberosum* (PT) using Stretcher program. Amino acid conservation across the aligned sequences is shown as (markup line) identical, (colon) conserved substitutions and (dot) semi-conserved substitutions. Catalytic residues are shown as highlight.

CG	1	MTARRFLNELADLYGVATSYTDYKGAHIEVSDDTLVKILRALGVNLDTSNLPNDDAIQRQ	60
EC	1	MESKR-LDNAALAAGISPNYINAHGKPKQSISAETKRRL-----DAMHQR	44
CG	61	IALFHDREFTRPLPPSVVAVEGDELVFPVHVHDGSPADVHIELEDGTQRDVSQVENWTAP	120
EC	45	TAT---KVAVTPVPNVVMVYTSQKGM--PMVVEGSGEYSWLLTTEEGTQ-----	87
CG	121	REIDGIRWGEASFKIPGDLPLGWHKHLKSNERSAECGLIITPARLSTADKYLDSPRS-G	179
EC	88	--YKGHVTGGKAFNLPKLPKPEGYHTLTLTQDDQRAHCRVIVAPKRCYEPQALLNKQKLWG	145
CG	180	VMAQIYSVRSTLSWGMGDFNDLGNLASVVAQDGADFLINPMHAAEPLPPTEDSPYLPTT	239
EC	146	ACVQLYTLRSEKNWIGDFGDLKAMLVDAKRGGSFIGNPIHALYPANPEASAPYSPSS	205
CG	240	RRFINPIYIRVEDIPEFNQLEIDLRRDIAEMAAEFERNLTSDIIEKNDVYAAKLQVLR	299
EC	206	RRWLVNIYIDVNAVEDFHLSEEAQAWWQLPTTQQTLQQARDADWDVYSTVTALKMTALRM	265
CG	300	IFE--MPRSEREANFVSVFVQREGQLIDFAT-----WCADRETAQS-	339
EC	266	AWKGFARDDQMAAFRQFVAEQGDSLFWQAALDALHAQQVKEDEMWRGWPAWPEMQRNV	325
CG	340	---ESVHGTEPDRDELTMFYMWLQWLQCEQLAAAQKRAVDAGMSIGIMADLAVGVHPGGA	396
EC	326	DSPEVRQFCEEHRDDVD-FYLWLQWLAYSQFAACWEISQGYEMPIGLYRDLAVGVAEGGA	384
CG	397	DAQNLSHVLAPDASVGAPPDGYNQGDWSQPPWHPVRLAEEGYIPWRNLLRRTVLRHSGG	456
EC	385	ETWCNRELYCLKASVGAAPPDILGPLQONWGLPPMDPHIITARAYEPFIELLRANMQNCGA	444
CG	457	IRVDHVLGLFRLFVMPRMQSPATGTYIRFDHNALVGLALEAELAGAVVIGEDLGTPEPW	516
EC	445	LRIDHVMSMLRLWVWIPYGETADQAGYVHYVDDLLSILALESKRHRMVIIGEDLGTVPVE	504
CG	517	VQDALAQRGIMGTSILWFEHSPSQGPERRQEEYRPLALTTVTTHDLPPTAGYLEGEHIAL	576
EC	505	IVGKLRSSGVYSYKVLVYFENDHEKTF-RAPKAYPEQSMVAATHDLPTRLRGYWECDLTL	563
CG	577	RERLGVLNTDPAAE-LAEDLQWQAE-ILDVAASANALPAREYVGLERDQRGELAELEGL	634
EC	564	GKTLGLYPDEVVLRGLYQDRELAKQLLDALHKYGLPKR--AGHKASLMSMTPTLNRGL	621
CG	635	HTFVAKTPSALTCVCLVDMVGKRAQNPQGTTRDMYPNWCIPLCDSEGNVLIIESLRE--	692
EC	622	QRYIADSNALLGLQPEDWLDMAEPVNIPTGTSYQ-YKNWRRKLSATLESMAFADDGVNKKL	680
CG	675	NELYHRVAKASKRD	706
EC	661	KDLDRRRRAAAKKK	694

Figure 3.9 Amino acid sequence alignment of amyloamylase from *Corynebacterium glutamicum* ATCC 13032 (CG) compared with amyloamylase from *Escherichia coli* K12 (EC) using Stretcher program. Amino acid conservation across the aligned sequences is shown as (markup line) identical, (colon) conserved substitutions and (dot) semi-conserved substitutions. Catalytic residues are shown as highlight.

Table 3.1 Percent similarity of deduced amino acid sequence of recombinant amyloamylase from *Corynebacterium glutamicum* ATCC 13032 compared with other 4 α GTases. The accession numbers were from NCBI and Swiss-Prot database.

Accession number	Organism	Number of amino acid	%Similarity
NP_601497	<i>Corynebacterium glutamicum</i>	706	100
EED09753	<i>Thermus aquaticus</i>	500	28
YP_144527	<i>Thermus thermophilus</i>	500	28
AAC06897	<i>Aquifex aeolicus</i>	485	30
Q06801	<i>Solanum tuberosum</i>	576	33
P15977	<i>Escherichia coli</i> K12	694	45

ศูนย์วิทยทรัพยากร
จุฬาลงกรณ์มหาวิทยาลัย

3.1.5 Expression of amyloamylase gene

The *E.coli* BL21(DE3) containing recombinant plasmid (p19AM) was cultivated in LB broth containing 100 µg/ml ampicillin antibiotic. The enzyme production was induced with IPTG at a final concentration of 0.4 mM for 0, 1, 2, 3, 4, 5 and 6 hours. The growth rate was followed by A_{600} . The cells were harvested and starch transglucosylation activity in crude extract was assayed as described in section 2.9.2. When recombinant clone was cultured without IPTG induction, the expression of amyloamylase gene was quite low and activity was undetectable. The expression was highest at induction time of 2 hours when 0.4 mM IPTG was used (Figure 3.10), this condition was selected for enzyme induction in further experiment. The specific activity of amyloamylase was about 2.2 Unit/mg protein. After 2 hours of induction, the enzyme specific activity decreased.

3.1.6 Protein pattern of cells

The 1.5 ml cell suspension was taken from recombinant clone (p19AM) grown at 0.4 mM IPTG at various times as described in 2.7 and then harvested by centrifugation. The cell pellets were resuspended in 100 µl of H₂O. Fifteen microliters of cell samples were added with SDS loading dye and boiled before subjected to electrophoresis on 7.5% SDS-polyacrylamide gel. The results in Figure 3.11 showed that the major protein band at around 80 kDa of cells at each induction time corresponded to the expected size of the enzyme.

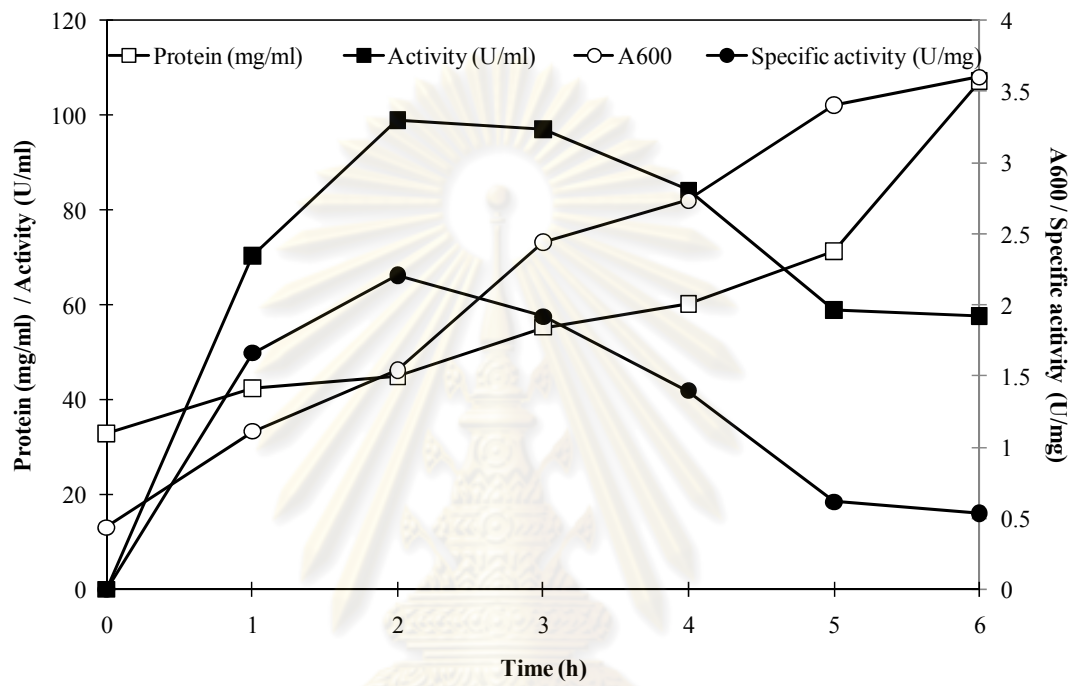


Figure 3.10 Expression of p19AM in *E. coli* BL21(DE3) at 0.4 mM IPTG

ศูนย์วิทยทรัพยากร
จุฬาลงกรณ์มหาวิทยาลัย

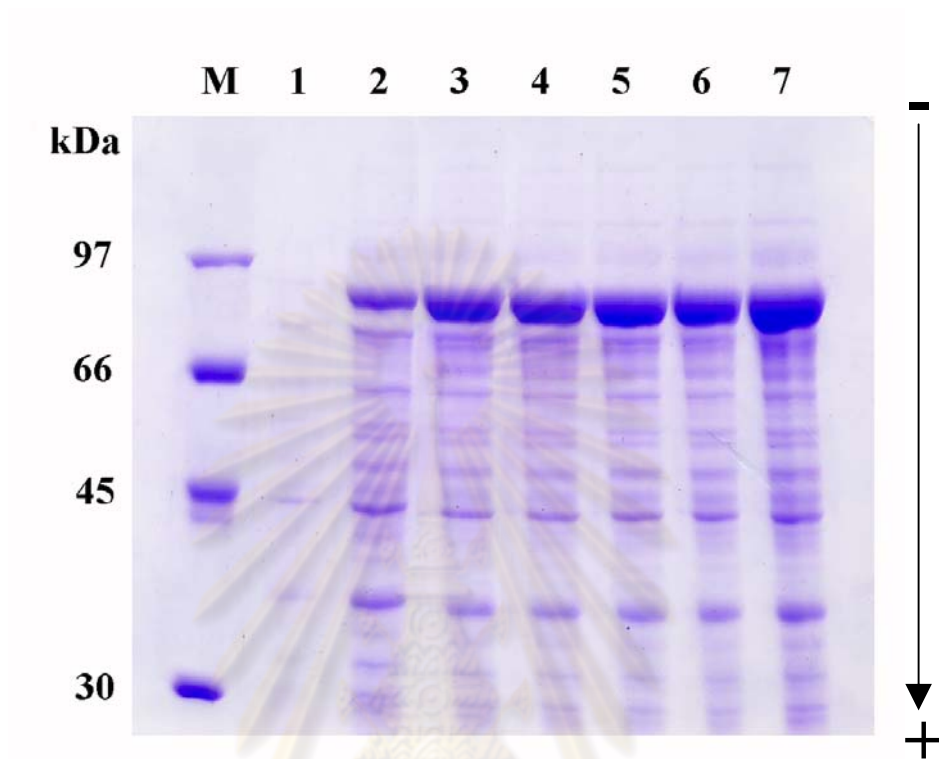


Figure 3.11 SDS-PAGE of whole cell suspensions of p19AM clone induced by 0.4 mM IPTG at various times

Lane M = protein LMW marker

Lane 1-7 = cell suspensions of p19AM clone at various induction times: 0, 1, 2, 3, 4, 5 and 6 h, respectively

จุฬาลงกรณ์มหาวิทยาลัย

3.2 Purification of amyloamylase from the recombinant clone harboring p19AM

3.2.1 Preparation of crude extract

Crude recombinant amyloamylase was prepared from 7 g of *E.coli* BL21(DE3) recombinant clone (p19AM) which was cultivated from 1.8 liter of medium as described in 2.8.2. Twelve milliliters of crude enzyme solution contained 740 mg protein with 1,633 Unit of starch transglucosylation activity was used for purification. The specific activity of the enzyme in crude preparation was 2.2 Unit/mg protein.

3.2.2 HisTrap FF™ column chromatography

The crude enzyme from recombinant clone was dialyzed against 20 mM phosphate buffer, pH 7.4. The enzyme solution was applied onto a HisTrap FF™ column as described in 2.8.3. The chromatographic profile is shown in Figure 3.12. The unbound proteins were washed off by the equilibrating buffer as the major protein peak with shoulder. The bound proteins were eluted in a rather sharp narrow peak by the buffer containing 500 mM imidazole, the peak in which high enzyme activity was observed. The fractions with starch transglucosylation activity were pooled and dialyzed against 20 mM phosphate buffer, pH 7.4. The specific activity of the enzyme at this step was 23.8 Unit/mg protein. The enzyme was 10.8 fold purified with 30.2% recovery (Table 3.2).

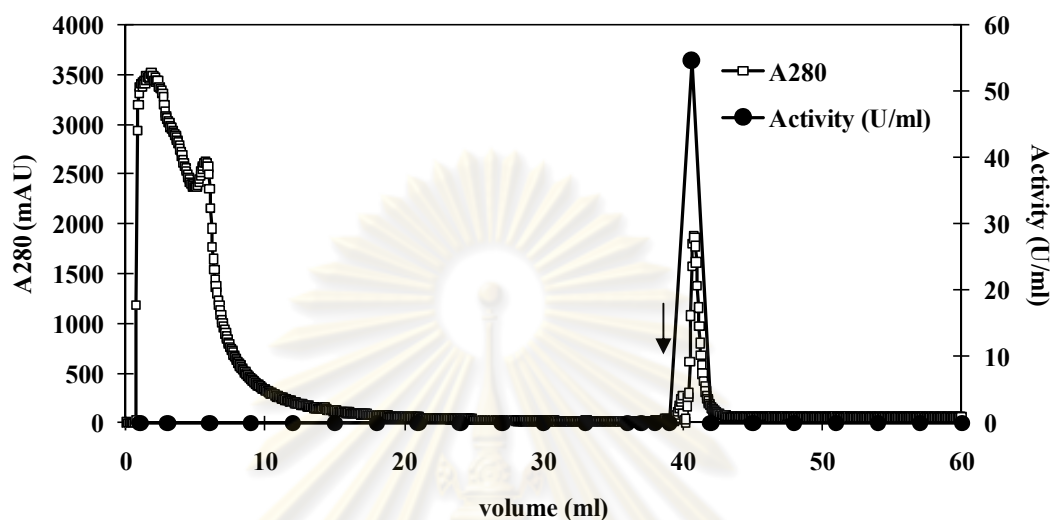


Figure 3.12 Purification profile of amyloamylase from the recombinant clone harboring p19AM by HisTrap FFTM column chromatography

The enzyme was applied to HisTrap FFTM column (0.7 x 2.5 cm, two columns consecutively) and washed with 20 mM phosphate buffer pH 7.4 containing 0.5 M NaCl and 20 mM imidazole until A_{280} of eluent decreased to baseline. The bound proteins were eluted by 500 mM imidazole in the same buffer at the flow rate of 1 ml/min. Fractions of 3 ml were collected. The arrow indicates where elution of the bound proteins started. The active protein and activity peaks were pooled.

Table 3.2 Purification of amyloamylase from the recombinant clone harboring p19AM^a

Purification step	Total protein (mg)	Total activity ^b (U)	Specific activity (U/mg)	Purification Fold	Yield (%)
Crude extract	740	1633	2.2	1	100
HisTrap FF TM	20.7	493	23.8	10.8	30.2

^aCrude extract was prepared from 1.8 liter (7 g cell wet weight) of cell culture.

^bAssayed by starch transglucosylation activity

ศูนย์วิทยทรัพยากร
จุฬาลงกรณ์มหาวิทยาลัย

3.2.3 Determination of enzyme purity by SDS and Native-PAGE

The enzyme from each step of purification was examined for purity and protein pattern by SDS-PAGE (Figure 3.13) as described in 2.11.1. In SDS-PAGE analysis, the purified enzyme showed a single band on the gel indicating the success of purification by only one step of affinity chromatography. In addition, the purified enzyme was subjected to non-denaturation PAGE followed by activity staining as described in 2.11.2 (Figure 3.14). In Native-PAGE, the purified enzyme showed one major band and another faint band which migrated faster than the major band.

3.3 Characterization of amyloamylase from the recombinant clone harboring p19AM

3.3.1 Molecular weight determination of amyloamylase

The molecular weight of recombinant amyloamylase containing his-tag residues was estimated to be about 84 kDa by SDS-PAGE (Figure 3.13b).

3.3.2 Effect of temperature on amyloamylase starch transglucosylation activity and stability

The effect of temperature on enzyme activity was investigated as described in 2.13.2. The temperature was varied from 20 °C to 60 °C. The result is shown in Figure 3.15a. The enzyme activity which showed highest activity was defined as 100% residual activity. The enzyme performed the highest activity at 30 °C while 90% of the activity still remained at 40 °C. It was observed that the activity was significantly dropped at 50 °C and higher.

The thermostability of amyloamylase was determined as described in 2.13.3. The enzyme was preincubated at various temperatures ranging from 20 °C to 60 °C

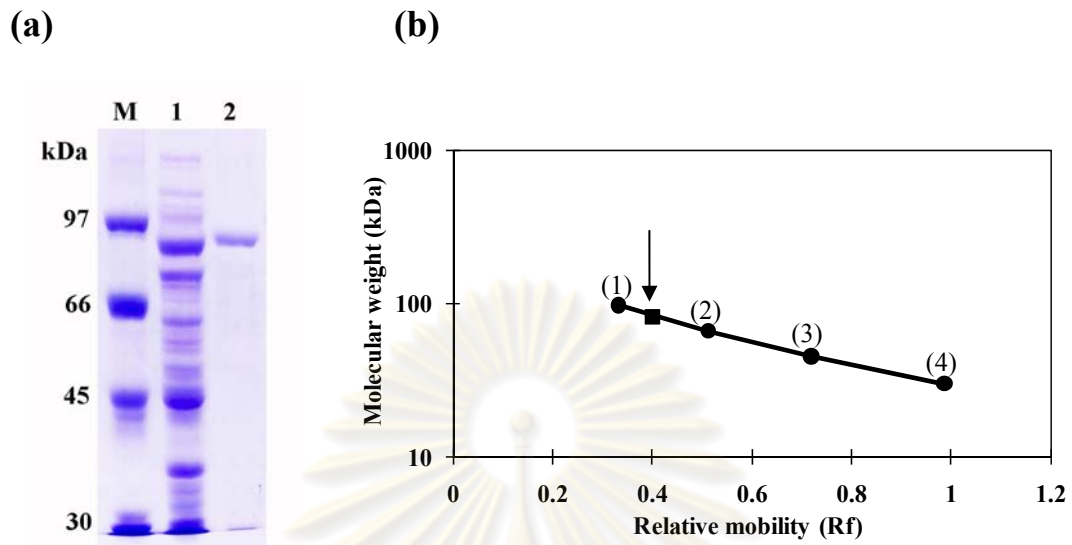


Figure 3.13 Molecular weight determination of amyloamylase

a) SDS-PAGE of the recombinant amyloamylase (p19AM) from each purification step

Lane M	=	Protein LMW marker	
Lane 1	=	Crude extract	15 μ g
Lane 2	=	HisTrap™ column	3 μ g

b) Calibration curve for molecular weight of recombinant amyloamylase containing his-tag by SDS-PAGE

- (1) = Phosphorylase b (MW 97,000 Da)
- (2) = Bovine serum albumin (MW 66,000 Da)
- (3) = Ovalbumin (MW 45,000 Da)
- (4) = Carbonic anhydrase (MW 30,000 Da)

Arrow indicates a determined molecular weight of amyloamylase



Figure 3.14 Native-PAGE of purified amyloamylase of the recombinant clone (p19AM) incubated with soluble starch substrate and stained with iodine solution

Lane 1 = HisTrap™ column 0.2 Units^a

Lane 2 = HisTrap™ column 0.4 Units^a

^aAssayed by starch transglucosylation activity

ศูนย์วิจัยทรัพยากร
จุฬาลงกรณ์มหาวิทยาลัย

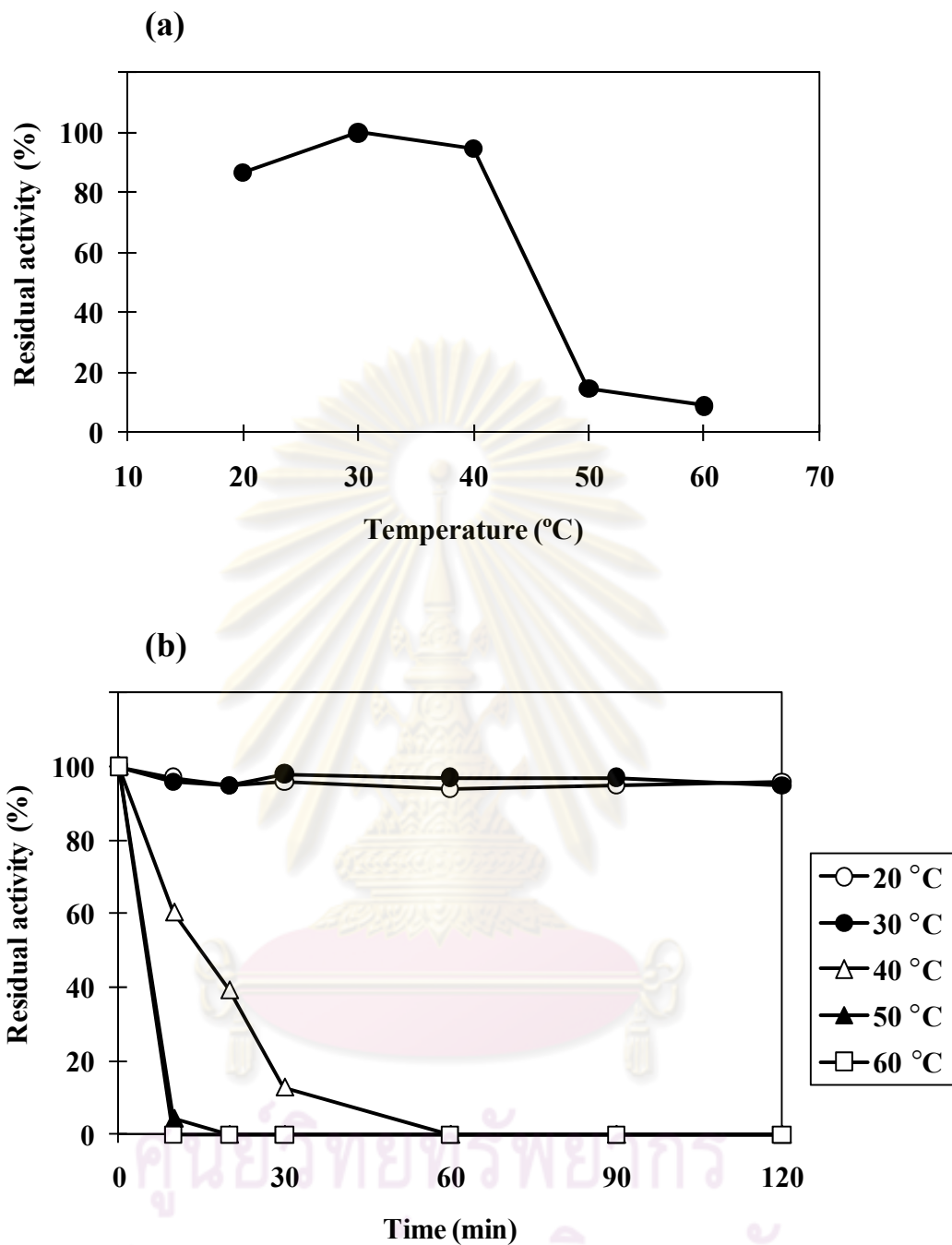


Figure 3.15 Effect of temperature on starch transglucosylation activity and stability

a) Effect of temperature on amyloamylase activity

b) Effect of temperature on amyloamylase stability

The enzyme sample was in 50 mM phosphate buffer, pH 6.0.

for 0-120 minutes. The activity of non-preincubated enzyme was defined as 100% residual activity. The result is shown in Figure 3.15b. The enzyme retained its activity at temperature up to 30 °C and lost about 60% of its activity at 40 °C after 20 minutes. At 50 °C and 60 °C, amyloamylase absolutely lost its activity after 10 minutes of incubation.

3.3.3 Effect of pH on amyloamylase starch transglucosylation activity and stability

The effect of pH on enzyme activity was examined at various pHs of buffers ranging from 4.0 to 9.0 as mentioned in 2.13.4. The result is shown in Figure 3.16a. The enzyme exhibited maximal activity at pH 6.0 and 85% of activity was observed at pH 8.0. Tris-HCl seemed to show negative buffer effect.

The pH stability of amyloamylase was determined as described in 2.13.5. The enzyme was preincubated at 30 °C for 1 hour in 50 mM buffers at various pHs ranging from 4.0 to 9.0. The result is shown in Figure 3.16b. The activity of non-preincubated enzyme was defined as 100% residual activity. The enzyme was found to be stable over the pH range from 5.5 to 9.0.

3.3.4 Transglucosylation reaction of amyloamylase

The transglucosylation reaction of amyloamylase was determined as described in 2.13.6. The enzyme was incubated with linear maltooligosaccharide substrates (G1, glucose to G7, maltoheptaose) in 50 mM phosphate buffer, pH 6.0 at 30 °C for 2 hours. The reaction mixture was analyzed by thin-layer chromatography (TLC) as described in 2.15.1. The result is shown in Figure 3.17. The enzyme could catalyze transglucosylation reaction from maltooligosaccharides G2 to G7 while G1 could not

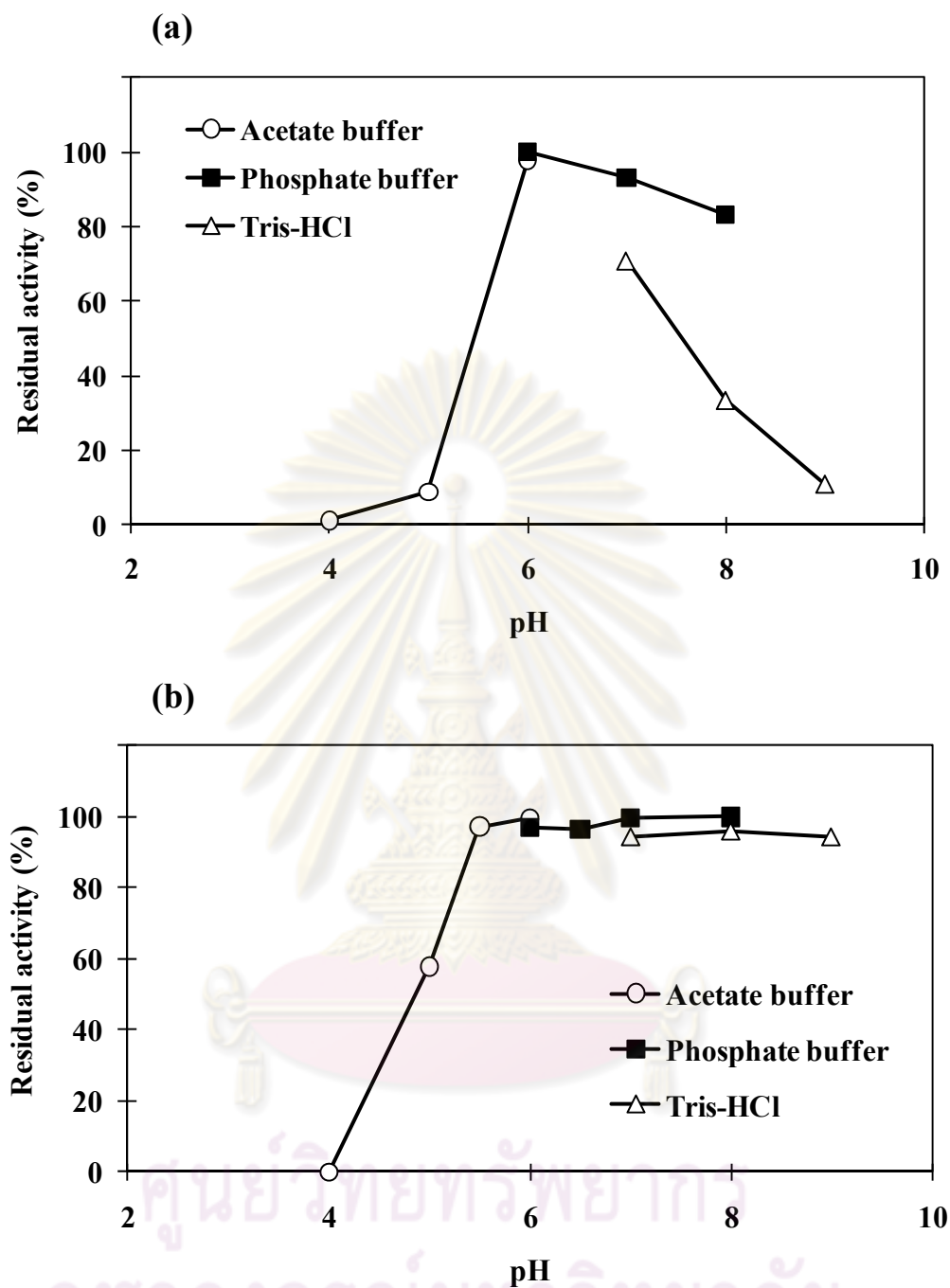


Figure 3.16 Effect of pH on amylomaltase starch transglucosylation activity and stability

a) Effect of pH on amylomaltase activity

b) Effect of pH on amylomaltase stability

The reactions were measured at 30 °C.

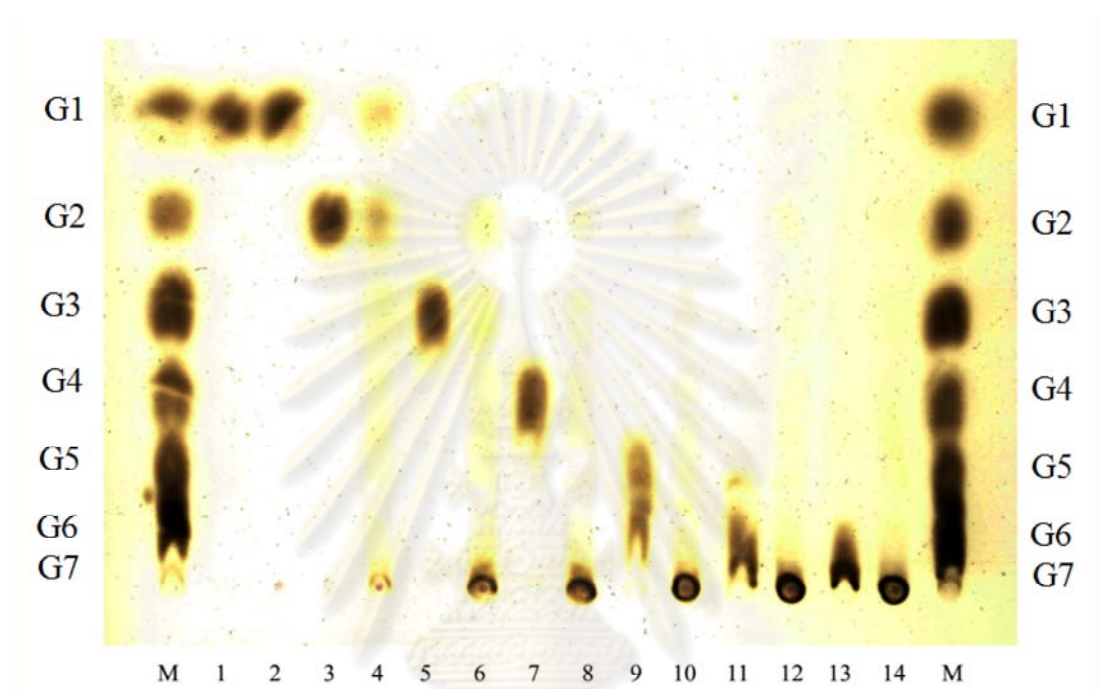


Figure 3.17 TLC chromatogram of the reaction products of amyloamylase incubated with maltooligosaccharides. Enzyme solution was incubated with 0.2% (w/v) of each substrate at 30°C for 2 h. Lane M, standard G1-G7; lane 1,2: G1 without/with enzyme; lane 3,4: G2 without/with enzyme; lane 5,6: G3 without/with enzyme; lane 7,8: G4 without/with enzyme; lane 9,10: G5 without/with enzyme; lane 11,12: G6 without/with enzyme; lane 13,14: G7 without/with enzyme

be a substrate. Various maltooligosaccharides of different length were produced from each reaction. When relatively long maltooligosaccharides (G5, G6, and G7) were used as a substrate, high molecular mass oligosaccharides were observed as the TLC spots of the products were hardly moved from the origin.

3.3.5 The synthesis of large-ring cyclodextrins

The production of large-ring cyclodextrins by amyloamylase was followed as described in 2.13.7. The enzyme was incubated with 0.2% (w/v) pea starch in 50 mM phosphate buffer, pH 6.0 at 30 °C for 30 minutes to 24 hours. The reaction mixture was analyzed by HPAEC-PAD as described in 2.15.2. The LR-CD products were depended on the incubation time used. At 0.15 Unit/ml enzyme, the principle product was changed from larger LR-CD (CD31) at shorter incubation time (30 minutes) to smaller size (CD25) at 24 hours (Figure 3.18a to f). It was observed that the principle product CD28 and CD26 was seen at 4 and 6 hours of incubation, respectively. When using higher concentration of the enzyme (0.5 Unit/ml), the amount of CD products was increased. However, the product pattern was not much different from that at low enzyme, consisted of mixtures of LR-CDs ranged from about CD19 to higher than CD50, with CD 27-28 as principle products obtained at 4 hours incubation time (Figure 3.19).

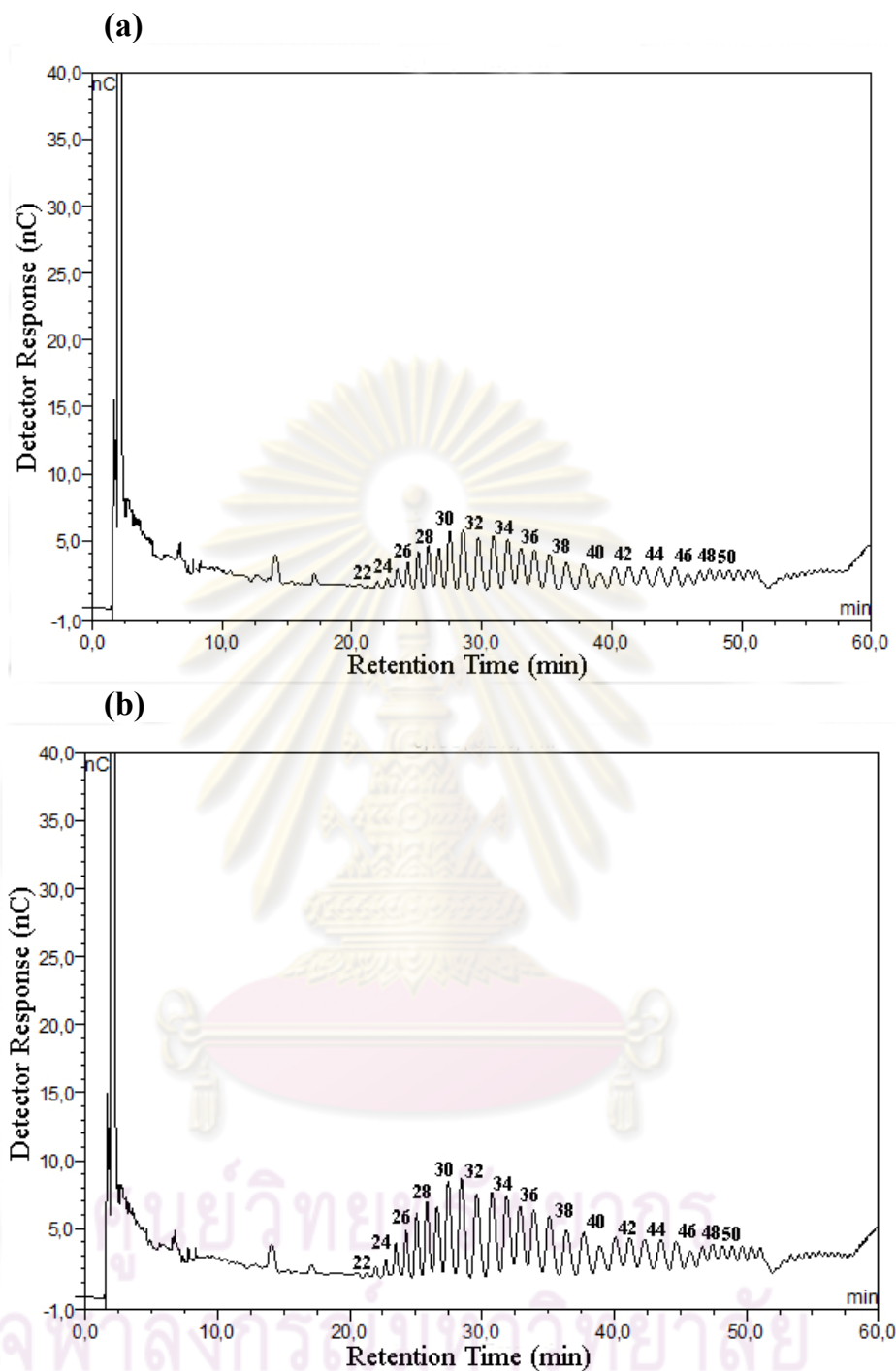


Figure 3.18 HPAEC analysis of large-ring cyclodextrins synthesized by amyloamylase at different incubation time. 0.2% (w/v) pea starch was incubated with 0.15 U/ml enzyme at 30 °C. Peak numbers indicate the degree of polymerization of identified LR-CDs based on comparison of R_t with CD20 and CD21. (a) Incubation of 30 min, (b) Incubation of 1 h.

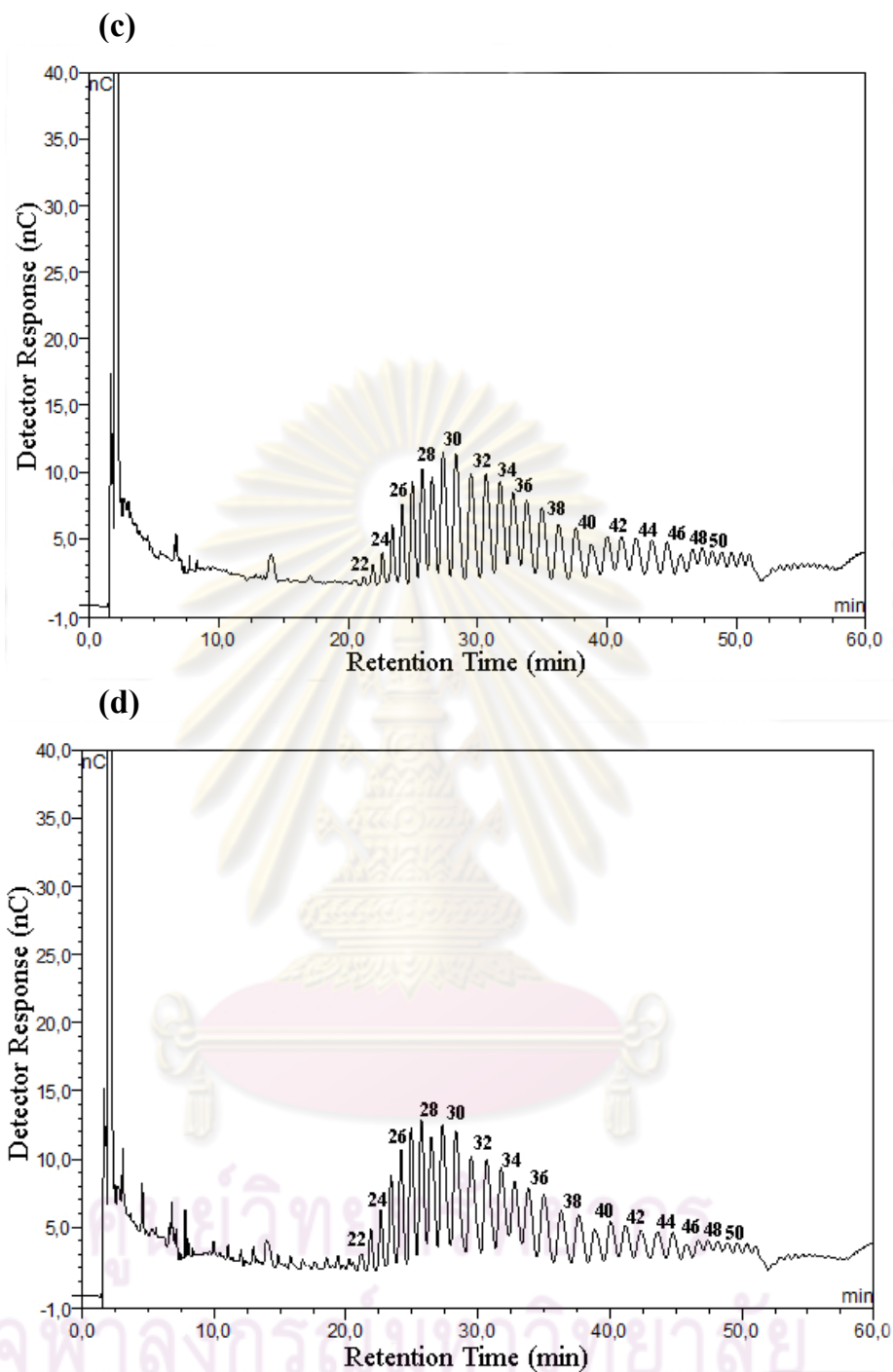


Figure 3.18 (continued) HPAEC analysis of large-ring cyclodextrins synthesized by amylo maltase at different incubation time. 0.2% (w/v) pea starch was incubated with 0.15 U/ml enzyme at 30 °C. Peak numbers indicate the degree of polymerization of identified LR-CDs based on comparison of R_t with CD20 and CD21. (c) Incubation of 2 h, (d) Incubation of 4 h.

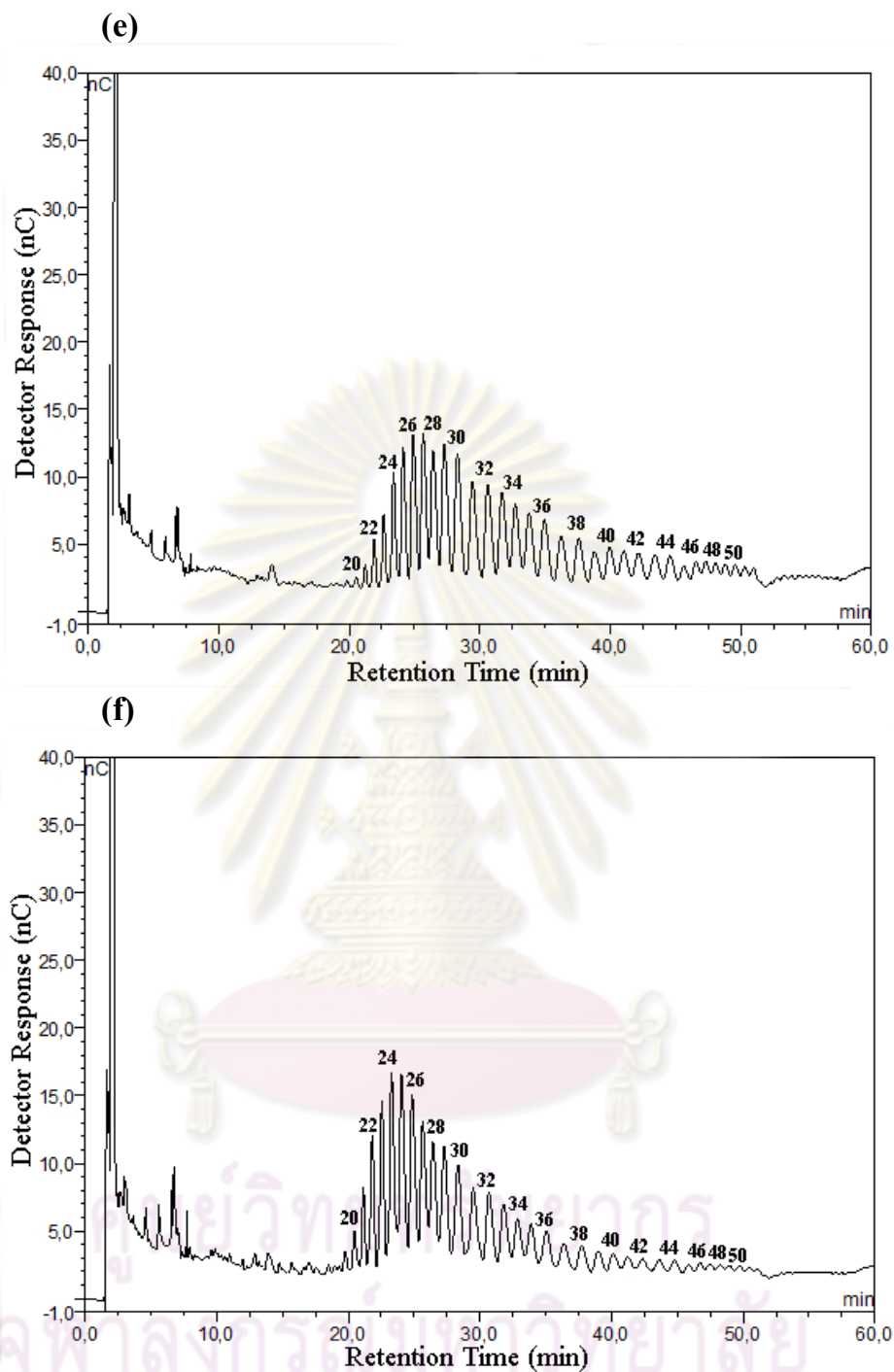


Figure 3.18 (continued) HPAEC analysis of large-ring cyclodextrins synthesized by amyloamylase at different incubation time. 0.2% (w/v) pea starch was incubated with 0.15 U/ml enzyme at 30 °C. Peak numbers indicate the degree of polymerization of identified LR-CDs based on comparison of R_t with CD20 and CD21. (e) Incubation of 6 h, (f) Incubation of 24 h.

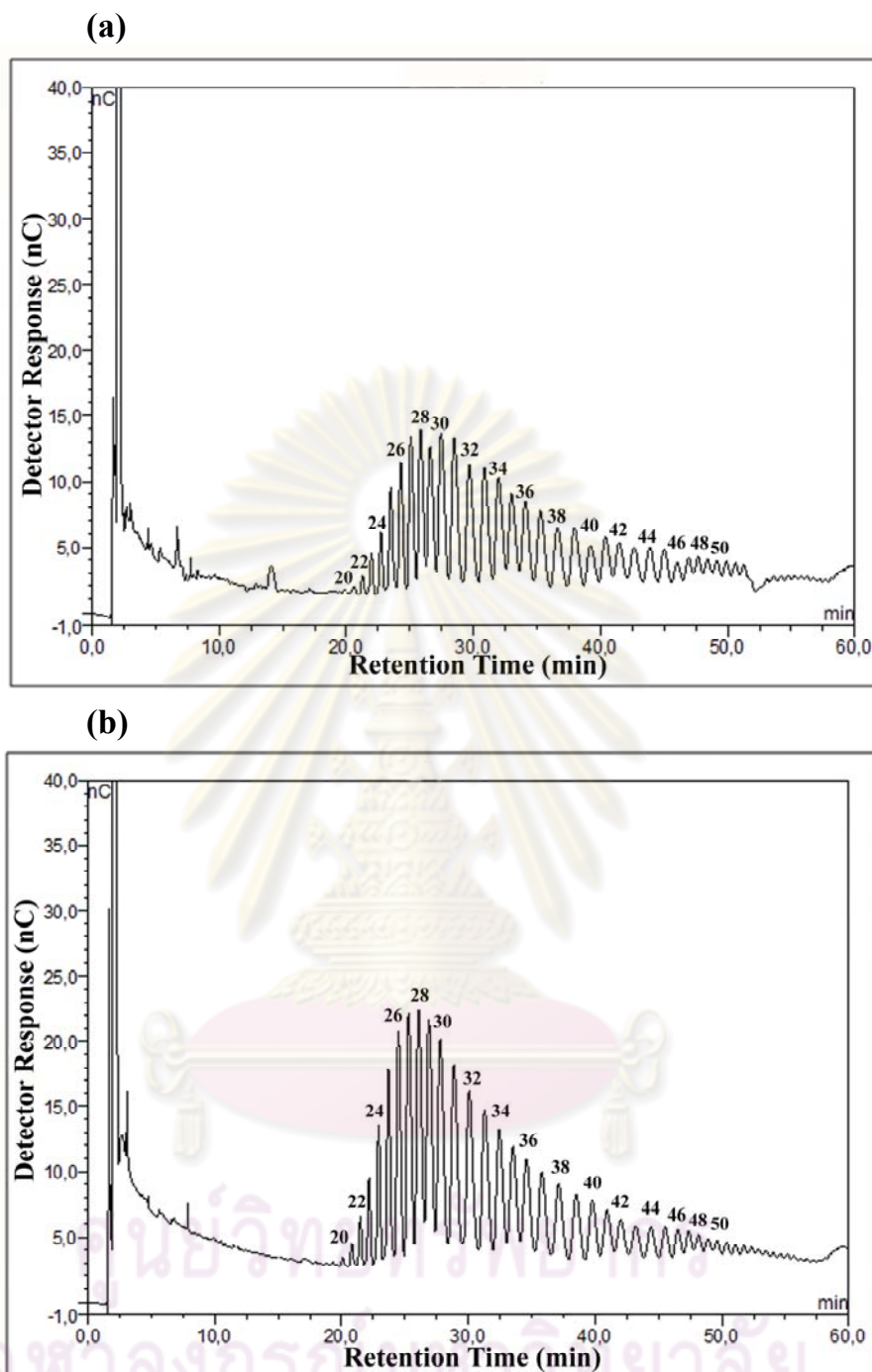


Figure 3.19 HPAEC analysis of large-ring cyclodextrins synthesized by amyloamylase at different amount of enzyme. 0.2% (w/v) pea starch was incubated with a) 0.15 U/ml and b) 0.5 U/ml enzyme at 30 °C for 4 h. Peak numbers indicate the degree of polymerization of identified LR-CDs based on comparison of R_t with CD20 and CD21.

3.4 Construction and expression of recombinant wild-type and Y172A mutated amyломaltase

After purification of recombinant wild-type amyломaltase from p19AM clone, the purified protein was treated with enterokinase to remove his-tag residues (23 amino acids in length). Unfortunately, the mature amyломaltase enzyme without his-tag residues showed no activity. So the change of the expression vector used for cloning was made. Instead of pET-19b which has his-tag sequence at N-terminal of expressed protein, pET-17b was chosen to be a new expression vector.

3.4.1 Extraction of plasmid DNA

The plasmid DNA (p17AM) was extracted and checked by agarose gel electrophoresis (Figure 3.20, Lane 1& 2). The ratio of $A_{260/280}$ values was 1.8 indicated that the purity of this extracted DNA was sufficient to be used for further experiment.

3.4.2 Transformation

The *malQ* gene fragment was digested with *NdeI* and *XhoI* from p19AM, then ligated with *NdeI-XhoI* digested pET-17b vector (Appendix 12) by T4 DNA ligase. Transformation into the competent cells of *E. coli* BL21(DE3) was performed as in section 3.1.3. The agarose gel electrophoresis pattern of the recombinant plasmid containing *malQ* (p17AM) is shown in Figure 3.20 (lane 3-6). The size of linear form of the recombinant plasmid and 2.1 kb corresponded to the size of *malQ*.

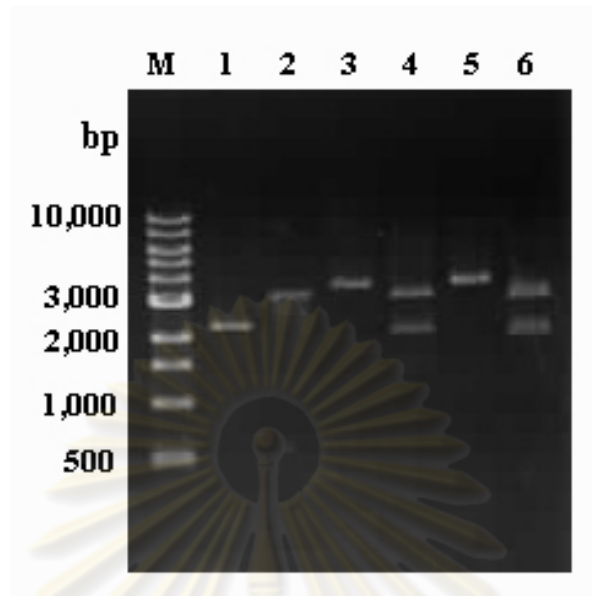


Figure 3.20 Agarose gel electrophoresis of recombinant *malQ* inserted in pET-17b vector. The DNA samples were separated on 1% agarose gel and visualized by ethidium bromide staining.

Lane M = 1 kb DNA ladder

Lane 1 = pET-17b vector

Lane 2 = pET-17b vector digested with *NdeI* and *XhoI*

Lane 3, 5 = pET-17b vector harboring *malQ*

Lane 4, 6 = pET-17b vector harboring *malQ*, digested with *NdeI* and *XhoI*

จุฬาลงกรณ์มหาวิทยาลัย

3.4.3 Nucleotide sequencing

To confirm the inserted fragment, the recombinant plasmid (p17AM) was subjected to DNA sequencing using the primers of T7 promoter and T7 terminator as in 3.1.4. The nucleotide sequence of *malQ* (2,121 bp) and the deduced amino acid sequence (706 residues) were identical to the sequences in Figure 3.4 except that the his-tag residues (the first 23 amino acids) were removed.

3.4.4 Site-directed mutagenesis at Y172A of amyloamylase

The sequence alignment of the obtained deduced amino acid sequence with *T. aquaticus* amyloamylase was performed (Figure 3.5). The Tyr-172 of *C. glutamicum* amyloamylase is in the corresponded position to Tyr-54 of *T. aquaticus* amyloamylase (Terada *et al.*, 1999) which was reported that the change of this residue affected the hydrolytic activity of *T. aquaticus* amyloamylase. In this study, the Tyr-172 of *C. glutamicum* amyloamylase was changed to alanine by PCR amplification as described in section 2.6. The colonies of mutant were confirmed by nucleotide sequencing (data not shown). The result indicated that mutated position had GCG instead of TAT which led to the change in amino acid from Tyr to Ala residue. The Y172A mutant was used for further experiment.

3.4.5 Expression of amyloamylase gene

The *E. coli* BL21(DE3) containing recombinant plasmid (p17AM) and Y172A mutated plasmid were cultivated in LB broth containing 100 µg/ml ampicillin. The result of amyloamylase expression was the same as for the enzyme with his-tag residues as described in 3.1.5. The specific activities of amyloamylase and Y172A mutated amyloamylase obtained were about 2 Unit/mg protein and 1.1 Unit/mg protein, respectively.

3.5 Purification of amyloamylase from the recombinant clone harboring p17AM and Y172A mutant

3.5.1 Preparation of crude extract

Crude recombinant amyloamylase was prepared from 4 g and 6 g of *E. coli* BL21(DE3) recombinant clone (p17AM) and Y172A mutant which was cultivated from 1 liter and 1.6 liter of the medium as described in 2.8.2. For recombinant wild type, ten milliliters of crude enzyme solution contained 304.5 mg protein with 612 Unit of starch transglucosylation activity. The specific activity of the enzyme in crude preparation was 2 Unit/mg protein (Table 3.3). For the mutant, 505 mg protein with 543 Unit of starch transglucosylation activity was detected in 10 milliliters of crude enzyme, and the specific activity was 1.1 Unit/mg protein (Table 3.4).

3.5.2 DEAE FFTM column chromatography

The crude enzyme from recombinant clone (p17AM) was dialyzed against 50 mM phosphate buffer, pH 7.4 and applied onto DEAE FFTM column as described in 2.8.4.1. The chromatographic profile is shown in Figure 3.21. The unbound proteins

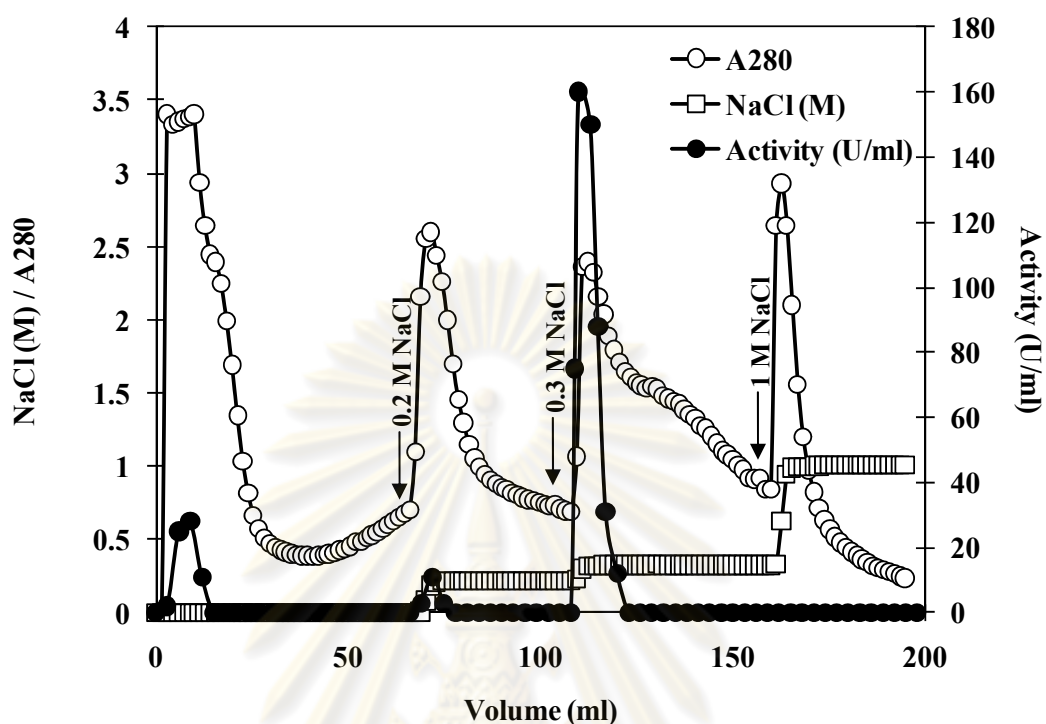


Figure 3.21 Purification profile of wild-type amylomaltase from recombinant clone (p17AM) by DEAE FFTM column chromatography

The crude enzyme was applied to DEAE FFTM column (0.7 x 2.5 cm) and washed with 50 mM phosphate buffer, pH 7.4 containing 0.01% β -mercaptoethanol until A₂₈₀ of eluent decreased to baseline. The bound proteins were stepwise eluted by 0.2 M NaCl, 0.3 M NaCl and 1 M NaCl in the same buffer at a flow rate of 1 ml/min. Fractions of 3 ml were collected. The arrows indicate where stepwise elution started. The active protein and activity peaks were pooled.

were eluted from the column by phosphate buffer, pH 7.4 containing 0.01% β -mercaptoethanol, this peak was found to contain little enzyme activity. The bound proteins were then eluted with stepwise of 0.2 M NaCl, 0.3 M NaCl and 1 M NaCl in the same buffer. The fractions eluted by 0.3 M NaCl were found to contain high starch glucosylation activity. They were pooled and dialyzed against 50 mM phosphate buffer, pH 7.4. The specific activity of the enzyme from this step was 13 Unit/mg protein. The enzyme was 6.5 fold purified with 36.4% recovery (Table 3.3).

For the mutated enzyme, the column condition and the elution steps were the same as in the recombinant wild type. The purification pattern obtained was similar, however, it was noticed that the protein and the activity peaks from 0.3 M NaCl elution were significantly reduced (Figure 3.22 as compared to Figure 3.21). The specific activity of the enzyme from this step was 3.6 Unit/mg protein. The enzyme was 3.3 fold purified with 11.6% recovery (Table 3.4).

3.5.3. Phenyl FFTM column chromatography

The pooled p17AM enzyme from DEAE FFTM was dialyzed against 50 mM phosphate buffer, pH 7.4 and applied onto Phenyl FFTM column as described in 2.8.4.2. The chromatographic profile is shown in Figure 3.23. The unbound proteins with no detectable amylomaltase activity were eluted from the column by 50 mM phosphate buffer, pH 7.4 containing 1 M ammonium sulfate and 0.01% β -mercaptoethanol. The bound proteins were then eluted with stepwise of 0.2 M ammonium sulfate and 0 M ammonium sulfate in the same buffer. The major protein with high activity peak was eluted by the buffer without ammonium sulfate. The fractions with starch transglucosylation activity were pooled and dialyzed against 50

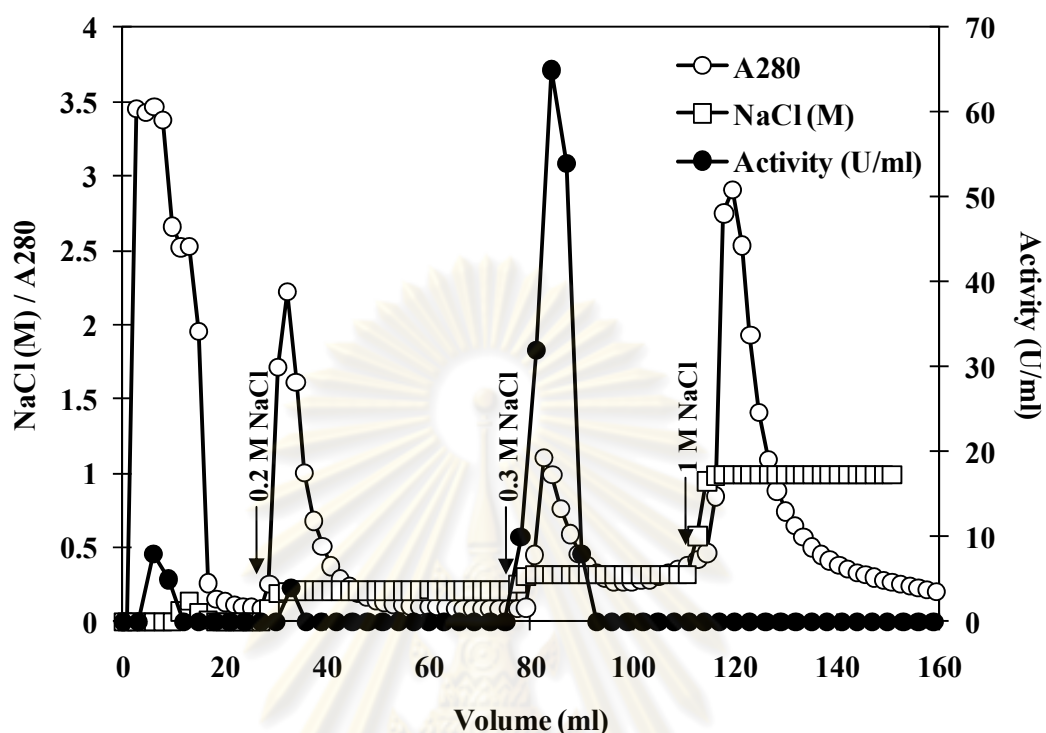


Figure 3.22 Purification profile of Y172A mutated amyloamylase by DEAE FF™ column chromatography

The crude enzyme was applied to DEAE FF™ column (0.7 x 2.5 cm) and washed with 50 mM phosphate buffer, pH 7.4 containing 0.01% β -mercaptoethanol until A_{280} of eluent decreased to baseline. The bound proteins were stepwise eluted by 0.2 M NaCl, 0.3 M NaCl and 1 M NaCl in the same buffer at a flow rate of 1 ml/min. Fractions of 3 ml were collected. The arrows indicate where stepwise elution started. The active protein and activity peaks were pooled.

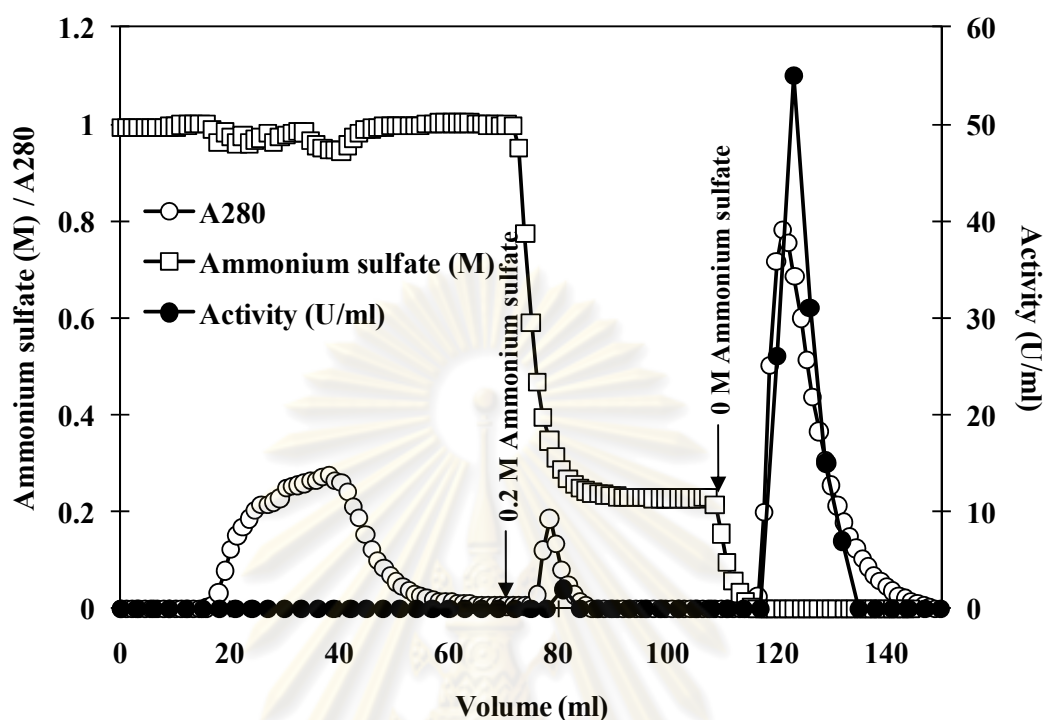


Figure 3.23 Purification profile of wild-type amyloamylase from recombinant clone (p17AM) by Phenyl FFTM column chromatography

The pooled enzyme from DEAE FFTM was applied to Phenyl FFTM column (1.6 x 10 cm) and washed with 50 mM phosphate buffer, pH 7.4 containing 1M ammonium sulfate and 0.01% β -mercaptoethanol until A_{280} of eluent decreased to baseline. The bound proteins were stepwise eluted by 0.2 M ammonium sulfate and 0 M ammonium sulfate in the same buffer at a flow rate of 1 ml/min. Fractions of 3 ml were collected. The arrows indicate where stepwise elution started. The active protein and activity peaks were pooled.

mM phosphate buffer, pH 7.4. The specific activity of the enzyme from this step was 25.3 Unit/mg protein. The enzyme was 12.6 fold purified with 17.3% recovery.

For the Y172A mutated enzyme, the pattern of elution from this DEAE FFTM step was the same as in the recombinant wild-type. It was observed that all the protein peaks and the activity peak were decreased (Figure 3.24 as compared to Figure 3.23). The specific activity of the enzyme from this step was 50 Unit/mg protein. The enzyme was 45 fold purified with 9% recovery.

The summary of purification of the recombinant wild-type and the Y172A mutated amyloamylase is shown in Table 3.3 and 3.4, respectively.

3.5.4 Determination of enzyme purity by SDS and Native-PAGE

The recombinant wild-type and Y172A mutated amyloamylase from each step of purification was examined for purity and protein pattern by SDS-PAGE (Figure 3.25 and Figure 3.26) as described in 2.11.1. In SDS-PAGE analysis, the recombinant wild type and Y172A mutated enzyme showed about 10 protein bands after purified through the first DEAE FFTM column. Then, only a single protein band was observed on the gel after the purification step of Phenyl FFTM. In addition, the purified enzyme was also subjected to non-denaturation PAGE followed by activity staining (Figure 3.27). In Native-PAGE analysis, the recombinant wild type and Y172A mutated enzyme showed a single activity band on the gel.

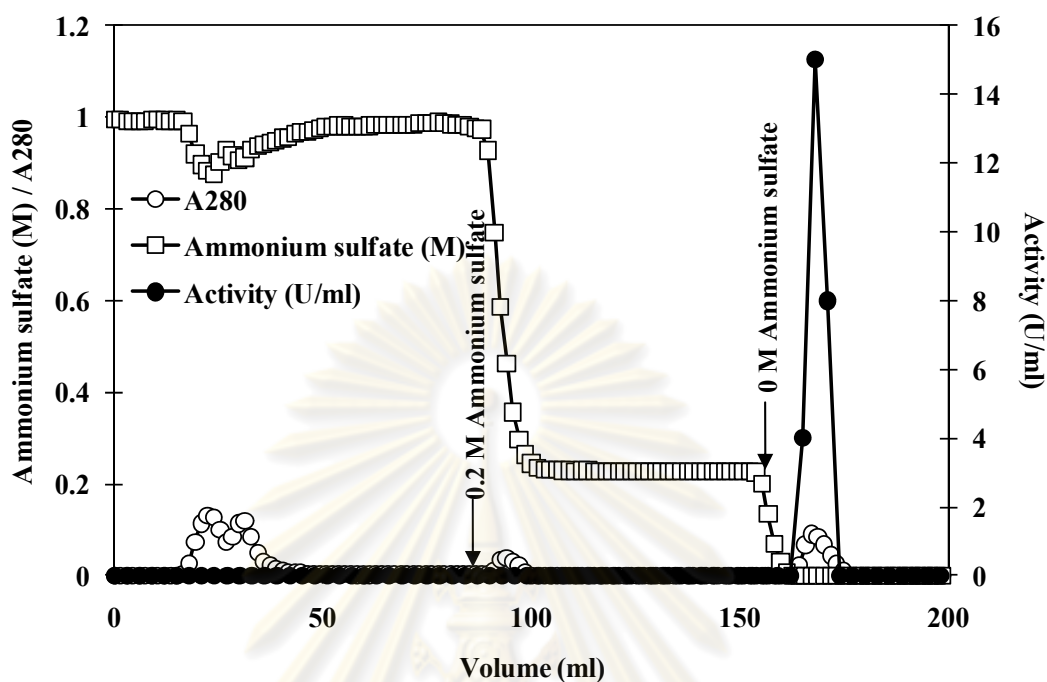


Figure 3.24 Purification profile of Y172A mutated amyloamylase by Phenyl FFTM column chromatography

The pooled enzyme from DEAE FFTM was applied to Phenyl FFTM column (1.6 x 10 cm) and washed with 50 mM phosphate buffer, pH 7.4 containing 1M ammonium sulfate and 0.01% β -mercaptoethanol until A₂₈₀ of eluent decreased to baseline. The bound proteins were stepwise eluted by 0.2 M ammonium sulfate and 0 M ammonium sulfate in the same buffer at a flow rate of 1 ml/min. Fractions of 3 ml were collected. The arrows indicate where stepwise elution started. The active protein and activity peaks were pooled.

Table 3.3 Purification of the recombinant wild-type amyloamylase (p17AM)^a

Purification step	Total protein (mg)	Total activity^b (U)	Specific activity (U/mg)	Purification Fold	Yield (%)
Crude extract	304.5	612	2	1	100
DEAE FF TM	13.7	178	13	6.5	36.4
Phenyl FF TM	2.2	56.6	25.3	12.6	17.3

^aCrude extract was prepared from 1 liter (4 g cell wet weight) of cell culture.

^bAssayed by starch transglucosylation activity

Table 3.4 Purification of Y172A mutated amyloamylase^a

Purification step	Total protein (mg)	Total activity^b (U)	Specific activity (U/mg)	Purification Fold	Yield (%)
Crude extract	505	543	1.1	1	100
DEAE FF TM	17	63	3.6	3.3	11.6
Phenyl FF TM	1.0	50	50	45	9.0

^aCrude extract was prepared from 1.6 liter (6 g cell wet weight) of cell culture.

^bAssayed by starch transglucosylation activity

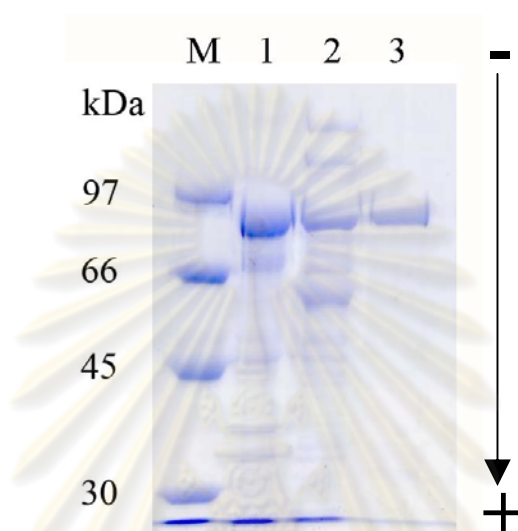


Figure 3.25 SDS-PAGE of the recombinant wild-type (p17AM) from each purification step

Lane M	=	Protein LMW marker	
Lane 1	=	Crude extract	15 μ g
Lane 2	=	DEAE FF™ column	8 μ g
Lane 3	=	Phenyl FF™ column	3 μ g

ศูนย์วิทยทรัพยากร
จุฬาลงกรณ์มหาวิทยาลัย

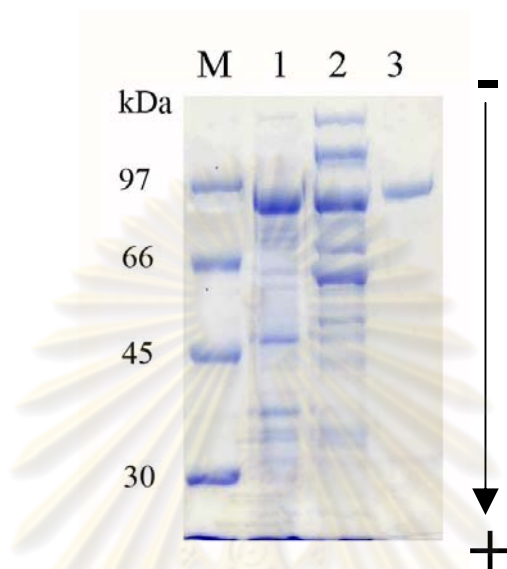


Figure 3.26 SDS-PAGE of the Y172A mutated amyloamylase from each purification step

Lane M	=	Protein LMW marker	
Lane 1	=	Crude extract	15 μ g
Lane 2	=	DEAE FF TM column	10 μ g
Lane 3	=	Phenyl FF TM column	3 μ g

จุฬาลงกรณ์มหาวิทยาลัย

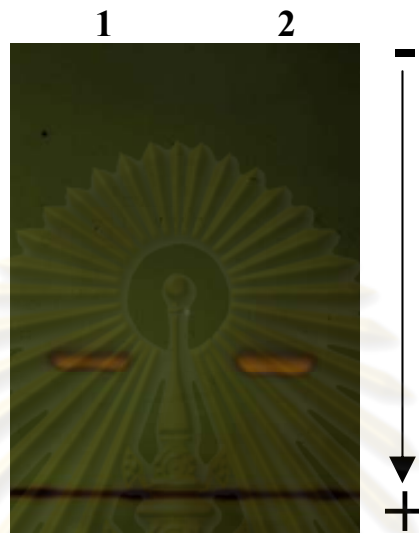


Figure 3.27 Native-PAGE of the purified amyloamylase from recombinant wild-type (p17AM) and Y172A mutant incubated with soluble starch substrate and stained with iodine solution

Lane 1 = p17AM amyloamylase 0.2 Units^a

Lane 2 = Y172A mutated amyloamylase 0.4 Units^a

^aAssayed by starch transglucosylation activity

จุฬาลงกรณ์มหาวิทยาลัย

3.6 Characterization of amyломaltase from recombinant clone p17AM and Y172A mutant

3.6.1 Molecular weight determination

The molecular weight of recombinant wild-type (p17AM) and Y172A mutated amylomaltase was estimated to be about 81 kDa by SDS-PAGE (Figure 3.28). The native molecular weight of the two enzyme forms was also determined from gel filtration chromatography on a Sephacryl S-200 column as mention in 2.13.1.2 (Figure 3.29). The molecular weight was estimated to be 83,000 Da. The value was consistent with the calculated molecular weight of the deduced amino acid sequence of the native enzyme which was 78,524.3 Da. The result indicated that this amylomaltase is a single protein chain with no subunit structure.

3.6.2 Effect of temperature on starch transglucosylation activity and stability

The effect of temperature on enzyme activity and stability was investigated. The result of the recombinant wild-type and Y172A mutated enzyme was the same as the enzyme with his-tag residues (p19AM, section 3.3.2). The enzymes performed the highest activity at 30 °C. After 2 hours incubation, the enzyme retained its full activity at temperature up to 30 °C, partially lost activity at 40 °C and absolutely lost activity at or above 50 °C.

3.6.3 Effect of pH on starch transglucosylation activity and stability

The effect of pH on enzyme activity and stability was investigated. The result of the recombinant wild-type and Y172A mutated enzyme was the same as the enzyme with his-tag residues (p19AM, section 3.3.3). At 30 °C, the enzyme exhibited maximal activity at pH 6.0 and was stable over the pH ranged from 5.5 to 9.0.

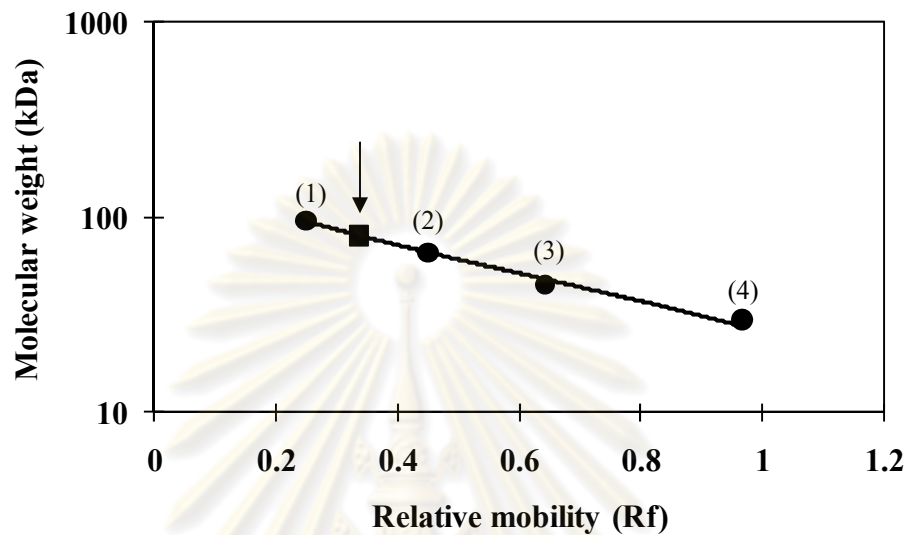


Figure 3.28 Calibration curve for molecular weight of recombinant wild-type and Y172A mutated amyloamylase by SDS-PAGE

- (1) = Phosphorylase b (MW 97,000 Da)
- (2) = Bovine serum albumin (MW 66,000 Da)
- (3) = Ovalbumin (MW 45,000 Da)
- (4) = Carbonic anhydrase (MW 30,000 Da)

Arrow indicates a determined molecular weight of recombinant wild-type and Y172A mutated amyloamylase

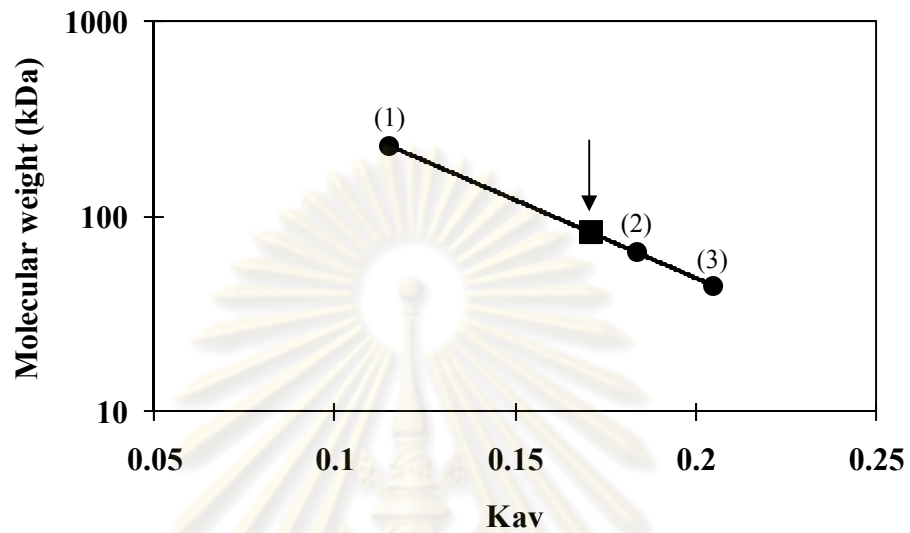


Figure 3.29 Calibration curve for molecular weight of recombinant wild-type and Y172A mutated amyloamylase by gel filtration on Sephacryl S-200 column

- (1) = Catalase (MW 232,000 Da)
 (2) = Bovine serum albumin (MW 66,000 Da)
 (3) = Ovalbumin (MW 44,000 Da)

Arrow indicates a determined molecular weight of recombinant wild-type and Y172A mutated amyloamylase

จุฬาลงกรณ์มหาวิทยาลัย

3.6.4 Determination of pI of amyloamylase

The recombinant wild-type amyloamylase, Y172A mutated enzyme and standard pI marker proteins were subjected to electrofocusing gel according to the method described in 2.12. The result is shown in Figure 3.30. A pI standard curve was constructed from the pI's and distance migrated from cathode of the standard proteins as shown in Figure 3.31. Both enzymes showed the same pI of 4.7. This value is consistent with the calculated value of 4.76 obtained by calculation from the deduced structure of the native enzyme using Program ProtParam (Gasteiger *et al.*, 2005).

3.6.5 Transglucosylation reaction of amyloamylase

The transglucosylation reaction of the recombinant wild-type and Y172A mutated amyloamylase was determined according to the method described in 2.13.6. The result was the same as the enzyme with his-tag residues (p19AM, section 3.3.4). The enzyme can catalyze transglucosylation reaction from G2 to G7 substrate to yield different maltooligosaccharides.

3.6.6 Activities of the recombinant wild-type and Y172A mutated amyloamylase

Four different activities of amyloamylase were measured as described in 2.9 and the activities of the recombinant wild-type p17AM and Y172A mutant were compared. The results are summarized in Table 3.5. Disproportionation activity is the measure of intermolecular transglucosylation activity of the enzyme. It was found that Y172A mutated enzyme showed about 3.5 fold lower activity than the wild-type enzyme. The cyclization activity of amyloamylase which measures intramolecular transglucosylation of the enzyme to yield the cyclic oligosaccharides is unique for

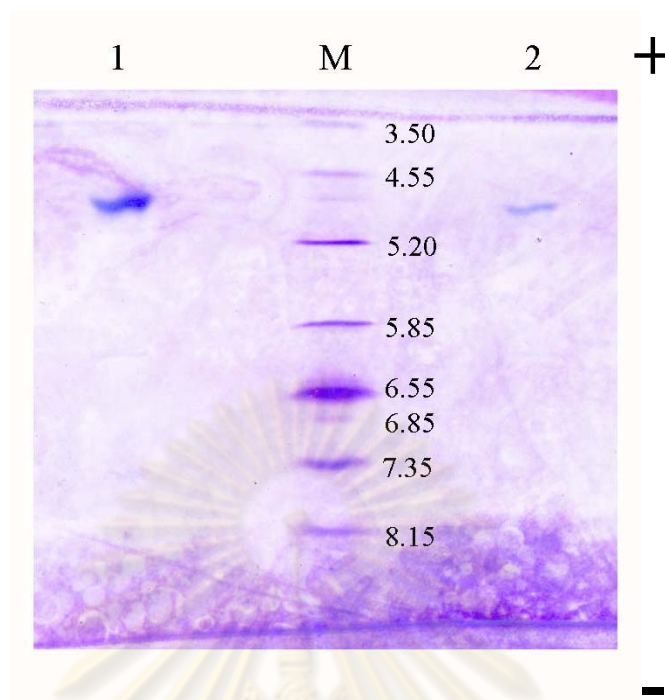


Figure 3.30 Isofocusing polyacrylamide gel electrophoresis of recombinant wild-type and Y172A mutated amyloamylase

Lane M	=	Standard pI markers;	
		Amyloglucosidase	pI 3.50
		Soybean trypsin Inhibitor	pI 4.55
		β -lactoglobulin A	pI 5.20
		Bovine carbonic anhydrase B	pI 5.85
		Human carbonic anhydrase B	pI 6.55
		Horse myoglobin-acidic band	pI 6.85
		Horse myoglobin-basic band	pI 7.35
		Lentil lectin-acidic band	pI 8.15
Lane 1	=	Purified recombinant wild-type amyloamylase	
Lane 2	=	Purified Y172A mutated amyloamylase	

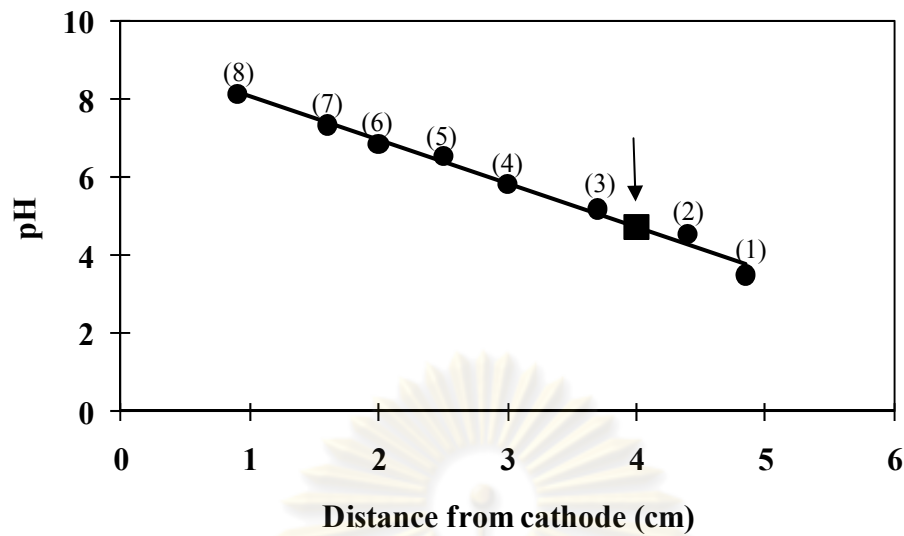


Figure 3.31 Calibration curve of standard pI markers.

The migration distances from cathode of the pI standard markers were measured and plotted against pI

- | | | |
|-------|-----------------------------|---------|
| (1) = | Amyloglucosidase | pI 3.50 |
| (2) = | Soybean trypsin Inhibitor | pI 4.55 |
| (3) = | β -lactoglobulin A | pI 5.20 |
| (4) = | Bovine carbonic anhydrase B | pI 5.85 |
| (5) = | Human carbonic anhydrase B | pI 6.55 |
| (6) = | Horse myoglobin-acidic band | pI 6.85 |
| (7) = | Horse myoglobin-basic band | pI 7.35 |
| (8) = | Lentil lectin-acidic band | pI 8.15 |

Arrow indicates a determined pI of recombinant wild-type and Y172A mutated amyloamylase

Table 3.5 Activity of the recombinant wild-type and Y172A mutated amyloamylase

Activity	Specific activity (U/mg protein)	
	Wild-type	Y172A
Disproportionation	21.76	6.18
Cyclization	0.502	0.283
Hydrolysis	7.13	4.22
Coupling	n.d.	n.d.

n.d. = not detectable

The methods for measuring disproportionation, cyclization, hydrolysis and coupling activities were as described in section 2.9.3, 2.9.4, 2.9.5 and 2.9.6, respectively.

ศูนย์วิทยทรัพยากร
จุฬาลงกรณ์มหาวิทยาลัย

4 α GTase including amyloamylase. The Y172A mutated enzyme catalyzed this reaction with 1.8 fold lower activity than the wild type. For hydrolysis activity on LR-CDs substrate, the Y172A mutated enzyme also showed 1.7 fold lower activity than wild-type enzyme. For coupling activity which is the reverse reaction of cyclization reaction, the activity could not be detected by any of the four described methods (section 2.9.6). The overall results showed that the recombinant wild-type amyloamylase demonstrated higher disproportionation, cyclization and hydrolysis activities than the Y172A mutated enzyme.

3.6.7 Substrate specificity

Substrate specificity of recombinant wild-type and Y172A mutated amyloamylase in disproportionation reaction was studied as described in 2.13.9. The ability of the recombinant wild-type and Y172A mutated amyloamylase to catalyze disproportionation reaction of various oligosaccharides (G2 to G7) was determined as shown in Figure 3.32 and 3.33, respectively. It found that maltotriose (G3) was the most preferred substrate for both enzymes. For recombinant wild-type enzyme, the descending order of preferred substrate was G3>G4>G5>G6>G7~G2 while the Y172A mutated enzyme showed the substrate order of G3>G4>G5>G6>G7>G2. It is noticed that the wild-type enzyme could use maltose (G2) better than Y172A mutated enzyme.

3.6.8 Determination of kinetic parameters

The kinetic of recombinant wild-type and Y172A mutated amyloamylase was evaluated by disproportionation reaction, where maltosyl group of maltotriose is transferred to another maltotriose to produce a glucose molecule. The

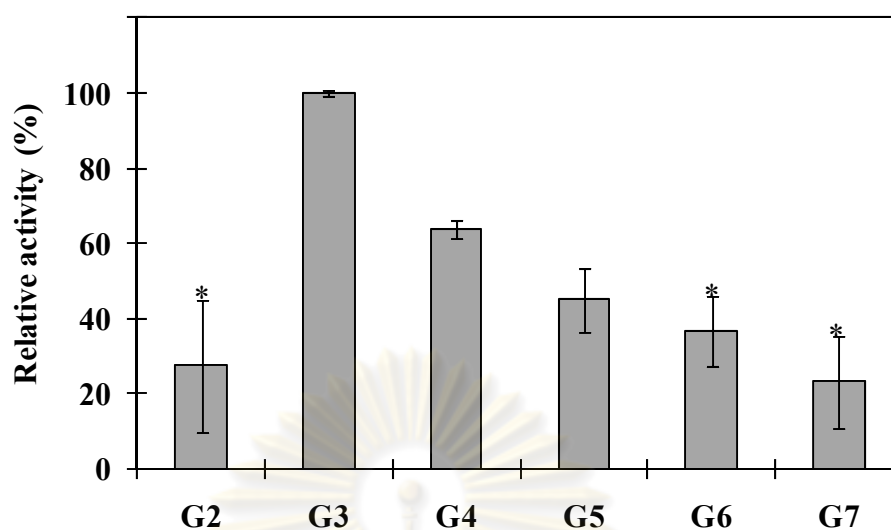


Figure 3.32 Substrate specificity of recombinant wild-type amyloamylase (p17AM) in disproportionation reaction. Data are presented as the mean \pm S.D. derived from three independent repeats. * $p < 0.05$ (Student's *t*-test) with respect to the disproportionation reaction with maltopentaose as substrate.

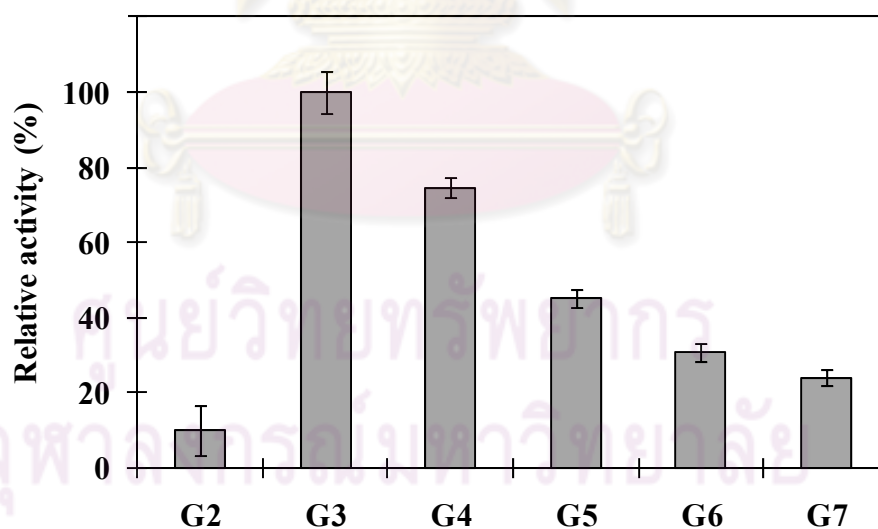


Figure 3.33 Substrate specificity of Y172A mutated amyloamylase in disproportionation reaction. Data are presented as the mean \pm S.D. derived from three independent repeats.

disproportionation reactions were performed at 30 °C for 5 minutes. The amount of released glucose was determined by glucose oxidase assay as described in 2.9.3. Lineweaver-Burk plot using nonlinear least square regression analysis of varying concentration of maltotriose was shown in Figure 3.34 and the summarized result was shown in Table 3.6. Under these conditions both enzymes showed different K_m and V_{max} values for maltotriose, and differed in their k_{cat} and the catalytic efficiency of the disproportionation reaction. The recombinant wild-type and Y172A mutated amyloamylase showed closed K_m values of 19.6 and 12.9 mM, respectively. When k_{cat} and catalytic efficiency were concerned, the recombinant wild-type amyloamylase gave higher value than Y172A mutated enzyme. These results showed that the reaction rate of the enzyme-substrate complex to give disproportionated products decreased after mutation. The k_{cat} and k_{cat}/K_m value of Y172A mutated enzyme was about 4.4 and 2.8-fold lower than that of the recombinant enzyme.

3.6.9 Time course of hydrolysis reaction

The glucose released from hydrolytic reaction of recombinant wild-type and Y172A mutated amyloamylase was determined as described in 2.13.8. The enzyme was incubated with 0.5 mg/ml of mixture of large-ring cyclodextrins at 30 °C and glucose released at various times was examined. The result (Figure 3.35) showed that the amount of glucose released by wild-type amyloamylase was significantly increased during the first six hours and kept on increasing gradually until 24 hours reaction. While the amount of glucose released by Y172A mutated enzyme was not increased but rather stable through 24 hours reaction time.

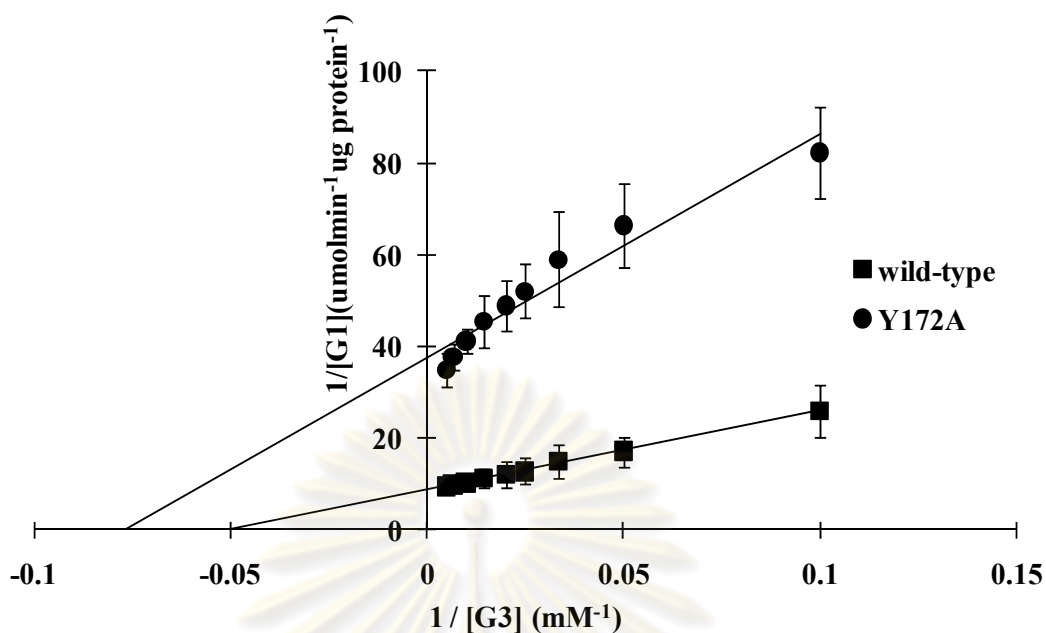


Figure 3.34 Lineweaver-Burk plot of recombinant wild-type and Y172A mutated amyloamylase on disproportionation reaction with maltotriose. The wild-type or Y172A mutated enzyme was incubated with various concentrations of maltotriose in 50 mM phosphate buffer, pH 6.0 at 30 °C for 5 min. Release of glucose was determined by glucose oxidase assay. Data are presented as the mean \pm S.D. derived from three independent repeats.

Table 3.6 Kinetic parameters of the recombinant wild-type and Y172A mutated amyloamylase from disproportionation reaction with maltotriose as substrate

Enzyme	K_m (mM)	V_{max} ($\mu\text{molmin}^{-1}\mu\text{g protein}^{-1}$)	k_{cat} (min^{-1})	k_{cat}/K_m ($\text{mM}^{-1}\text{min}^{-1}$)
Wild-type	19.6	0.116	9,374	479
Y172A	12.9	0.026	2,165	168

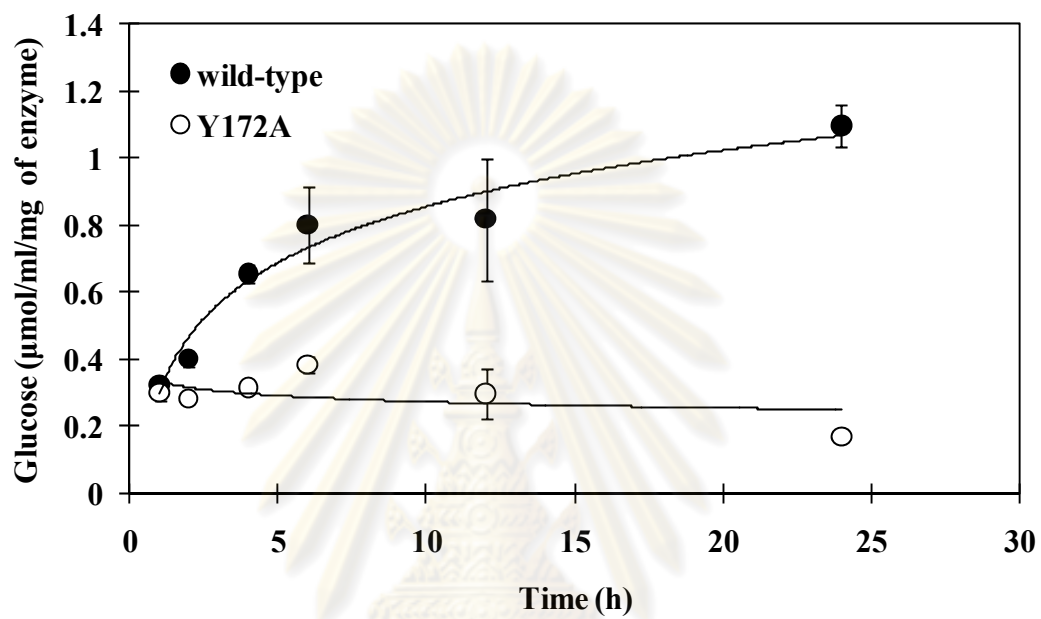


Figure 3.35 Glucose released at various time points.

ศูนย์วิทยทรัพยากร
จุฬาลงกรณ์มหาวิทยาลัย

3.6.10 The synthesis of large-ring cyclodextrins

When compared the wild-type and the Y172A mutated amyloamylase, it was found that at early incubation time (0-4 hours), Y172A mutated enzyme produced a significant lower amount of product than the wild-type enzyme, however, the product pattern was similar (Figure 3.36a to c). At long incubation time (24 hours), the product pattern of these enzymes was different (Figure 3.36b). The principal product of large-ring cyclodextrin was changed from larger (CD30-CD31 at 0-4 hours for both forms of enzyme) to the smaller size (CD26 and CD29 at 24 hours for the wild-type and mutated enzyme, respectively) when incubation time was extended. The changing rate of principal product formation from larger to smaller ring size in the recombinant wild-type amyloamylase was faster than that of Y172A mutated enzyme. It was noticed that at 24 hours incubation, the mutated enzyme had higher amounts of CD28-CD31 and of the rather large CDs (CD35-CD40) when compared to the wild-type.

When the amount of enzyme was varied, the effect on LR-CDs production was also seen (Figure 3.37). At 1 hour incubation, the increase in LR-CDs was corresponded with the increase in unit enzyme for both wild-type and mutated enzyme (Figure 3.37a and 3.37b). At long incubation (24 hours), the amount of LR-CDs of high unit enzyme (0.15 U) was lower than those produced by lower units of enzyme (0.1 U and 0.05 U) except for the smaller ring size CD21 for the wild-type enzyme (Figure 3.37c) and CD21-25 for the mutated enzyme (Figure 3.37d). The LR-CDs produced by 0.15 U enzyme were tend to be smaller than those produced from 0.1 and 0.05 U (Figure 3.37c and 3.37d). Thus, the size and the amount of LR-CDs product was decreased when the amount of enzyme increased at long incubation time. The changing rate of principal product formation from larger to smaller ring in the presence of higher unit was faster than in lower unit of enzyme. In addition, the

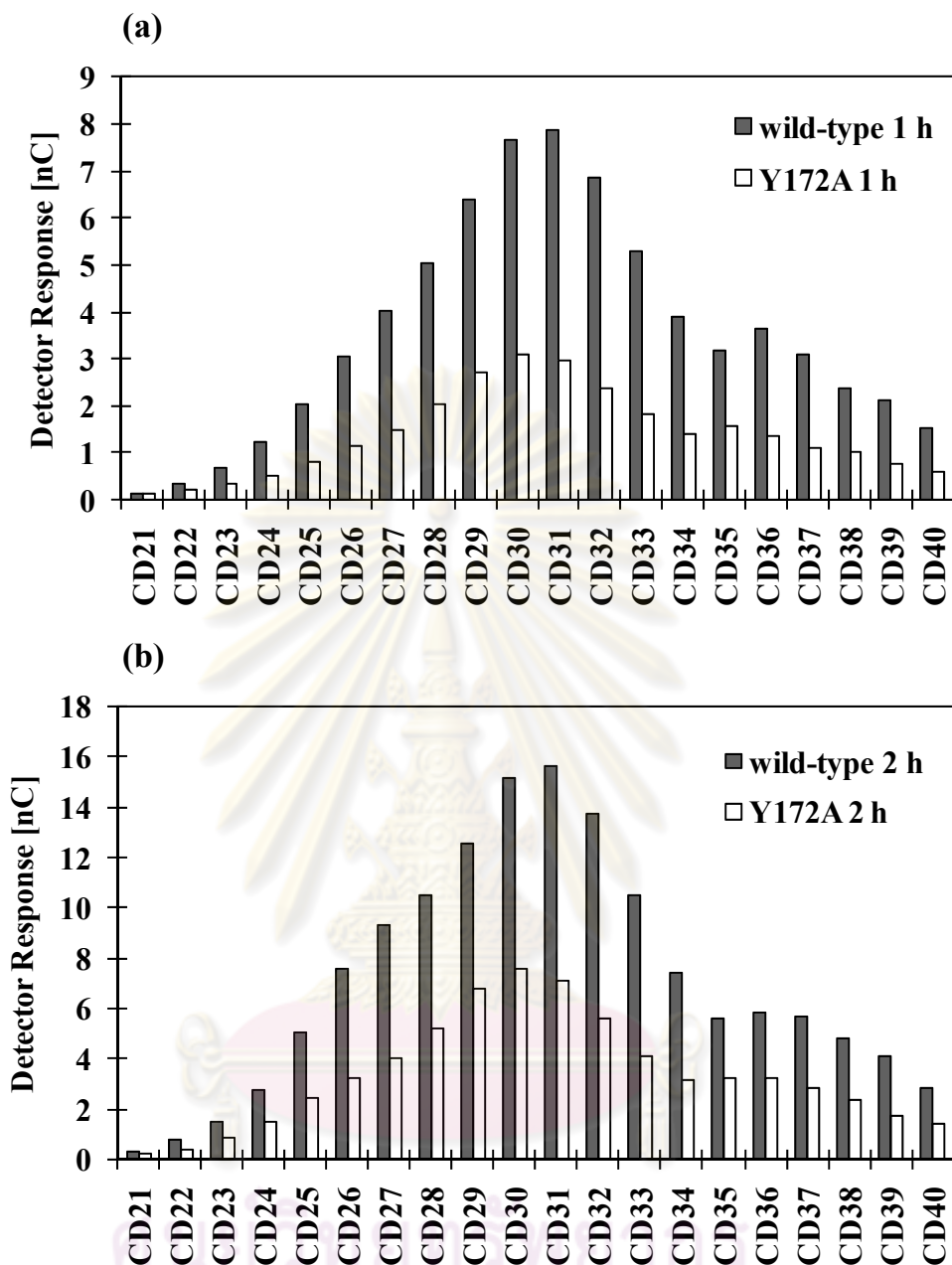


Figure 3.36 Profiles of large-ring cyclodextrin products at different incubation time as analyzed by HPAEC-PAD. 0.2% (w/v) pea starch was incubated with 0.05 U/ml enzyme at 30 °C. (a) Incubation of 1 h, (b) Incubation of 2 h, (c) Incubation of 4 h, (d) Incubation of 24 h. Grey and white bars are products of the recombinant wild-type and Y172A mutated amyloamylase, respectively. The results were averaged from two independent measurements.

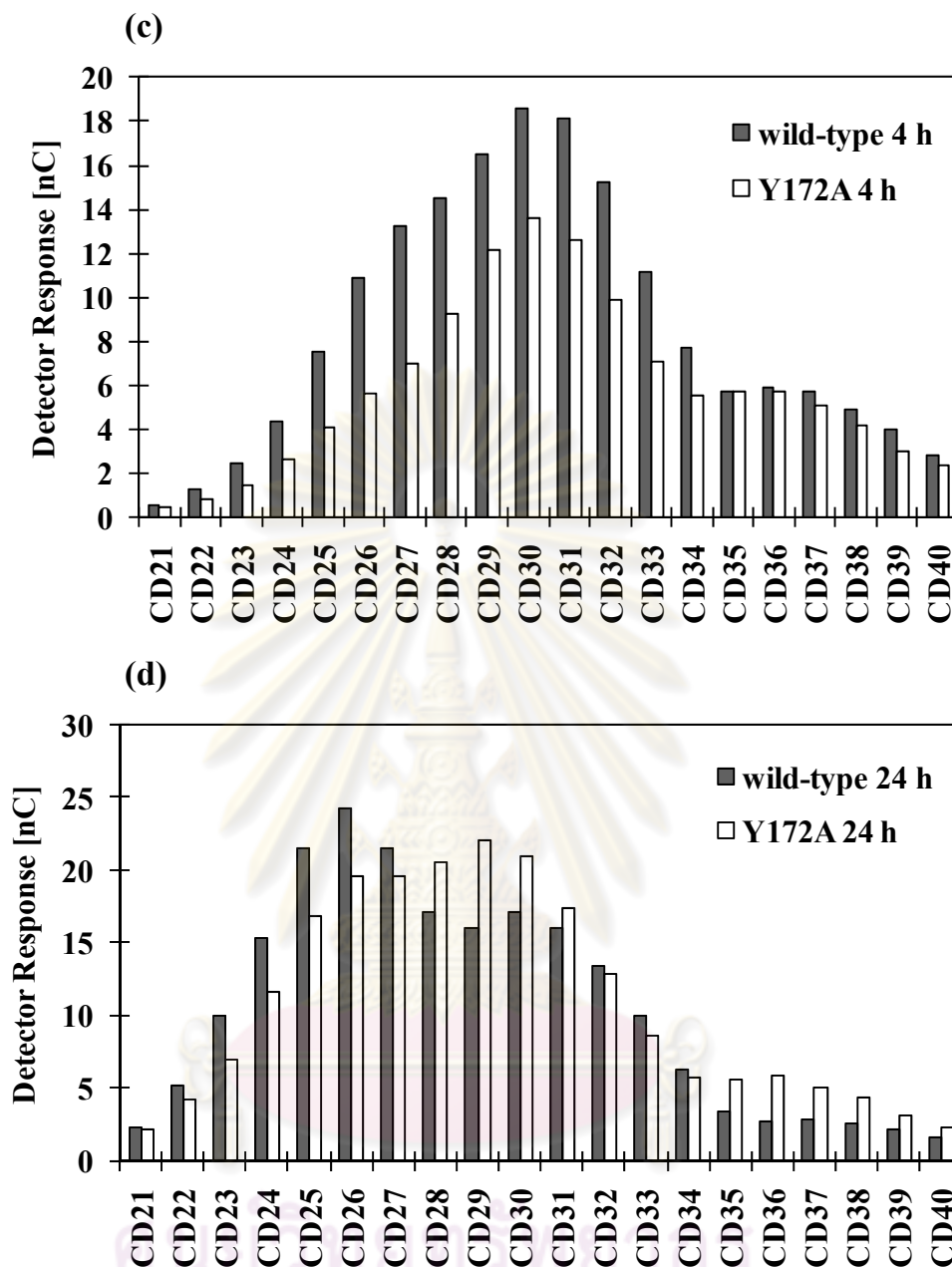


Figure 3.36 (continued) Profiles of large-ring cyclodextrin products at different incubation time as analyzed by HPAEC-PAD. 0.2% (w/v) pea starch was incubated with 0.05 U/ml enzyme at 30 °C. (a) 1 h incubation, (b) 2 h incubation, (c) 4 h incubation, (d) 24 h incubation. Grey and white bars are products of the recombinant wild-type and Y172A mutated amyloamylase, respectively. The results were averaged from two independent measurements.

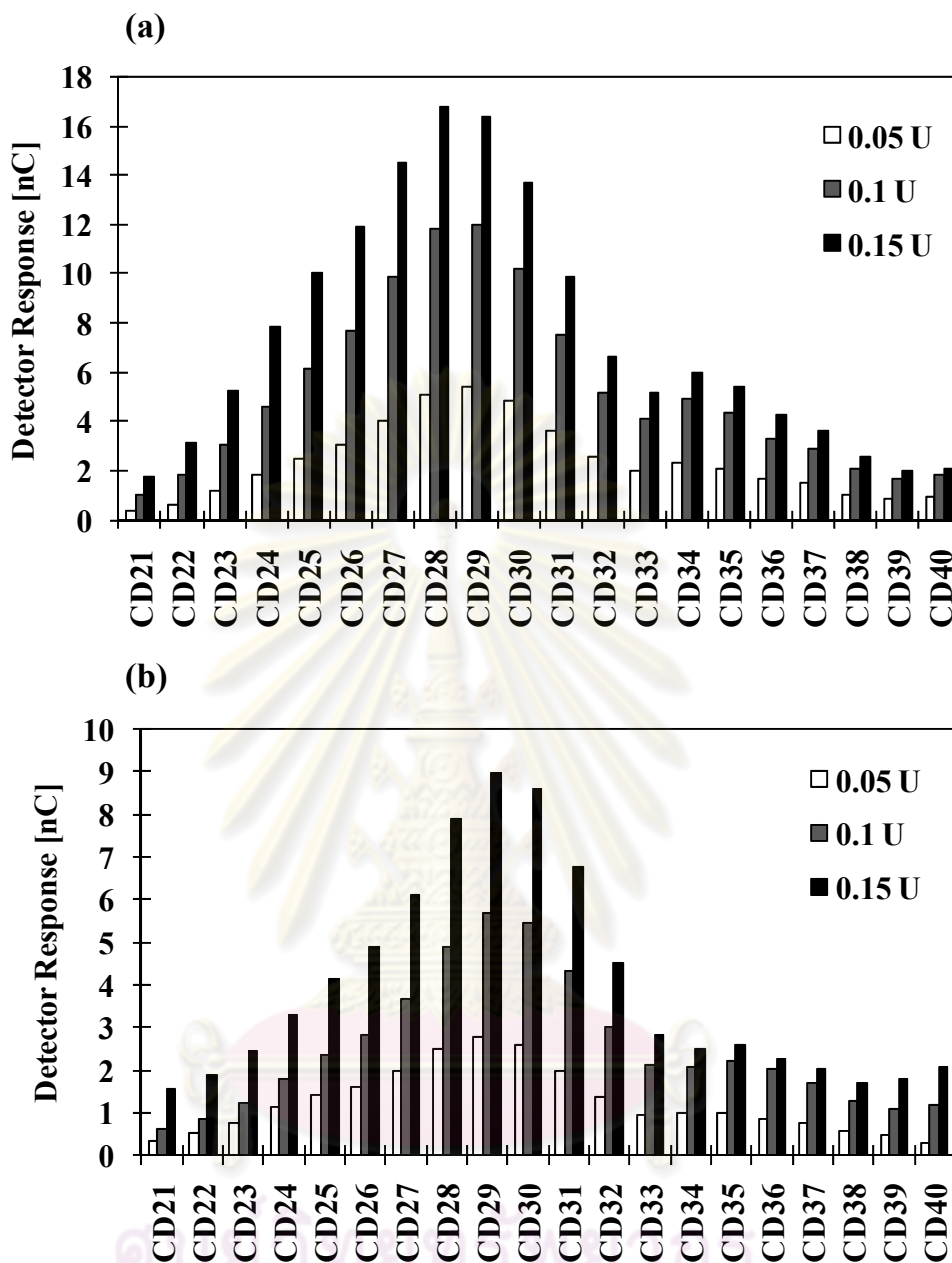


Figure 3.37 Profiles of large-ring cyclodextrin products at different amount of recombinant amyloamylase as analyzed by HPAEC-PAD. 0.2% (w/v) pea starch was incubated at 30 °C. (a) the wild-type enzyme, 1 h incubation, (b) Y172A enzyme, 1 h incubation, (c) the wild-type enzyme, 24 h incubation, (d) Y172A enzyme, 24 h incubation. Black, gray and white bars are products from 0.05, 0.1 and 0.15 U enzyme, respectively.

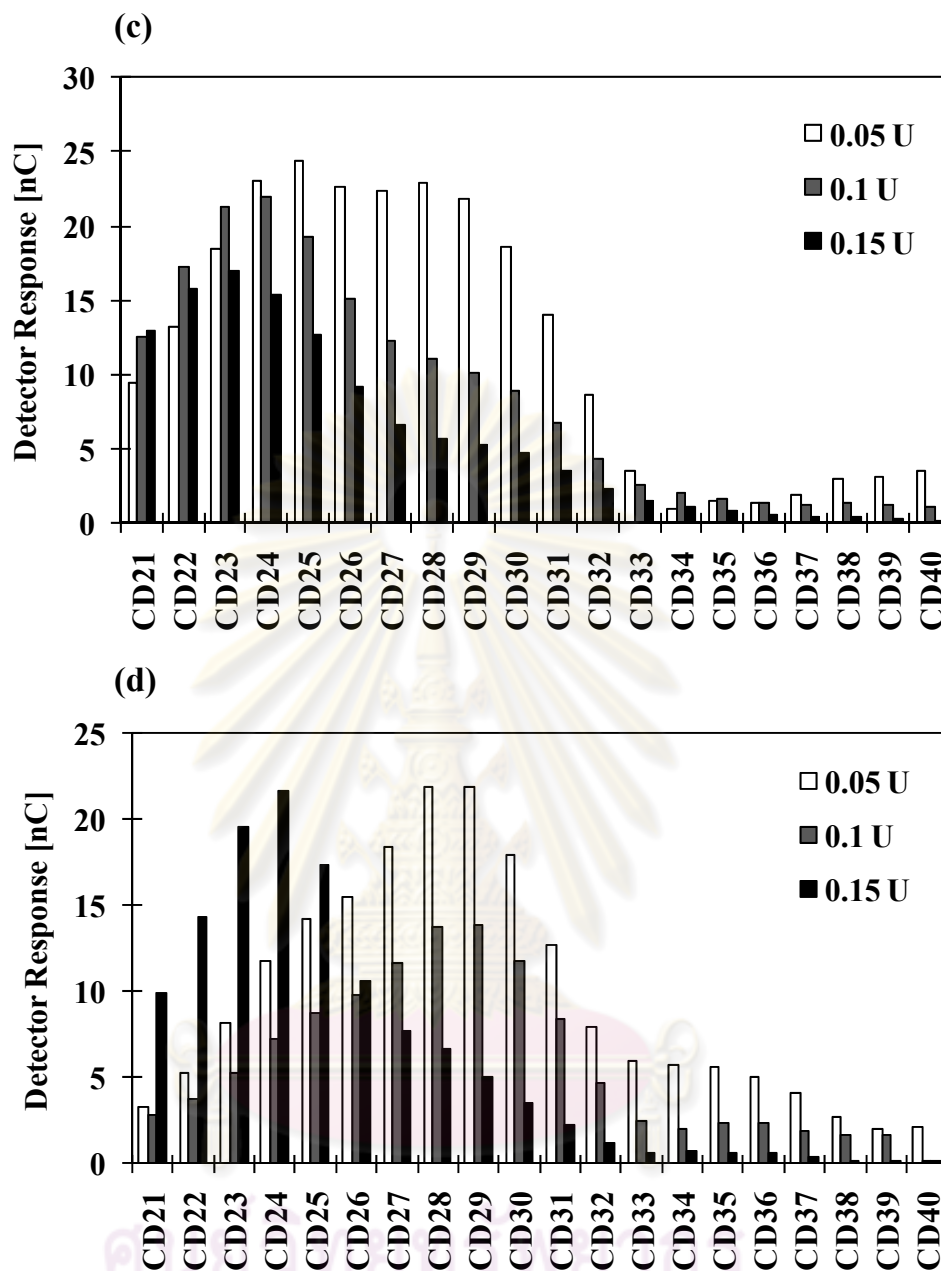


Figure 3.37 (continued) Profiles of large-ring cyclodextrin products at different amount of recombinant amylamaltase as analyzed by HPAEC-PAD. 0.2% (w/v) pea starch was incubated at 30 °C. (a) the wild-type enzyme, 1 h incubation, (b) Y172A enzyme, 1 h incubation, (c) the wild-type enzyme, 24 h incubation, (d) Y172A enzyme, 24 h incubation. Black, gray and white bars are products from 0.05, 0.1 and 0.15 U enzyme, respectively.

changing rate of principal product formation from larger to smaller ring size by the recombinant enzyme was faster than that of Y172A mutated enzyme (Table 3.7).

3.6.11 Analysis of large-ring cyclodextrins by MALDI-TOF

In order to get larger amount of products, the larger-scale production of large-ring cyclodextrins was performed using 0.024 U/ml wild-type enzyme as described in 2.14. The product was analyzed by HPAEC-PAD (Figure 3.38) and the size confirmed by MALDI-TOF as described in 2.16. The result of MALDI-TOF of the precipitate of reaction products was shown in Figure 3.39. The pseudomolecular ion peaks $[M+Na]^+$ at m/z corresponded to the size of products were then assigned for each LR-CD. The spectra showed that the products consisted of reliably observed amount of CD23 to CD45. The smaller and larger CDs could also be observed but with a very low amount. CD30 was the product with the highest amount. The results confirms the assignment of LR-CDs using the retention time in HPAEC (Figure 3.38) that the recombinant wild-type enzyme can synthesize large-ring cyclodextrins from CD19 up to about CD70.

ศูนย์วิทยทรัพยากร
จุฬาลงกรณ์มหาวิทยาลัย

Table 3.7 The effect of amount of enzyme and incubation time on formation of principal large-ring cyclodextrin products of the wild-type and Y172A mutated amyloamylase

Amount of enzyme (U)	Incubation time (h)	Principal CD
Wild-type		
0.05	1	CD28-30
0.1	1	CD28-29
0.15	1	CD28-29
0.05	24	CD24-28
0.1	24	CD23-24
0.15	24	CD22-24
Y172A		
0.05	1	CD28-30
0.1	1	CD29-30
0.15	1	CD29-30
0.05	24	CD28-29
0.1	24	CD28-29
0.15	24	CD24

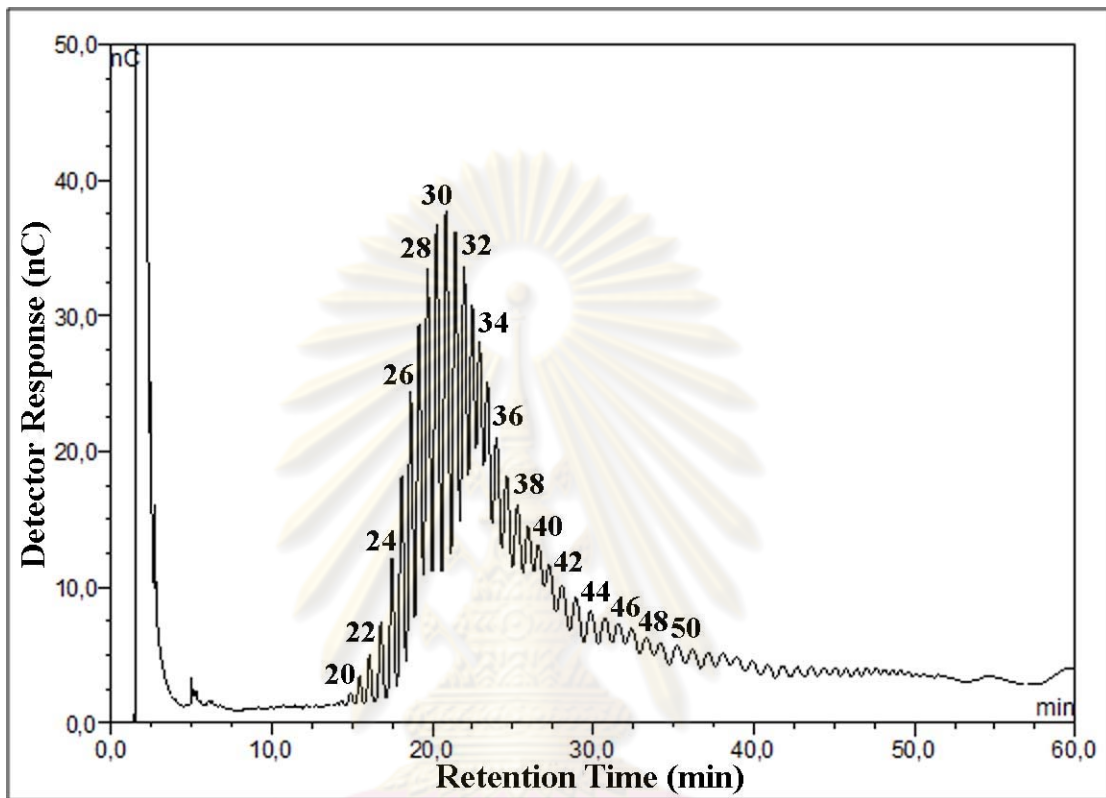


Figure 3.38 HPAEC analysis of the larger-scale production of large-ring cyclodextrins. 0.2% (w/v) pea starch was incubated with 0.024 U/ml enzyme at 30 °C for 24 h. Peak numbers indicate the degree of polymerization of identified LR-CDs based on comparison of R_t with CD20 and CD21.

ศูนย์วิทยาศาสตร์การ
จุฬาลงกรณ์มหาวิทยาลัย

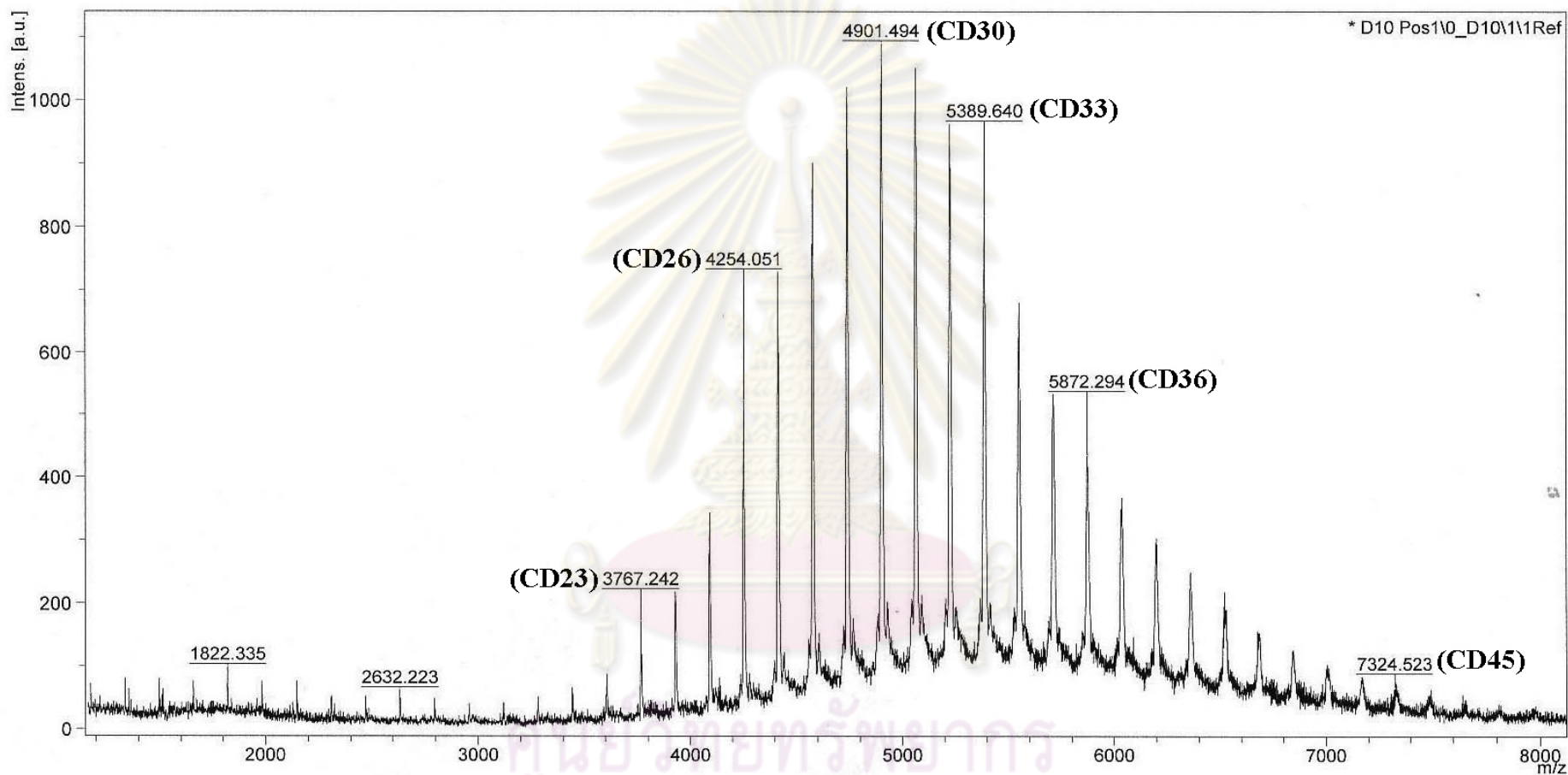


Figure 3.39 Mass spectra of mixture of large-ring cyclodextrin products. Peak numbers indicate the size of LR-CD products.

CHAPTER IV

DISCUSSION

Since large-ring cyclodextrins show several potential applications in pharmaceuticals, food science and biotechnology (Endo *et al.*, 2002, Tomono *et al.*, 2002), investigation on LR-CDs producing enzyme is required. Bacteria and archaea are known as main sources for amyloamylase enzyme. Molecular cloning has also been used to produce new clone of bacteria with the desired LR-CDs producing property. In some organisms such as *Corynebacterium glutamicum* (Kalinowski *et al.*, 2003; Ikeda and Nakagawa, 2003), only the putative amyloamylase gene was reported with no studies on the enzyme. Interestingly, we found that the nucleotide sequence of amyloamylase from *C. glutamicum* had low similarity to those from *T. aquaticus* (Terada *et al.*, 1999) and *A. aeolicus* (Bhuiyan *et al.*, 1999) in which the cycloamylose production from enzymatic action on starch substrate have been reported. The aim of the present study was to biochemically characterize this novel amyloamylase from *C. glutamicum* with the emphasis on the profile of LR-CDs production. The work includes overexpression of amyloamylase by construction of the recombinant enzyme, enzyme purification and site-directed mutagenesis to determine structure-function relationship.

4.1 Identification of amyloamylase gene from *Corynebacterium glutamicum*

Amyloamylase was first found in *Escherichia coli* as a maltose-inducible enzyme which is essential for the metabolism of maltose (Monod and Torriani, 1984). The amyloamylase gene has been cloned from several bacteria and archaea e.g. *Streptococcus pneumoniae* (Stassi *et al.*, 1981), *E. coli* (Pugsley and Dubreuil, 1988),

hyperthermophilic archaeon *Thermococcus litoralis* (Jeon *et al.*, 1997), *Thermus aquaticus* ATCC 33923 (Terada *et al.*, 1999), *Aquifex aeolicus* (Bhuiyan *et al.*, 2003) and *Thermus brockianus* (Bo-young *et al.*, 2006). However, only a few amyloamylases were biochemically characterized.

The *C. glutamicum* amyloamylase gene (*malQ*) had an ORF of 2,121 bp and was deduced into a protein with 706 amino acids. PCR technique using oligonucleotides (primers) from known sequence of gene (Sambrook and Russell, 2001) was employed to identify *malQ* gene from *C. glutamicum*. The DNA polymerase with 3'→5' exonuclease (proof reading) was used to reduce the error in PCR product. For our experiment, *pfu* DNA polymerase was employed because it is useful for polymerization reaction requiring high fidelity synthesis (Lundberg *et al.*, 1991).

The result (Figure 3.2) showed that the designed primers were specific to *malQ* gene from *C. glutamicum*. The PCR product was used for insertion into pET-19b vector and transformed to *E. coli* BL21(DE3). The pET-19b is an expression vector using bacteriophage T7 promoter as the expression system. The system has the following advantages (Sambrook *et al.*, 2001). First, bacteriophage T7 RNA polymerase, unlike *E. coli* RNA polymerase, is not inhibited by rifampicin. The antibiotic can therefore be used to extinguish transcripts of host cell genes. Second, the bacteriophage-encoded enzyme recognizes only bacteriophage T7 promoters which are not present in *E. coli* chromosomal DNA. Finally, bacteriophage T7 RNA polymerase as processive enzyme will transcribe around a circle plasmid several times and may therefore produce genes that are efficiently transcribed by *E. coli* RNA polymerase. Therefore, T7 promoter was suitable for expression of *malQ* gene and pET-19b vector was selected. *E. coli* BL21(DE3) was used for host expression vector

because this strain had gene encoding bacteriophage T7 RNA polymerase, which is integrated into the chromosome of BL21. To insert *malQ* gene fragment into pET-19b at the right position, both gene fragment and pET-19b must have similar restriction sites. In this experiment *NdeI* and *XhoI* restriction sites were selected. The gene fragment was amplified with 5' end primer containing *NdeI* restriction site and 3' end primer that contained *XhoI* restriction site. The whole gene fragment amplified was digested with *NdeI* and *XhoI*, then ligated to *NdeI-XhoI* sites of pET-19b and transformed into *E. coli* BL21(DE3) host cells. The transformant containing pET-19b vector harboring *malQ* was grown on LB agar containing ampicillin plate and was used for plasmid extraction and sequence determination.

Based on the deduced amino acid sequence, *C. glutamicum* amyloamylase exhibited low level of homology with previously reported 4 α GTases especially those well-characterized enzymes from *Thermus* and *Aquifex* (17 % identity with *T. aquaticus* (Terada *et al.*, 1999), 18% identity with *T. thermophilus* (Terada *et al.*, 1999) 13% identity with *A. aeolicus* (Bhuiyan *et al.*, 2003), 12% identity with potatoes (Takaha *et al.*, 1993) and the highest identity of 26% with *E. coli* K12 enzyme (Pugsley and Dubreuil, 1988) (Table 3.1).

4.2 Expression of amyloamylase from the recombinant clone harboring p19AM

Because the recombinant gene fragment did not have their own promoter, they were expressed under T7 promoter on the plasmid pET-19b. In this pET system, T7 RNA polymerase gene was under the control of the lacUV5 promoter, and the plasmid vector equipped with a bacteriophage T7 promoter upstream of the gene. Both promoters contain the *lac* operator (*lacO*) in such position that binding of a lac repressor to the operator site blocks transcription. IPTG can bind to the repressor

which results in the loss of affinity for the lac operator. Therefore, adding IPTG should allow transcription of *malQ* gene in pET system vector. Transformants, which showed the highest amyloamylase activity were grown in LB medium containing ampicillin. At mid-log growth phase, IPTG was added, the suitable concentration was 0.4 mM and further grew for 2 hours before harvested, and the enzyme specific activity obtained was about 2.2 U/mg protein (Table 3.2). The *E. coli* is a normally used host for amyloamylase expression (Takaha *et al.*, 1993; Terada *et al.*, 1999; Jeon *et al.*, 1997; Bhuiyan *et al.*, 2003; Bo-young *et al.*, 2006; Goda *et al.*, 2007;), however, a few studies used *Bacillus subtilis* as an expression host. All expressed amyloamylases were reported to be located in the cells (Espinosa *et al.*, 1984; Kang *et al.*, 2010). Recently, expression of amyloamylase gene from *Thermus scotoductus* in *B. subtilis* using constitutive promoters were reported (Kang *et al.*, 2010). They found that the activity of amyloamylase expressed by *B. subtilis* was only 4% of that in previous *E. coli* system.

4.3 Purification of amyloamylase from the recombinant clone harboring p19AM

Several methods have been used to purify amyloamylase. Heat treatment at 85 °C, 80% ammonium sulfate precipitation and Phenyl-Sepharose HR 5/5 column were used to purify 4 α GTase from *Pyrococcus* sp. KOD1 (Tachibana *et al.*, 1997). 30% ammonium sulfate precipitation, DEAE-Sephadex column, ultrogel AcA column, hydroxylapatite column and 1,6-hexanediamine Sepharose 4B column were purification steps for *E. coli* IFO 3806 enzyme (Kitahata *et al.*, 1989). For sweet potato D-enzyme, 30-70% ammonium sulfate precipitation, Sephadex G10 column, DEAE-toyopearl 650M column and Cellulofine GCL-2000-sf were used (Suganuma *et al.*, 1991). Heat treatment, Q-Sepharose HR 16/10 column, mono Q HR 5/5 column

and Superose 12 HR 10/30 column were used to purify 4 α GTase from *Thermotoga maritima* (Liebl *et al.*, 1992). One popular approach is to attach an oligonucleotide that encodes six consecutive histidine residues. The expressed “his-tag” protein binds to chromatographic supports that contain an immobilized divalent metal ion such as Ni²⁺ (Murray *et al.*, 2003). The amyloamylase from p19AM (the recombinant clone containing pET-19b inserted with *malQ* gene from *C. glutamicum*) was expressed as enzyme containing his-tag residues at N-terminal. The enzyme was purified by HisTrap FFTM which is a prepacked column containing 90 μ m highly cross-linked agarose bead with an immobilized chelating group. The matrix has been charged with Ni²⁺-ion. This column selectively binds histidine-tag protein which has specific affinity for Ni²⁺. The amyloamylase was purified to homogeneity with 10.8 purification fold and 30.2% yield (Table 3.2). In previous reports, amyloamylase from *Synechocystis* sp. PCC 6803 was 2.9-fold purified with 84.5% yield (Lee *et al.*, 2009) and that from *Thermus brockianus* was 35-fold purified with 67% yield after heat treatment and Ni²⁺-NTA column chromatography (Bo-young *et al.*, 2006).

In SDS-PAGE analysis, the purified enzyme showed a single band on the gel (Figure 3.13a). This result suggested that the enzyme was highly purified. However, the native-PAGE revealed one major and one minor band (Figure 3.14). Native-PAGE can be sensitive to any process that alters either the charge or the conformation of a protein, such as, the change in charge due to post-translational modification (e.g. deamidation), unfolded or other modified conformations, oligomers and aggregates (both covalent and non-covalent) and binding events (protein-protein or protein-ligand) (Copeland, 2000).

4.4 Characterization of amyloamylase from the recombinant clone with p19AM

4.4.1 Molecular weight determination

The molecular weight of amyloamylase containing his-tag residues from recombinant clone with p19AM was 84 kDa (Figure 3.13b). The size was closed to 4 α GTase from *Thermococcus litoralis* (79 kDa, Xavier *et al.*, 1999), but different from that in *Thermus aquaticus* (57 kDa, Terada *et al.*, 1999), *Synechocystis* sp. PCC 6803 (57 kDa, Lee *et al.*, 2009) and in *E. coli* IFO3806 (93 kDa, Kitahata *et al.*, 1989). D-enzyme in potatoes was 60 kDa (Takaha *et al.*, 1993)

4.4.2 Effect of temperature on starch transglucosylation activity and stability

From our result, the enzyme showed optimum temperature for starch transglucosylation activity at 30 °C (Figure 3.15a). For temperature stability, full activity was retained at temperature up to 30 °C while at 50°C and higher, amyloamylase absolutely lost its activity after 10 minutes of incubation (Figure 3.15b). The optimum temperature and temperature stability was closed to those of 4 α GTases from mesophilic bacteria such as *E. coli* IFO3806 (optimum temperature at 35 °C and stable up to 45 °C, Kitahata *et al.*, 1989), *Pseudomonas stutzeri* (optimum temperature at 37 °C and stable up to 50 °C, Schmidt *et al.*, 1979) and *Synechocystis* sp. PCC 6803 (optimum temperature at 45 °C and stable up to 50 °C, Lee *et al.*, 2009). While amyloamylases from thermophilic microorganism were different such as those from *T. aquaticus* (optimum temperature at 75 °C and stable up to 85 °C, Terada *et al.*, 1999) and *Thermotoga maritime* (optimum temperature at 70 °C and stable up to 80 °C, Leibl *et al.*, 1992).

4.4.3 Effect of pH on starch transglucosylation activity and stability

Amylomaltase from *C. glutamicum* showed optimum pH for starch transglucosylation activity at pH 6.0 (Figure 3.16a). This enzyme was stable at pH range 5.5-9.0 when incubated at 30 °C for 1 hour, activity was retained above 80%, suggesting that this amylomaltase was stable in the wide range of pH (Figure 3.16b). These pH characteristics were similar to those of *T. aquaticus* with optimum pH at 5.5-6.0 and stable at pH 4.0-10.0 when incubated at 70 °C for 10 minutes (Terada *et al.*, 1999). While the enzyme from *E. coli* IFO3806 was not alkali stable, optimum pH at 6.5 and stable at pH 6.0-7.3 when incubated at 40 °C for 30 minutes (Kitahata *et al.*, 1989). Amylomaltases with higher optimum pH were reported in *Pseudomonas stutzeri* (pH 7.7, Schmidt *et al.*, 1979), in *Thermotoga maritime* (pH 7.0-8.0, Leibl *et al.*, 1992) and in *Synechocystis* sp. PCC 6803 (pH 7.0, Lee *et al.*, 2009).

4.4.4 Transglucosylation reaction

In addition to an intramolecular transglucosylation, amylomaltase also catalyzes an intermolecular transglucosylation reaction or disproportionation on maltooligosaccharides in which a glucan moiety is transferred from one α -1,4-glucan molecule to another α -1,4-glucan (Takaha and Smith, 1999). The result showed that the recombinant amylomaltase can transfer glucose units from one 1,4- α -glucan to another and the enzyme requires at least maltose unit for the transglucosylation reaction. The amylomaltase from *C. glutamicum* was similar to those from *T. aquaticus* (Terada *et al.*, 1999), *Clostridium butyricum* NCIMB 7423 (Goda *et al.*, 1997), *E. coli* IFO3806 (Kitahata *et al.*, 1989), *Thermococcus litoralis* (Jeon *et al.*, 1997) and *Synechocystis* sp. PCC 6803 (Lee *et al.*, 2009) in which the smallest molecule required for intermolecular transglucosylation was maltose. The plant D-

enzymes from potatoes (Takaha *et al.*, 1993) and *Arabidopsis thaliana* (Lin and Preiss, 1988) also catalyze an intermolecular transglucosylation but the smallest molecule required was maltotriose. This characteristic differentiates amyloamylase from D-enzyme (Takaha and Smith, 1999).

4.4.5 The synthesis of large-ring cyclodextrins

The 4 α GTase mainly catalyzes intramolecular transglucosylation or cyclization reaction to form cycloamylose or cyclodextrin. Small-ring CDs (CD6-CD8) are produced by CGTase while LR-CDs are produced by amyloamylase or D-enzyme (Takaha and Smith, 1999; Endo *et al.*, 2002). The ability of amyloamylase from *C. glutamicum* to produce LR-CDs was examined using pea starch as substrate. The results showed that the LR-CD products were depended on the incubation time used. At early incubation time, the principle product was larger LR-CD. This time dependence behavior was also reported in *T. aquaticus* (Terada *et al.*, 1999) and potato D-enzyme (Takaha *et al.*, 1996). We also found that when using higher concentration of the enzyme, the amount of CD products was increased. However, the product pattern was not much different from that at low enzyme concentration, consisted of mixtures of LR-CDs ranged from about CD19 to higher (Figure 3.19). Our product profile was different from other amyloamylases in which the smallest CD produced were CD17 (*E. coli* K12, Takaha and Smith, 1999), CD22 (*T. aquaticus*, Terada *et al.*, 1999, *Synechocystis* sp. PCC 6803, Lee *et al.*, 2009). While potato D-enzyme produced CD17 as smallest product (Takaha *et al.*, 1996).

4.5 Construction and expression of recombinant wild-type p17AM and Y172A mutated enzyme

Frequently, removal of the purification tag is necessary, either to restore protein function, enhance its solubility or, for therapeutic processes, because the purification fusion is antigenic (Sussenfeld, 1990; Esposito and Chatterjee, 2006). Difficulties are often encountered when attempts are made to remove the tag (Baneyx, 1999). In some case, the protease cleavage fails, owing perhaps to steric issues or aggregation. In other cases, the protease cleavage is successful, but the protein does not remain soluble or function once the tag is removed (Esposito and Chatterjee, 2006). There have been reports on misfolded, aggregated and precipitated of proteins after tag removal bacterial proteins such as elongation factor Tu, DNA gyrase subunit A (Ashraf *et al.*, 2004) and also in eukaryotic proteins such as glucocorticoid receptor, small heterodimer partner and HPV E6 oncoprotein (Ashraf *et al.*, 2004; Nominé *et al.*, 2001).

After purification of recombinant wild-type amyloamylase from p19AM clone, the his-tag residue (23 amino acids in length) was removed. Unfortunately, the mature amyloamylase enzyme showed no activity. A new expression vector without his-tag, pET-17b, has then been chosen. The *malQ* gene fragment was excised from pET-19b, ligated with pET-17b and the new transformant was constructed. The recombinant wild-type p17AM was expressed as similar to the p19AM and the specific activity of the crude enzyme obtained was 2 U/mg protein (Table 3.3) which was about the same as that for p19AM.

To construct the mutated amyloamylase for structure-function study, Tyr-172 was chosen according to previous work in *T. aquaticus*. The Tyr-54 and Tyr-101 at secondary binding site of *T. aquaticus* amyloamylase were proposed to be important

for the formation of LR-CD product due to hydrophobic interaction (Sträter *et al.*, 2002). Later, by site-directed mutagenesis, residues at the second binding site have been reported to involve in LR-CD production by exerting the effect on hydrolysis activity of this enzyme (Fujii *et al.*, 2005). The corresponding position in *C. glutamicum*, Tyr-172, was then our target for site-directed mutagenesis (Figure 3.21). The Tyr-172 of *C. glutamicum* amyloamylase was changed to alanine by PCR amplification. The Y172A mutant was grown in the LB medium containing ampicillin and determined for starch transglucosylation activity. The specific activity of the crude Y172A mutated amyloamylase was 1.1 U/mg protein (Table 3.4) which was about half of that of the wild-type enzyme due to the decrease in activity after mutation.

4.6 Purification of amyloamylase from the recombinant clone harboring p17AM and Y172A mutant

To purify the wild-type p17AM and Y172A mutated amyloamylase, DEAE FFTM and Phenyl FFTM column were used. The DEAE FFTM column is a weak anion exchanger which is a positively charged solid matrix. Proteins with a net negative charge migrate through the matrix more slowly than those with a net positive charge. After this step, both the wild-type and mutated enzyme still revealed many protein bands on SDS-PAGE (Figure 3.26 and 3.27). Second step of purification was then performed on Phenyl FFTM column, a hydrophobic interaction chromatography which separate proteins on the basis of their varying hydrophobic interaction with hydrophobic groups. Binding is promoted by the presence of moderately high concentration of anti-chaotropic salts and elution is improved by decreasing the affinity of the protein for the hydrophobic group on the matrix, usually by decreasing

the ionic strength of the elution buffer (Nelson and Cox, 2005). Both enzymes were purified to homogeneity after this step since a single band was observed on SDS-PAGE (Figure 3.26 and 3.27) and also native-PAGE (Figure 3.28).

4.7 Characterization of amyloamylase from the recombinant clone with p17AM and Y172A mutant

4.7.1 Molecular weight determination

The molecular weights of the wild-type p17AM and Y172A mutated amyloamylase were the same at 81 kDa when estimated from SDS-PAGE (Figure 3.29) and 83 kDa from gel filtration chromatography (Figure 3.30). This result suggests that this amyloamylase is a single protein chain with no subunit structure. The amyloamylases from *Thermococcus litoralis* (Jeon *et al.*, 1997), *Thermotoga maritima* (Liebl *et al.*, 1992) and D-enzyme from potatoes (Takaha *et al.*, 1993) were monomeric proteins. However, the enzyme from *Pseudomonas stutzeri* Terada *et al.* (1999) and pea chloroplast (Kakefuda and Duke, 1989) were reported to be dimer.

4.7.2 Effect of pH and temperature on starch transglucosylation activity and stability

The optimum pH and temperature and also stability of the wild-type p17AM and Y172A mutated enzyme were the same as the enzyme with his-tag residues (p19AM). These results suggested that his-tag and mutagenesis at Tyr-54 did not result in any change of these characteristics.

4.7.3 Determination of pI

The purified amyloamylase from recombinant clone with p17AM and Y172A mutant showed the same pI of 4.7 (Figure 3.32). This value is consistent with the calculated value obtained by calculation from the deduced amino acid sequence. This result suggested that the mutagenesis at Tyr-54 had no effect on the pI value of this enzyme.

4.7.4 Measurement of activities

The four activities of the wild-type p17AM and Y172A mutated amyloamylase were measured (Table 3.5). Disproportionation activity was determined by using maltotriose (G3) as substrate and glucose released was detected by glucose oxidase method. The Y172A mutated enzyme showed about 3.5-fold lower activity than the wild-type. Cyclization activity was measured by using pea starch as substrate and LR-CD produced was detected by HPAEC-PAD. The Y172A mutated enzyme catalyzed this reaction with 1.8-fold lower activity than the wild type. For hydrolysis activity, LR-CDs were used as substrate and reduced sugar was detected by bicinchoninic acid assay. The mutated enzyme also showed 1.7-fold lower activity than the wild-type. For coupling activity which is the reverse reaction of cyclization reaction, the activity was determined by many methods (section 2.9.6), but the activity was not at all detectable. From the overall results, substitution at Tyr-172 with Ala not only decreased the hydrolytic activity but also decreased disproportionation and cyclization activities of the enzyme. In addition, the coupling activity of this enzyme was extremely low. The substitution of Tyr-172 with Ala affected both inter- and intramolecular transglucosylation because all four reactions has been operated by the same

catalytic mechanism but using different donor and acceptor molecules (Przylas *et al.*, 2000, Sträter *et al.*, 2002).

In *T. aquaticus* amyloamylase, after Tyr-54 was replaced by Ala, the three activities, disproportionation, hydrolytic and coupling activities were decreased. On the contrary, cyclization activity was increased (Fujii *et al.*, 2005; Fujii *et al.*, 2007). For disproportionation and hydrolytic activities, the substitution of Tyr-54 in *T. aquaticus* amyloamylase by Ala showed 4.4-fold and 2.6-fold lower activity than wild-type, whereas the substitution of Tyr-172 in *C. glutamicum* showed 3.5-fold and 1.7-fold lower activity than wild-type, respectively. These suggested that the substitution in *T. aquaticus* showed higher effect than in *C. glutamicum* amyloamylase when disproportionation and hydrolytic activities were compared. For cyclization reaction, the substitution in *T. aquaticus* amyloamylase showed 1.9-fold higher activity than wild-type, while the substitution in *C. glutamicum* showed 1.8-fold lower activity than wild-type.

When disproportionation reaction using linear maltooligosaccharide substrates (G1, glucose to G7, maltoheptaose) was investigated, the wild-type p17AM and Y172A enzyme showed the same result as p19AM. The enzymes require at least maltose unit for this reaction to occur.

The wild-type p17AM and Y172A mutated amyloamylase were different when hydrolytic reaction at various time points using LR-CDs as substrate was compared. The glucose released at each time point was detected by bicinchoninic acid assay. The amount of glucose released by the wild-type enzyme was significantly increased during the first six hours and kept on increasing gradually until 24 hours reaction. While that released by Y172A enzyme was rather stable. These results showed that the hydrolytic ability of the enzyme significantly decreased after mutation. In *T.*

aquaticus amyloamylase, substitution at the second binding site residues (Tyr-54 and Tyr-101) affected the reducing power (ability to break down substrate to produce glucose product, when all of substrate was broken down is defined as 100%) of the mutated enzyme (Fujii *et al.*, 2005 and 2007). Time course analysis showed that the wild-type enzyme resulted in an increase in the reducing power, while the increase in the reducing power was less in the mutated enzyme with lower hydrolytic activity. This suggested that the second binding site involved in reaction specificity and the binding of glucan to the second binding site could cause a conformational change in this enzyme, which might alter the reaction specificity.

4.7.5 Substrate specificity

Substrate specificity of the wild-type p17AM and Y172A mutated amyloamylase in disproportionation reaction was investigated using various oligosaccharides (G2 to G7) as substrate. The result showed that maltotriose (G3) was the most preferred substrate for both enzymes (Figure 3.33 and 3.34). For the wild-type enzyme, the descending order of preferred substrate was G3>G4>G5>G6>G7~G2 while the Y172A enzyme showed the substrate order of G3>G4>G5>G6>G7>G2. From transglucosylation reaction, the wild-type and mutated amyloamylase could catalyze maltooligosaccharide from maltose (G2) and higher. The descending order of preferred substrate was similar in both enzymes and the results suggested that the wild-type enzyme could use maltose (G2) better than Y172A mutated enzyme. Different substrate specificity was reported for amyloamylase from *Thermus thermophilus* HB8 (Kaper *et al.*, 2007), maltose (G2) was a poor substrate whereas maltotriose was an efficient substrate and the descending order of catalytic efficiency of the enzyme (k_{cat}/K_m) was

G3>G4>G5>G6>G7>G2. In addition, the descending order of catalytic efficiency of the *Pyrobaculum aerophilum* IM2 amyloamylase also showed similar result (G3>G4>G7>G5>G6) (Kaper *et al.*, 2005).

4.7.6 Kinetic study

Disproportionation activity was employed to determine the kinetic parameters. The maltotriose was used as substrate and glucose product was determined by glucose oxidase method. Both enzymes showed closed K_m values for maltotriose (12.9 mM for Y172A compared to 19.6 mM for wild-type). However, values of k_{cat} and the catalytic efficiency were different. The k_{cat} and k_{cat}/K_m values of Y172A mutated enzyme were about 4.4 and 2.8-fold lower than that of the wild-type enzyme. The results suggested that the amino acid substitution at Tyr-172 caused the change in kinetic parameters towards maltotriose, the binding at the active site was not much affected but the rate of catalysis was significantly reduced. Similarly, a decrease in k_{cat} was previously found in amino acid substitution at binding site which is outside catalytic region of α -amylase enzyme (Bozonnet *et al.*, 2007, Nielsen *et al.*, 2009). We thus proposed there was a conformational change at catalytic region that was affected from amino acid substitution at Tyr-172. The effect of substitution at the distal binding site on catalytic efficiency might be due to a requirement of a secondary binding site outside of the active site for the optimal activity (Oudjeriouat *et al.*, 2003), which might be corrupted by surface site mutation. This suggested that Tyr-54 might be a second binding site of this enzyme.

The second substrate binding site has been reported in α -amylase family from sources such as in bacteria (Knetzel *et al.*, 1995, Lyhne-Iversen *et al.*, 2006), archaea (Linden *et al.*, 2003) and plants (Robert *et al.*, 2003), and has been reported to affect

activities of the enzymes (Bozonnet *et al.*, 2007, Nielsen *et al.*, 2009). In CGTase that resembles amyloamylase in terms of catalytic reaction but differs in structure, the aromatic amino acid residue identified outside catalytic site region was shown to involve in the reaction specificity (Kelly *et al.*, 2008). In *T. aquaticus* amyloamylase, the Tyr-54 which was corresponded to Tyr-172 of *C. glutamicum* amyloamylase is located in subdomain B2 between second and third barrel strands (Przylas *et al.*, 2000). This position is proposed to trigger enzyme structure to a completely active conformation (Fujii *et al.*, 2007). The amino acid substitution at Tyr-172 affected at least three catalytic reactions of *C. glutamicum* amyloamylase, activities were reduced, not abolished suggesting that this position was not directly involved in the catalytic mechanism and substitution at this position might affect conformation of this enzyme. In addition, subtle conformational change from amino acid substitution at this residue is sufficient to retain catalytic function.

4.7.7 The synthesis of large-ring cyclodextrins

The LR-CDs production of recombinant wild-type p17AM and the Y172A mutated amyloamylase was compared (Figure 3.37). The results demonstrated that the amount of LR-CDs from Y172A mutated enzyme was lower than wild-type enzyme at early incubation time. However, the wild-type with and without his-tag and the Y172A mutated amyloamylase all produced the smallest LR-CDs as CD19. When incubation time was extended, the principal product of LR-CDs was changed from larger to smaller size in both enzymes, in addition, the product pattern of these enzymes was different at longer incubation time. The changing rate of principal product formation from larger to smaller ring size in the wild-type amyloamylase was faster than that of Y172A mutated enzyme. The changing of principle product of LR-

CD from larger to smaller ring size was also observed with his-tag containing amyloamylase (Figure 3.18), *T. aquaticus* amyloamylase (Terada *et al.*, 1999) and potato D-enzyme (Takaha *et al.*, 1996).

The amount of enzyme also had an effect on LR-CDs production (Figure 3.38). The increase in LR-CDs was corresponded with the increase in unit enzyme for both wild-type and mutated enzyme at early incubation time, however, the size and the amount of LR-CDs product was decreased when the amount of enzyme increased at long incubation time. The changing rate of principal product formation from larger to smaller ring size by the wild-type enzyme was faster than that of Y172A mutated enzyme. These results might be due to lower hydrolytic activity of Y172A mutated enzyme.

4.7.8 Analysis of large-ring cyclodextrins by MALDI-TOF

In HPAEC analysis, the size of LR-CD product was identified by comparing with two standard LR-CDs (CD20 and CD21). The other LR-CDs were identified by speculation from their relative R_f comparing to CD20 and CD21. To confirm the size of LR-CDs by MALDI-TOF, the reaction product from the wild-type p17AM was precipitated with acetone and dried. The precipitation of LR-CDs from potato D-enzyme and *T. aquaticus* amyloamylase have been reported using ethanol and dry under vacuum (Takaha *et al.*, 1996; Terada *et al.*, 1999; Fujii *et al.*, 2005 and 2007). Then, the precipitate was redissolved in water or NaOH and analyzed by HPAEC-PAD. Koizumi *et al.* (1999) precipitated LR-CDs from *Bacillus macerans* CGTase by using nine volume of acetone and recovered the pellet by centrifugation.

From the mass spectra (Figure 3.40), CD23 to CD45 were identified in reliably observed amounts. The determined size of LR-CDs by MALDI-TOF agreed

with HPAEC-PAD result. However, the smaller and larger CDs could also be observed but with a very low amount. The molecular weight of LR-CDs from *Bacillus macerans* CGTase (Koizumi *et al.*, 1999) and *T. aquaticus* amyloamylase (Taira *et al.*, 2006) were also determined by MALDI-TOF.



ศูนย์วิทยทรัพยากร
จุฬาลงกรณ์มหาวิทยาลัย

CHAPTER V

CONCLUSIONS

1. Amylomaltase gene (*malQ*) from *Corynebacterium glutamicum* ATCC 13032 consisted of an ORF of 2,121 bp and was deduced to 706 amino acid residues.
2. The deduced amino acid sequence showed only 18-26% identity with previously reported 4 α GTases.
3. Expression of amyломaltase was highest after induction with 0.4 mM IPTG for 2 hours. The amyломaltase from p19AM (*malQ* ligated with pET-19b) was purified to homogeneity by HisTrap FFTM column with final 30.2% yield and 10.8 purification fold.
4. The enzyme exhibited optimum temperature and pH for starch transglucosylation activity at 30 °C and pH 6.0. It was stable up to 30 °C in the pH range 5.5-9.0.
5. The p19AM enzyme could catalyze intermolecular transglucosylation reaction from maltooligosaccharides G2 to G7 while G1 could not be a substrate.
6. The intramolecular transglucosylation yielded LR-CDs from CD19 and higher.
7. Recombinant amyломaltase was reconstructed using pET-17b. The p17AM enzyme was purified to homogeneity by DEAE FFTM and Phenyl FFTM column with final 17.3% yield and 12.6 purification fold.
8. The single mutant Y172A was constructed. The Y172A amyломaltase was purified to homogeneity by DEAE FFTM and Phenyl FFTM column with final 9% yield and 45 purification fold.
9. The amyломaltase has no subunit structure since its molecular weight was 81 and 83 kDa by SDS-PAGE and gel filtration chromatography, respectively.

10. The wild-type and Y172A mutated amyloamylase showed the same optimal pH and temperature and the same pI of 4.7. Intermolecular transglucosylation activity for maltooligosaccharides was similar.
11. The wild-type amyloamylase showed higher disproportionation, cyclization and hydrolysis activities than Y172A mutated enzyme.
12. For substrate specificity, the descending order of preferred substrate of amyloamylase from p17AM was G3>G4>G5>G6>G7≈G2 while that of the Y172A enzyme was G3>G4>G5>G6>G7>G2.
13. For disproportionation activity, K_m and k_{cat} of the wild-type enzyme for maltotriose was 19.6 mM and 9,374 min⁻¹, while those for Y172A was 12.9 mM and 2,165 min⁻¹.
14. The increase in glucose released from hydrolytic reaction as a function of time was observed for the wild-type enzyme. No increase was found in Y172A reaction.
15. In the synthesis of LR-CDs, Y172A amyloamylase produced a lower amount of product than the wild-type enzyme at early incubation time. And the change in principal product from larger to smaller LR-CDs was observed at longer incubation time. The changing rate was faster for the wild-type enzyme.
16. The amount of LR-CDs was depended on the amount of enzyme, while the size changed with incubation time.
17. LR-CDs produced from wild-type amyloamylase was successfully precipitated by acetone. The size of LR-CDs was confirmed by MALDI-TOF.
18. Amyloamylase from *C. glutamicum* was a novel enzyme. The amino acid sequence and the LR-CDs product profile were different from those previously reported. Tyr-172 is important in determining the product profile.

REFERENCES

- Alting, A.C., *et al.* Improved creaminess of low-fat yoghurt: The impact of amyloamylase-treated starch domains. Food Hydrocolloids 23 (2009): 980–987.
- Ashraf, S.S., Benson, R.E., Payne, E.S., Halbleib, C.M., and Grøn, H. A novel multi-affinity tag system to produce high levels of soluble and biotinylated proteins in *Escherichia coli*. Protein Expression and Purification 33 (2004): 238-245.
- Baneyx, F. Recombinant protein expression in *Escherichia coli*. Current Opinion in Biotechnology 10 (1999): 411-421.
- Barends, T.R.M., Bultema, J.B., Kaper, T., van der Maarel, M.J.E.C., Dijkhuizen, L., and Dijkstra, B.W. Three-way stabilization of the covalent intermediate in amyloamylase, an α -amylase-like transglycosylase. The Journal of Biological Chemistry 282 (2007): 17242-17249.
- Barends, T.R.M., Korf, H., Kaper, T., van der Maarel, M.J.E.C., Dijkhuizen, L., and Dijkstra, B.W. Structural influences on product specificity in amyloamylase from *Aquifex aeolicus*. [Online]. 2004. Available from: <http://www.rcsb.org/pdb/explore.do?structureId=1TZ7> [2009, August 11]
- Bhuiyan, S.H., Kitaoka, M., and Hayashi, K. A cycloamylose-forming hyperthermostable 4- α -glucanotransferase of *Aquifex aeolicus* expressed in *Escherichia coli*. Journal of Molecular Catalysis B: Enzymatic 22 (2003): 45-53.
- Bollag, D.M., and Edelstein, S.J. Protein Methods. 1st ed. New York: A John Wiley & Sons, INC., Publication, 1991.
- Bollag, D.M., Rozycki, M.D., and Edelstein, S.J. Protein Methods. 2nd ed. New York: Wiley-Liss, 1996.

- Bloch, M.A., and Raibaud, O. Comparison of the malA regions of *Escherichia coli* and *Klebsiella pneumoniae*. Journal of Bacteriology 168 (1986): 1220-1227.
- Bo-young, B., *et al.* Cloning and overexpression of 4- α -glucanotransferase from *Thermus brockianus* (TBGT) in *E. coli*. Journal of Microbiology and Biotechnology 16 (2006): 1809-1813.
- Bozonnet, S., *et al.* The 'pair of sugar tongs' site on the non-catalytic domain C of barley α -amylase participates in substrate binding and activity. FEBS Journal 274 (2007): 5055-5067.
- Bradford, M.M. A rapid and sensitive method for the quantitation of microgram quantities of protein utilizing the principle of protein dye binding. Analytical Biochemistry 72 (1976): 248-254.
- Chaplin, M.F., and Kennedy, J.F. Carbohydrate Analysis: a Practical Approach. 2nd ed. New York: Oxford University Press Inc., 1994.
- Copeland, R.A. Enzyme: a Practical Introduction to Structure Mechanism and Data Analysis. 2nd ed. New York: A John Wiley & Sons, Inc., 2000.
- Dawson, R.M.C., Elliott, D.C., Elliott, W.H., and Jones, K.M. Data for Biochemical Research. 3rd ed. New York: Oxford University Press., 1986.
- Deckert, G., *et al.* The complete genome of the hyperthermophilic bacterium *Aquifex aeolicus*. Nature 392 (1998): 353-358
- Endo, T., Zheng, M., and Zimmermann, W. Enzymatic synthesis and analysis of large-ring cyclodextrins. Australian Journal of Chemistry 55 (2002): 39-48.
- Endo, T., *et al.* Production of large-ring cyclodextrins composed of 9~12 α -D-glucopyranose units by cyclodextrin glucanotransferase-effect of incubation temperature and molecular weight of amylose. Heterocycles 74 (2007): 991-997.

- Espinosa, M., Lopez, P., and Lacks, S.A. Transfer and expression of recombinant plasmids carrying pneumococcal *mal* genes in *Bacillus subtilis*. Gene 28 (1984): 301-310.
- Esposito, D., and Chatterjee, D.K. Enhancement of soluble protein expression through the use of fusion tags. Current Opinion in Biotechnology 17 (2006): 353-358.
- Fleischmann, R.D., *et al.* Whole-genome random sequencing and assembly of *Haemophilus influenzae* Rd. Science 269 (1995): 496-512.
- French, D., Pulley, A.O., Effenberger, J.A., Rougvie, M.A., and Abdullah, M. Studies on the Schardinger dextrans XII. The molecular size and structure of the δ -, ϵ -, ζ -, and η -dextrans. Archives of Biochemistry and Biophysics 111 (1965): 153-160.
- Fujii, K., *et al.* Use of random and saturation mutageneses to improve the properties of *Thermus aquaticus* amyloamylase for efficient production of cycloamyloses. Applied and Environmental Microbiology 71 (2005): 5823-5827.
- Fujii, K., *et al.* Function of second glucan binding site including tyrosines 54 and 101 in *Thermus aquaticus* amyloamylase. Journal of Bioscience and Bioengineering 103 (2007): 167-173.
- Furuishi, T., Endo, T., Nagase, H., Ueda, H., and Nagai, T. Solubilization of C₇₀ into water by complexation with δ -cyclodextrin. Chemical & Pharmaceutical Bulletin 46 (1998): 1658-1659.
- Gasteiger, E., *et al.* Protein Identification and Analysis Tools on the ExPASy Server. In J.M. Walker (ed.), The Proteomics Protocols Handbook, pp.571-607. New York: Humana Press, 2005.

- Gessler, K., *et al.* V-Amylose at atomic resolution: X-ray structure of a cycloamylose with 26 glucose residues (cyclomaltohexacosaeose). Proceedings of the National Academy of Sciences of the United States of America 96 (1999): 4246-4251.
- Goda, S.K., Eissa, O., Akhtar, M., and Minton, N.P. Molecular analysis of a *Clostridium butyricum* NCIMB 7423 gene encoding 4-alpha-glucanotransferase and characterization of the recombinant enzyme produced in *Escherichia coli*. Microbiology 143 (1997): 3287-3294.
- Hames, B.D., Hooper, N.M., and Hames, B.D. Instant Notes: Biochemistry. New York: Bios:Springer-verlag, 2000.
- Hansen, M.R., Blennow, A., Pedersen, S., and Engelsen, S.B. Enzyme modification of starch with amylomaltase results in increasing gel melting point. Carbohydrate Polymers 78 (2009): 72-79.
- Hansen, M.R., Blennow, A., Pedersen, S., Nørgaarda, L., and Engelsen, S.B. Gel texture and chain structure of amylomaltase-modified starches compared to gelatin. Food Hydrocolloids 22 (2008): 1551–1566.
- Harata, K., Akasaka, H., Endo, T., Nagase, H., and Ueda, H. X-ray structure of the δ -cyclodextrin complex with cycloundecanone. Chemical Communications 17 (2002): 1968-1969.
- Hashimoto, H. Present status of industrial application of cyclodextrins in japan. Journal of Inclusion Phenomena and Macrocylic Chemistry 44 (2002): 57-62.
- Ikeda, M., and Nakagawa, S. The *Corynebacterium glutamicum* genome: features and impacts on biotechnological processes. Applied Microbiology and Biotechnology 62 (2003): 99-109.

- Jeon, B.S., Taguchi, H., Sakai, H., Ohshima, T., Wakagi, T., and Matsuzawa, H. 4- α -glucanotransferase from the hyperthermophilic archaeon *Thermococcus litoralis*: enzyme purification and characterization, and gene cloning, sequencing and expression in *Escherichia coli*. European Journal of Biochemistry 248 (1997): 171-178.
- Jung, J.H., *et al.* Structural and functional analysis of substrate recognition by the 250s loop in amyloamylase from *Thermus brockianus*. Proteins 79 (2011): 633-644.
- Kakefuda, G., and Duke, S.H. Characterization of pea chloroplast D-enzyme (4- α -D-glucanotransferase). Plant Physiology 91 (1989): 136-143.
- Kakefuda, G., Duke, S.H., and Hostak, M.S. Chloroplast and extrachloroplastic starch-degrading enzymes in *Pisum sativum* L. Planta 168 (1986): 175-182.
- Kalinowski, J., *et al.* The complete *Corynebacterium glutamicum* ATCC 13032 genome sequence and its impact on the production of L-aspartate-derived amino acids and vitamins. Journal of Biotechnology 104 (2003): 5-25.
- Kang, H.K., Jang, J.H., Shim, J.H., Park, J.T., Kim, Y.W., and Park, K.H. Efficient constitutive expression of thermostable 4- α -glucanotransferase in *Bacillus subtilis* using dual promoters. World Journal of Microbiology and Biotechnology 26 (2010): 1915-1918.
- Kaper, T., *et al.* Identification of acceptor substrate binding subsites +2 and +3 in the amyloamylase from *Thermus thermophilus* HB8. Biochemistry 46 (2007): 5261-5269.
- Kaper, T., Talik, B., Ettema, T.J., Bos, H., van der Maarel, M.J., and Dijkhuizen, L. Amyloamylase of *Pyrobaculum aerophilum* IM2 produces thermoreversible starch gels. Applied and Environmental Microbiology 71 (2005): 5098-5106.

- Kaper, T., van der Maarel, M.J., Euverink, G.J., and Dijkhuizen, L. Exploring and exploiting starch-modifying amylomaltases from thermophiles. Biochemical Society Transactions 32 (2004): 279-282.
- Kelly, R.M., Leemhuis, H., Rozeboom, H.J., Oosterwijk, N.V., Dijkstra, B.W., and Dijkhuizen, L. Elimination of competing hydrolysis and coupling side reactions of a cyclodextrin glucanotransferase by directed evolution. Biochemical Journal 413 (2008): 517-525.
- Kennedy, J.K., and Pagliuca, G. Oligosaccharides. In M.F Chaplin, *et al.* (eds.), Carbohydrate Analysis, pp.48-50. New York: Oxford University Press, 1994.
- Kinoshita, S., Udaka, S., and Shimono, M. Studies on amino acid fermentation. Part I. Production of l-glutamic acid by various microorganisms. The Journal of General and Applied Microbiology 3 (1957): 193–205.
- Kinoshita, S., and Nakayama, K. Amino acids. In A.H. Rose (ed.), Primary Products of Metabolism, pp.209–261. London: Academic press, 1978.
- Kitahata, S., Murakami, H., and Okada, S. Purification and some properties of amylomaltase from *Escherichia coli* IFO 3806. Agricultural and Biological Chemistry 53 (1989): 2653- 2659.
- Kitamura, S., Nakatani, K., Takaha, T., and Okada, S. Complex formation of large-ring cyclodextrins with iodine in aqueous solution as revealed by isothermal titration calorimetry. Macromolecular Rapid Communications 20 (1999): 612–615.
- Knegtel, R.M.A., *et al.* Crystallographic studies of the interaction of cyclodextrin glycosyltransferase from *Bacillus circulans* strain-251 with natural substrates and products. The Journal of Biological Chemistry 270 (1995): 29256-29264.

- Koizumi, K., Sanbe, H., Kubota, Y., Terada, Y., and Takaha, T. Isolation and characterization of cyclic α -(1 \rightarrow 4)-glucans having degrees of polymerization 9–31 and their quantitative analysis by high-performance anion-exchange chromatography with pulsed amperometric detection. Journal of Chromatography A 852 (1999): 407-416.
- Kumagai, H. Microbial production of amino acids in Japan. Advances in Biochemical Engineering/Biotechnology 69 (2000): 71–85.
- Kuriki, T., *et al.* The concept of the α -amylase family: A rational tool for interconverting glucanohydrolase/glucanotransferases, and their specificities. Journal of Applied Glycoscience 53 (2006): 155-161.
- Lacks, S.A., Dunn, J.J., and Greenberg, B. Identification of base mismatches recognized by the heteroduplex-DNA-repair system of *Streptococcus pneumoniae*. Cell 31(1982): 327-336.
- Larsen, K.L. Large cyclodextrins. Journal of Inclusion Phenomena and Macrocyclic Chemistry 43 (2002): 1-13.
- Lee, B.H., Oh, D.K., and Yoo, S.H. Characterization of 4- α -glucanotransferase from *Synechocystis* sp. PCC 6803 and its application to various corn starches. New Biotechnology 26 (2009): 29-36.
- Lee, H.S., *et al.* Cooperative action of alpha-glucanotransferase and maltogenic amylase for an improved process of isomaltooligosaccharide (IMO) production. Journal of Agricultural and Food Chemistry 50 (2002): 2812-2827.
- Lee, K.Y., Kim Y., Park, K.H., and Lee, H.G. Effects of α -glucanotransferase treatment on the thermo-reversibility and freeze-thaw stability of a rice starch gel. Carbohydrate Polymers 63 (2006): 347–354.

- Leuchtenberger, W. Amino acids-technical production and use. In M. Roehr (ed.), Biotechnology, vol 6. Products of Primary Metabolism, pp.465–502. 2nd ed. Weinheim: VCH, 1996.
- Liebl, W. Corynebacterium – nonmedical. In M. Dworkin, *et al.* (eds.), The Prokaryotes: A Handbook on the Biology of Bacteria, Vol. 3: Archaea and Bacteria: Firmicutes, Actinomycetes, pp.796–818. New York: Springer, 2001.
- Liebl, W. Corynebacterium taxonomy. In L. Eggeling, *et al.* (eds.), Handbook of Corynebacterium glutamicum, pp.9–34. Boca Raton: CRC Press, 2005.
- Liebl, W., Feil, R., Gabelsberger, J., Kellermann, J., and Schleifer, K.H. Purification and characterization of a novel thermostable 4- α -glucanotransferase of *Thermotoga maritime* cloned in *Escherichia coli*. European Journal of Biochemistry 207 (1992): 81-88.
- Lin, T.P., and Preiss, J. Characterization of D-enzyme (4- α -glucanotransferase) in *Arabidopsis* leaf. Plant Physiology 86 (1988): 260-265.
- Linden, A., Mayans, O., Meyer-Klaucke, W., Antranikian, G., and Wilmanns, M. Differential regulation of a hyperthermophilic R-amylase with a novel (Ca,Zn) two-metal center by zinc. The Journal of Biological Chemistry 278 (2003): 9875-9884.
- Lundberg, K.S., Shoemaker, D.D., Adams, M.W.W., Short, J.M., Sorge, J.A., and Mathur, E.J. High-fidelity amplification using a thermostable DNA polymerase isolated from *Pyrococcus furiosus*. Gene 108 (1991): 1–6.
- Lütken, H., *et al.* Repression of both isoforms of disproportionating enzyme leads to higher malto-oligosaccharide content and reduced growth in potato. Planta 232 (2010): 1127-1139.

- Lyhne-Iversen, L., Hobley, T.J., Kaasgaard, S.G., and Harris, P. Structure of *Bacillus halmapalus* R-amylase crystallized with and without the substrate analogue acarbose and maltose. Acta Crystallographica F62 (2006): 849-854.
- Machida, S., and Hayashi, K. Kit for artificial chaperone. Japanese Patent Publication number: 2001-261697, 2001.
- Machida, S., Hayashi, K., Tokuyasu, T., and Takaba, T. Refolding method of antibody. Japanese Patent Publication number: 2003-128699, 2003.
- Machida, S., Ogawa, S., Xiaohua, S., Takaha, T., Fujii, K., and Hayashi, K. Cycloamylose as an efficient artificial chaperone for protein refolding. FEBS Letters 486 (2000): 131-135.
- Machius, M., Vértesy, L., Huber, R., and Wiegand, G. Carbohydrate and protein-based inhibitors of porcine pancreatic α -amylase: structure analysis and comparison of their binding characteristics. Journal of Molecular Biology 260 (1996): 409-421.
- Maniatis, T., Fritsch, E.F., and Sambrook, J. Molecular Cloning: a Laboratory Manual. 1st ed. New York: Cold Spring Harbor Laboratory, 1982.
- Manners, D.J., and Rowe, K.L. Studies on carbohydrate-metabolising enzymes: Part XXI. The α -glucosidase and d-enzyme activity of extracts of carrots and tomatoes. Carbohydrate Research 9 (1969): 441-450.
- Miyazawa, I., Ueda, H., Nagase, H., Endo, T., Kobayashi, S., and Nagai, T. Physicochemical properties and inclusion complex formation of δ -cyclodextrin. European Journal of Pharmaceutical Sciences 3 (1995): 153-162.
- Monod, J., and Torriani, A.M. Amylomaltase of *Escherichia coli*. Annales de l'Institut Pasteur 78 (1950): 65-77.

- Mun, S., Kim, Y., Kang, C., Park, K., Shim, J., and Kim, Y. Development of reduced-fat mayonnaise using 4 α Gase-modified rice starch and xanthan gum. International Journal of Biological Macromolecules 44 (2009): 400–407.
- Murray, R.K., Granner, D.K., Mayes, P.A., and Rodwell, V.W. Harper's Illustrated Biochemistry. 26th ed. New York: Lange Medical Books/McGraw Hill, 2003.
- Nakamura, A., Haga, K., and Yamane, K. Four aromatic residues in the active center of cyclodextrin glucanotransferase from alkalophilic *Bacillus* sp. 1011: effects of replacements on substrate binding and cyclization characteristics. Biochemistry 33 (1994): 9929-9936.
- Nelson, D.L., and Cox, M.M. Lehninger Principles of Biochemistry. 4th ed. New York: W.H. Freeman, 2005.
- Nielsen, M.M., *et al.* Two secondary carbohydrate binding sites on the surface of Barley R-amylase 1 have distinct functions and display synergy in hydrolysis of starch granules. Biochemistry 48 (2009): 7686-7697.
- Nominé, Y., Ristriani, T., Laurent, C., Lefèvre, J.F., Weiss, É., and Travé, G. Formation of soluble inclusion bodies by HPV E6 oncoprotein fused to maltose-binding protein. Protein Expression and Purification 23 (2001): 22-23.
- Oudjeriouat, N., Moreau, Y., Santimone, M., Svensson, B., Marchis-Mouren, G., and Desseaux, V. On the mechanism of α -amylase: Acarbose and cyclodextrin inhibition of barley amylase isozymes. European Journal of Biochemistry 270 (2003): 3871-3879.
- Park, J., *et al.* The action mode of *Thermus aquaticus* YT-1 4- α -glucanotransferase and its chimeric enzymes introduced with starch-binding domain on amylose and amylopectin. Carbohydrate Polymers 67 (2007): 164–173.

- Peat, S., Whelan, W.J., and Rees, W.R. The enzymic synthesis and degradation of starch. Part XX. The disproportionating enzyme (D-enzyme) of the potato. Journal of the American Chemical Society 1956 (1956): 44-53.
- Penninga, D., *et al.* Site-directed mutations in tyrosine 195 of cyclodextrin glycosyltransferase from *Bacillus circulans* strain 251 affect activity and product specificity. Biochemistry 34 (1995): 3368-3376.
- Przylas, I., Terada, Y., Fujii, K., Takaha, T., Saenger, W., and Sträter, N. X-ray structure of acarbose bound to amyloamylase from *Thermus aquaticus*: Implications for the synthesis of large cyclic glucans. European Journal of Biochemistry 267 (2000): 6903-6913.
- Pugsley, A.P., and Dubreuil, C. Molecular characterization of malQ, the structural gene for the *Escherichia coli* enzyme amyloamylase. Molecular Microbiology 2 (1988): 473-479.
- Pully, O. A., and French, D. Studies on the Schardinger dextrin XI: The isolation of new Schardinger dextrin. Biochemical and Biophysical Research Communications 5 (1961): 11-15.
- Robert, X., *et al.* The structure of barley R-amylose isozyme 1 reveals a novel role of domain C in substrate recognition and binding: A pair of sugar tongs. Structure 11 (2003): 973-984.
- Saenger, W., *et al.* Structures of the common cyclodextrins and their larger analogues- Beyond the doughnut. Chemical Reviews 98 (1998): 1787-1802.
- Sahm, H., Eggeling, L., and de Graaf, A.A. Pathway analysis and metabolic engineering in *Corynebacterium glutamicum*. Biological Chemistry 381 (2000): 899-910.

- Sambrook, J., and Russell, W.D. Molecular Cloning: a Laboratory Manual. 3rd ed. Cold spring harbor: Cold spring harbor laboratory press, 2001.
- Sassenfeld, H.M. Engineering proteins for purification. TIBTECH 8 (1990): 88-93.
- Schmidt, A.K., Cottaz, S., Driguez, H., and Schulz, G.E. Structure of cyclodextrin glycosyltransferase complexed with a derivative of its main product β -cyclodextrin. Biochemistry 37 (1998): 5909-5915.
- Schmidt, J., and John, M. Starch metabolism in *Pseudomonas stutzeri*. II. Purification and properties of a dextrin glucosyltransferase (D-enzyme) and amyloamylase. Biochimica et Biophysica Acta 566 (1979): 100-114.
- Schwartz, M. The maltose regulon. In F.C. Neidhardt, *et al.* (eds.), Escherichia coli and Salmonella typhimurium: Cellular and Molecular Biology, pp.1482-1502. Washington DC: American Society for Microbiology, 1987.
- Sinner, M., and Puls, J. Non-corrosive dye reagent for detection of reducing sugars in borate complex ion-exchange chromatography. Journal of Chromatography 156 (1978): 197-204.
- Stackebrandt, E., Rainey, F.A., and Ward-Rainey, N.L. Proposal for a new hierarchical classification system, Actinobacteria classis nov. International Journal of Systematic Bacteriology 47 (1997): 479-491.
- Stassi, D.L., Lopez, P., Espinosa, M., and Lacks, S.A. Cloning of chromosomal genes in *Streptococcus pneumoniae*. Proceedings of the National Academy of Sciences of the United States of America 78 (1981): 7028-7032.
- Sträter, N., Przylas, I., Saenger, W., Terada, Y., Fujii, K., and Takaha, T. Structural basis of the synthesis of large cycloamyloses by amyloamylase. Biologia, Bratislava 57(Suppl. 11) (2002): 93-99.

- Suganuma, T., Setoguchi, S., Fujimoto, S., and Nagahama, T. Analysis of the characteristic action of D-enzyme from sweet potato in terms of subsite theory. Carbohydrate Research 212 (1991): 201-212.
- Szejtli, J. Introduction and general overview of cyclodextrin chemistry. Chemical Reviews 98 (1998): 1743-1753.
- Tachibana, Y., Fujiwara, S., Takagi, M., and Imanaka, T. Cloning and expression of the 4- α -glucanotransferase gene from the hyperthermophilic archaeon *Pyrococcus* sp. KOD1, and characterization of the enzyme. Journal of Fermentation and Bioengineering 83 (1997): 540-548.
- Taira, H., Nagase, H., Endo, T., and Ueda, H. Isolation, purification and characterization of large-ring cyclodextrins (CD₃₆-CD₃₉). Journal of Inclusion Phenomena and Macrocyclic Chemistry 56 (2006): 23-28.
- Takaha, T., and Smith, S.M. The function of 4- α -glucanotransferase and their use for the production of cyclic glucans. Biotechnology and Genetic Engineering Reviews 16 (1999): 257-280.
- Takaha, T., Yanase, M., Okada, S., and Smith, S.M. Disproportionating enzyme (4- α -glucanotransferase; EC 2.4.1.25). Purification, molecular cloning, and potential in starch metabolism. The Journal of Biological Chemistry 268 (1993): 1391-1396.
- Takata, H., *et al.* Action of neopullulanase: Neopullulanase catalyzes both hydrolysis and transglycosylation at α -(1 \rightarrow 4)- and α -(1 \rightarrow 6)-glucosidic linkages. The Journal of Biological Chemistry 267 (1992): 18447-18452.
- Terada, Y., Fujii, K., Takaha, T., and Okada, S. *Thermus aquaticus* ATCC 33923 amyloamylase gene cloning and expression and enzyme characterization:

- Production of cycloamylose. Applied and Environmental Microbiology 65 (1999): 910-915.
- Tomono, K., *et al.* Interaction between cycloamylose and various drugs. Journal of Inclusion Phenomena and Macrocyclic Chemistry 44 (2002): 267–270.
- Udaka, S. Screening method for microorganisms accumulating metabolites and its use in the isolation of *Micrococcus glutamicus*. Journal of Bacteriology 79 (1960): 754–755.
- Ueda, H. Physicochemical properties and complex formation abilities of large-ring cyclodextrins. Journal of Inclusion Phenomena and Macrocyclic Chemistry 44 (2002): 53-56.
- Ueda, H., Wakisaka, M., Nagase, H., Takaha, T., and Okada, S. Physicochemical properties of large-ring cyclodextrins (CD₁₈~CD₂₁). Journal of Inclusion Phenomena and Macrocyclic Chemistry. 44 (2002): 405-405.
- Uitdehagg, J.C.M., Enverink, G.J., van der Veen, B.A., van der Maarel, M., and Dijkstra, B.W. Structure and mechanism of the amylomaltase from *Thermus thermophilus* HB8. [Online]. 2000. Available from: <http://www.rcsb.org/pdb/explore/explore.do?structureId=1FP8> [2009, August 11]
- Uitdehaag, J.C.M., *et al.* X-ray structures along the reaction pathway of cyclodextrin glycosyltransferase elucidate catalysis in the α -amylase family. Nature Structural Biology 6 (1999): 432-436.
- van der Maarel, M.J.E.C., van der Veen, B., Uitdehaag, J.C.M., Leemhuis, H., and Dijkhuizen L. Properties and applications of starch-converting enzymes of the α -amylase family. Journal of Biotechnology 94 (2002): 137–155.

- van der Veen, B.A., Joost, C.M., Uitdehaag, B.W.D., and Lubbert. D. Engineering reaction and production specificity of cyclodextrin glycosyltransferase from *Bacillus circulans* strain 251. Biochemica et Biophysica Acta: Protein and Proteomic 1543 (2000): 336-360.
- Vertès, A.A., Inui, M., and Yukawa, H. Manipulating corynebacteria from individual genes to chromosome. Applied and Environmental Microbiology 71 (2005): 7633–7642.
- Voet, D. and Voet, J.G. Biochemistry. New York: J. Wiley & Sons, 2004.
- Xavier, K.B., Peist, R., Kossmann, M., Boos, W., and Santos, H. Maltose metabolism in the hyperthermophilic archaeon *Thermococcus litoralis*: Purification and Characterization of key enzymes. Journal of Bacteriology 181 (1999): 3358-3367.
- Yoshio, N., Maeda, I., Taniguchi, H., and Nakamura, M. Purification and properties of D-enzyme from malted barley. Journal of the Japanese Society of Starch Science 33 (1986): 244-252.



APPENDICES

ศูนย์วิทยทรัพยากร
จุฬาลงกรณ์มหาวิทยาลัย

Appendix 1

Preparation for SDS-polyacrylamide gel electrophoresis

1) Stock reagents

2 M Tris-HCl pH 8.8

Tris(hydroxymethyl)-aminomethane 24.2 g

Adjusted pH to 8.8 with 1 N HCl and adjusted volume to 100 ml with distilled water

1 M Tris-HCl pH 6.8

Tris(hydroxymethyl)-aminomethane 12.1 g

Adjusted pH to 6.8 with 1 N HCl and adjusted volume to 100 ml with distilled water

10% (w/v) SDS

Sodium dodecyl sulfate 10 g

Adjusted volume to 100 ml with distilled water

50% (v/v) Glycerol

100% Glycerol 50 ml

Added 50 ml distilled water

1% (w/v) Bromophenol blue

Bromophenol blue 100 mg

Brought to 10 ml with distilled water and stir until dissolved. Filtration was performed to remove aggregated dye.

2) Working Solutions

Solution A

30% Acrylamide, 0.8% bis-acrylamide, 100 ml

Acrylamide	29.2	g
------------	------	---

N,N'-methylene-bis-acrylamide	0.8	g
-------------------------------	-----	---

Adjusted volume to 100 ml with distilled water

Solution B

4x Separating Gel Buffer

2 M Tris-HCl pH 8.8	75	ml
---------------------	----	----

10% SDS	4	ml
---------	---	----

Distilled water	21	ml
-----------------	----	----

Solution C

4x Stacking Gel Buffer

1 M Tris-HCl pH 6.8	50	ml
---------------------	----	----

10% SDS	4	ml
---------	---	----

Distilled water	46	ml
-----------------	----	----

10% Ammonium persulfate

Ammonium persulfate	0.5	g
---------------------	-----	---

Distilled water	5	ml
-----------------	---	----

Electrophoresis Buffer

Tris(hydroxymethyl)-aminomethane	3	g
----------------------------------	---	---

Glycine	14.4	g
---------	------	---

Sodium dodecyl sulfate	1	g
------------------------	---	---

Adjusted volume to 1 liter with distilled water

5x Sample buffer

1 M Tris-HCl pH 6.8	0.6	ml
50% Glycerol	5	ml
10% SDS	2	ml
2-Mercaptoethanol	0.5	ml
1% Bromophenol blue	1	ml
Distilled water	0.9	ml

Coomassie Gel Stain

Coomassie Blue R-250	1	g
Methanol	450	ml
Distilled water	450	ml
Glacial acetic acid	100	ml

Coomassie Gel Destain

Methanol	100	ml
Glacial acetic acid	100	ml
Distilled water	800	ml

ศูนย์วิทยทรัพยากร
จุฬาลงกรณ์มหาวิทยาลัย

Solution B**4x Seperating Gel Buffer**

2 M Tris-HCl pH 8.8	75	ml
Distilled water	25	ml

Solution C**4x Stacking Gel Buffer**

1 M Tris-HCl pH 6.8	50	ml
Distilled water	50	ml

10% Ammonium persulfate

Ammonium persulfate	0.5	g
Distilled water	5	ml

1% Glycogen

Glycogen from oyster	0.05	g
Distilled water	5	ml

Electrophoresis Buffer

Tris(hydroxymethyl)-aminomethane	3	g
Glycine	14.4	g
Adjusted volume to 1 liter with distilled water		

5x Sample buffer

1 M Tris-HCl pH 6.8	3.1	ml
50% Glycerol	5	ml
1% Bromophenol blue	0.5	ml
Distilled water	1.4	ml

Appendix 3

Preparation for isoelectric focusing (IEF)

Stock reagents

24.25% Acrylamide, 0.75% bis-acrylamide, 100 ml

Acrylamide	24.25	g
N,N'-methylene-bis-acrylamide	0.75	g
Adjusted volume to 100 ml with distilled water		

0.1% Riboflavin

Riboflavin	50	mg
Distilled water	40	ml

Heat until soluble and adjusted volume to 50 ml with distilled water

Monomer-ampholyte solution

25% Acrylamide	1	ml
Distilled water	2.75	ml
25% Glycerol	1	ml
Ampholyte	0.25	ml
0.1% Riboflavin	50	μl
10% Ammonium persulfate	15	μl
TEMED	5	μl

Fixative solution, 100 ml

Sulfosalicylic acid	4	g
Trichloroacetic acid	12.5	g
Methanol	30	ml

Immersed gel in this solution for 30 minutes

Staining Solution, 100 ml

Ethanol	27	ml
Acetic acid	10	ml
Coomassie brilliant blue R-250	0.04	g
CuSO ₄	0.5	g
Distilled water	63	ml

Dissolved the CuSO₄ in water before adding the methanol. Either dissolved the dye in alcohol and filtrated or added it to the solution at the end. Immersed the gel into staining solution for approximately 1-2 hours.

Destaining solution**First destaining solution**

Ethanol	12	ml
Acetic acid	7	ml
CuSO ₄	0.5	g
Distilled water	81	ml

Dissolved the CuSO₄ in water before adding the ethanol. Immersed the gel in two or three changes of this solution until the background was nearly clear.

Second destaining solution

Ethanol	25	ml
Acetic acid	7	ml
Distilled water	68	ml

Immersed the gel in this solution to remove residuals of CuSO₄

Appendix 4**Preparation for Iodine solution****Iodine solution****0.2% I₂ / 2% KI**

Potassium iodide 2 g

Iodine 0.2 g

Adjusted to 100 ml with distilled water



ศูนย์วิทยทรัพยากร
จุฬาลงกรณ์มหาวิทยาลัย

Appendix 5

Preparation for bicinchoninic acid assay

Bicinchoninic acid reagent

Solution A

4,4'-Dicarboxy-2,2'-biquinoline 0.1302 g

Dissolved in 85 ml of distilled water

NaCO₃ 6.2211 g

Adjusted to 100 ml with distilled water

Solution B

Component (1)

L-aspartic acid 0.642 g

NaCO₃ 0.8681 g

Dissolved in 15 ml of distilled water

Component (2)

CuSO₄ 0.1736 g

Dissolve in 5 ml of distilled water

Mixed component (1) and (2), then adjusted to 25 ml with distilled water

Mixed 24 ml of solution A and 1 ml of solution B and used within 24 hours

Appendix 6

Preparation for DNS reagent

DNS Reagent

2-hydroxy-3,5-dinitrobenzoic acid	5	g
2 N NaOH	100	ml
Potassium sodium tartrate	150	g

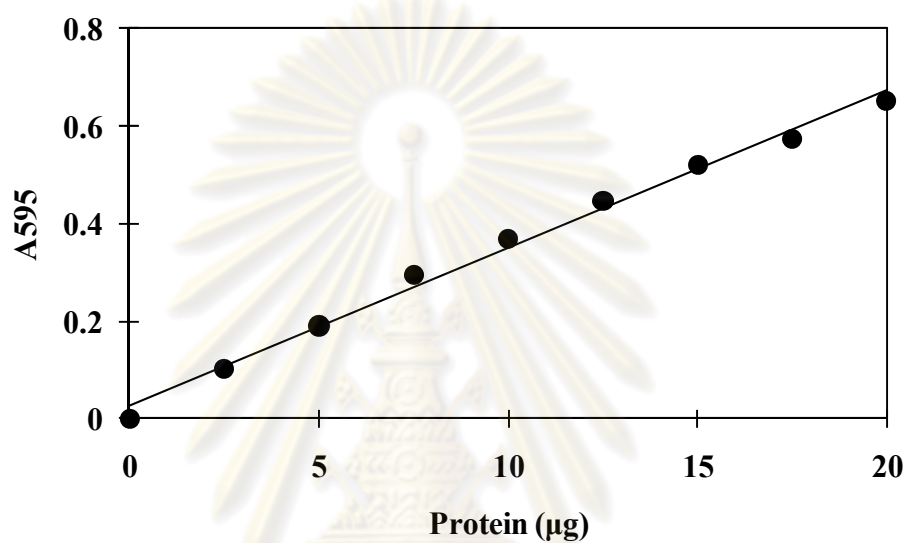
Adjusted to 500 ml with distilled water



ศูนย์วิทยทรัพยากร
จุฬาลงกรณ์มหาวิทยาลัย

Appendix 7

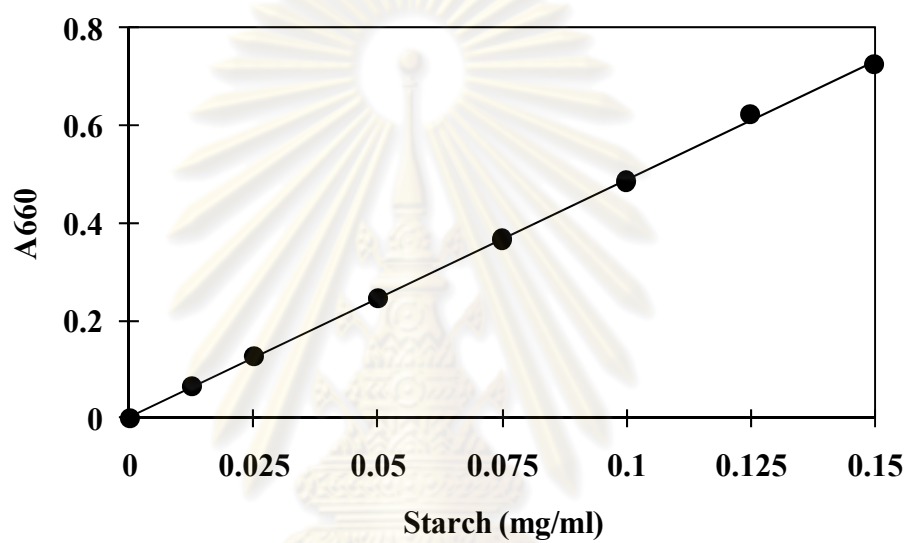
Standard curve for protein determination by Bradford's method



ศูนย์วิทยทรัพยากร
จุฬาลงกรณ์มหาวิทยาลัย

Appendix 8

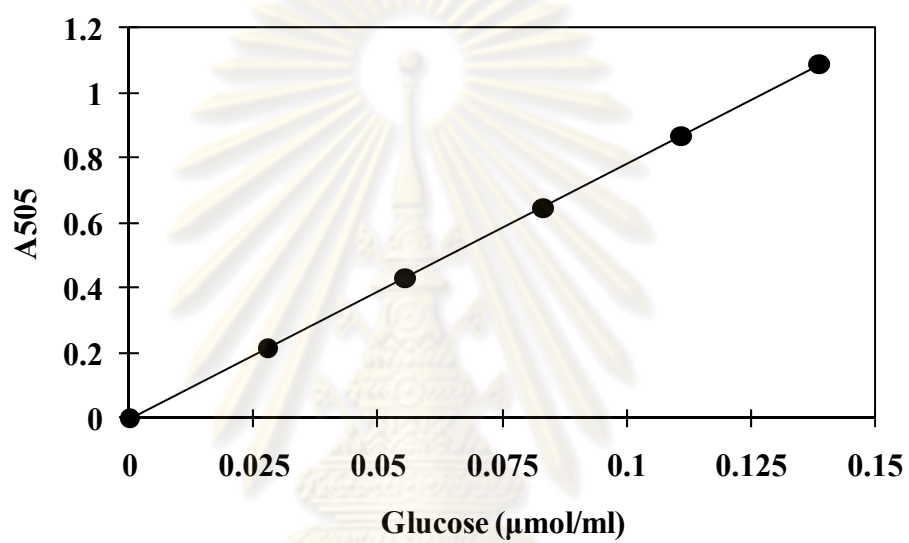
Standard curve for starch determination by starch degrading assay



ศูนย์วิทยทรัพยากร
จุฬาลงกรณ์มหาวิทยาลัย

Appendix 9

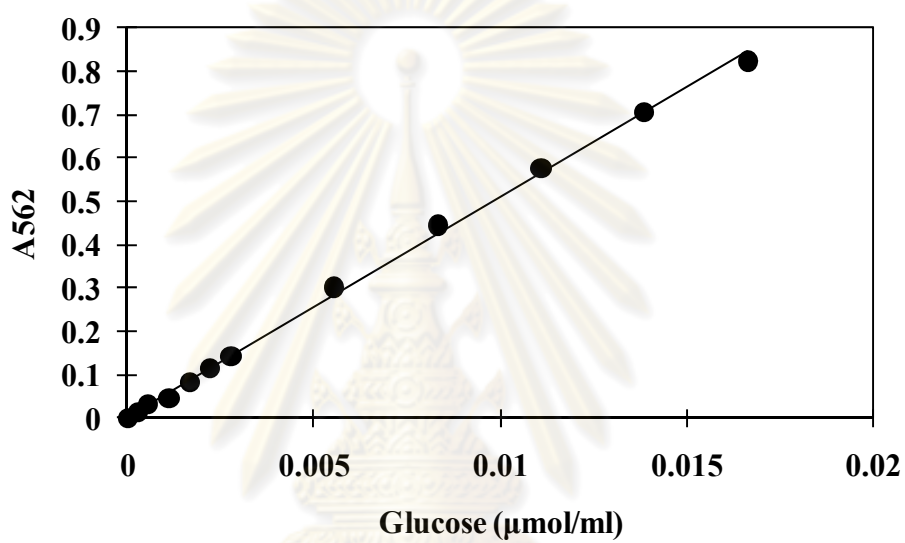
Standard curve for glucose determination by glucose oxidase assay



ศูนย์วิทยทรัพยากร
จุฬาลงกรณ์มหาวิทยาลัย

Appendix 10

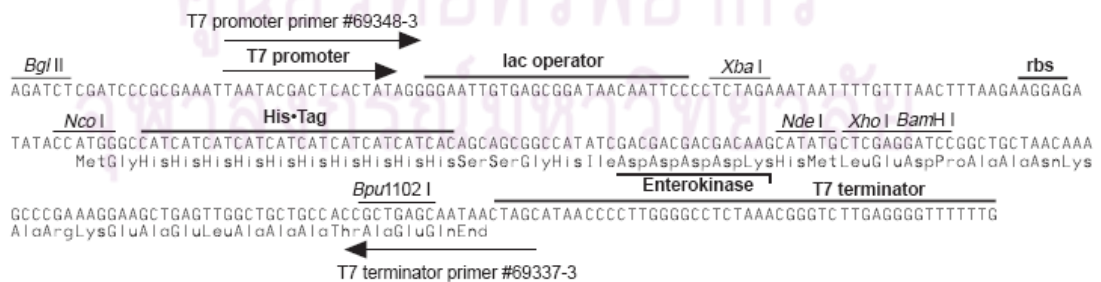
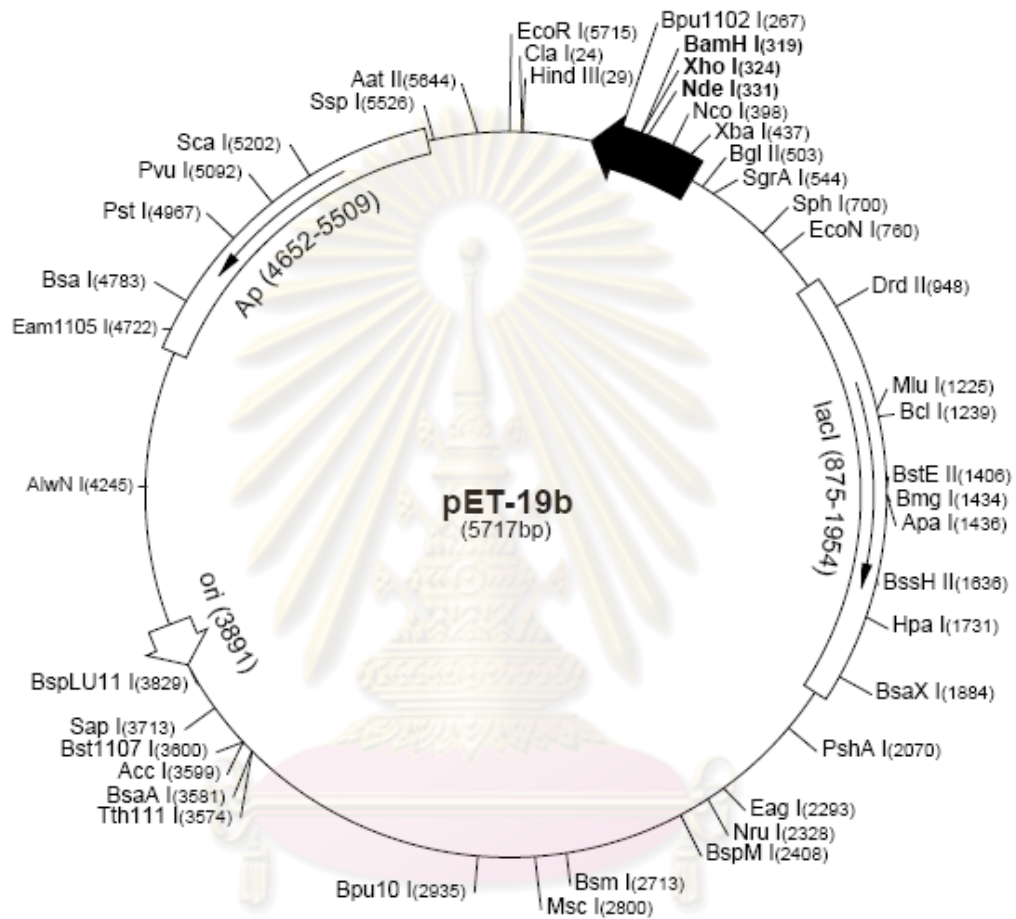
Standard curve for glucose determination by bicinchoninic acid assay



ศูนย์วิทยทรัพยากร
จุฬาลงกรณ์มหาวิทยาลัย

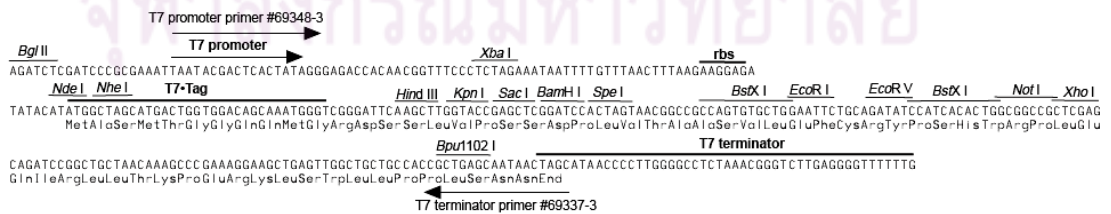
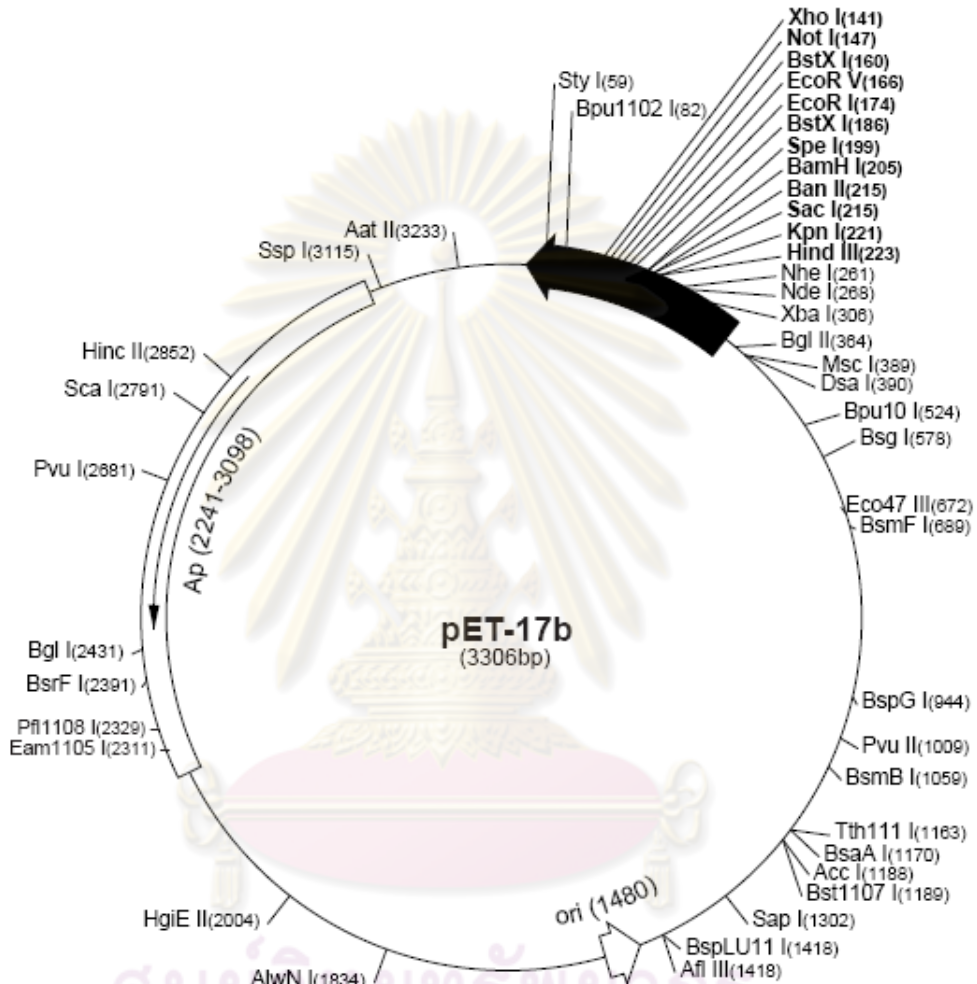
Appendix 11

Restriction map of pET-19b



Appendix 12

Restriction map of pET-17b



BIOGRAPHY

Miss Wiraya Srisimararat was born on June 2, 1982. She graduated with the Bachelor Degree of Science in Biotechnology from King Mongkut's Institute of Technology Ladkrabang in 2004. She graduated with Master Degree of Science in Biochemistry from Chulalongkorn University in 2007. Then, she continued studying Ph.D. in Biochemistry, faculty of Science, Chulalongkorn University.

Publications:

Srisimararat, W., Powviriyakul, A., Kaulpiboon, J., Krusong, K., Zimmermann, and Pongsawasdi, P. (2010) "A novel amyloamylase from *Corynebacterium glutamicum* and analysis of the large-ring cyclodextrin products" *Journal of Inclusion Phenomena and Macrocyclic Chemistry*, DOI 10.1007/s10847-010-9890-5

Srisimararat, W., and Pongsawasdi, P. (2008) "Enhancement of the oligosaccharide synthetic activity of β -galactosidase in organic solvents by cyclodextrin" *Enzyme and Microbial technology*, 43, 436-441.

Srisimararat, W., and Pongsawasdi, P. (2007) "Effect of cyclodextrin on oligosaccharide synthetic activity of beta-galactosidase" *Proceedings of the First Biochemistry and Molecular Biology (BMB) Conference: Biochemistry and Molecular Biology for the integration of life*, April 26-27, Thailand. pp. 122-130.

Grants and Fellowships:

2008-present Research Institution Partnership Grant from Alexander von Humboldt Foundation

2007-present The Royal Golden Jubilee Ph.D. Program from Thailand Research fund

2006 Graduate Thesis Grant from Graduate School, Chulalongkorn University

2002 Tokai-KMITL Internship Grant from Tokai University and King Mongkut's Institute of Technology Ladkrabang